Plasma Pre-Treatment for Adhesive Bonding of Aerospace Composite Components

A thesis submitted for the degree of Master of Philosophy

by

Berta Navarro Rodríguez

College of Engineering, Design and Physical Sciences

Department of Mechanical, Aerospace and Civil Engineering

Brunel University London

August 2016

The research on 'Plasma Treatment for Adhesive Bonding of Aerospace Composite Components' was carried out as a part-time MPhil programme, between February 2015 and August 2016 at the National Structural Integrity Research Centre (NSIRC, Cambridge), and awarded by Brunel University London (Department of Mechanical, Aerospace and Civil Engineering). This research was also performed in collaboration with TWI Ltd (Cambridge).

ABSTRACT OF THE DISSERTATION

Plasma Treatment for Adhesive Bonding of Aerospace Composite Components

by

Berta Navarro Rodríguez

Master of Philosophy in *Mechanical, Aerospace and Civil Engineering*

Brunel London University, 2016

Senior Lecturer Aerospace Engineering – Cristinel Mares

Consultant Adhesive Technology TWI – Ewen Kellar

Key words: composites, aerospace, cold atmospheric pressure plasma, adhesive bonding, surface pre-treatment

A cold atmospheric pressure plasma source was investigated as an alternative pre-treatment for carbon fibre reinforced epoxy substrates prior to bonding.

For reference, common surface pre-treatments were also investigated (peel ply, manual abrasion, and grit blasting). In the aerospace industry, the peel ply, is usually added to one side of the composite surface during manufacture and peeled off prior to bonding.

Peel ply can be used independently or in combination with other techniques. The strength of the bonded joints of the different pre-treatments was assessed through tensile lap shear tests. It was found that combining peel ply with plasma increased the joint strength by 10% whereas manual abrasion or grit blasting after peel ply improved the strength of the joints by 15% and 20% respectively.

The effect of pre-treating the composite substrate side without peel ply (bag side) was also investigated. The strength of the joints produced without any

pre-treatment was increased by 99% for manual abrasion, 134% for grit blasting and by 146% for plasma.

Comparing both surfaces of the composite substrates, it was found that using peel ply improved the performance of the joints by 91%.

In order to understand better the effects of the different pre-treatments, surface characterisation of the substrates (surface roughness, surface free energy, and analysis of chemical changes) was also conducted.

The effect of roughness did little to affect the strength values (for both surfaces of the composite). The adhesive used in this research was very good at wetting the surface, regardless of the roughness.

However, when the adhesive was able to wet the surface, the relationship between bond strength and surface free energy was unclear.

Plasma was shown to increase levels of oxygen at the surface and reduce/eliminate the concentration of fluorine at the surface on the bag side of the composite.

ACKNOWLEDGEMENTS

First of all I would like to express my gratitude to Brunel University (London), NSIRC (Cambridge) and TWI Ltd (Cambridge) for giving me the possibility to execute my studies in these prestigious centres. Thanks to my academic supervisor, Cristinel Mares (Senior Lecturer in the Aerospace Department of Brunel University), and my industrial supervisor, Ewen Kellar (TWI's Adhesive Bonding and Surface Preparation Consultant), for their support and guidance, and to my manager, Mihalis Kazilas, who has always believed in me.

I would like to thank also HEXCEL Composites Ltd, especially Matt Cleaver, for the supply of the materials, the use of their facilities and their kind support and help during my research.

I am highly indebted to my colleague David Williams for his guidance and support enabling me to have a better understanding of the research topic.

I would like to thank Helen Wickens, Jacob Greenwood, and Stuart Lewis for always helping me with a lovely smile.

I am heartily thankful to my flat mates, work mates and really good friends Karthik and Rashmi for all our moments together. With them, I have learnt what the real meaning of sharing is. I thank them for their kindness, for taking care of me and for their endless support.

Particular thanks to Emmanouela and Silvia for their love and interminable positivity, making me smile and for being full of energy whenever I see them.

I would like to give my special thanks to my lovely friends Marta and Antonio, who have been always there for me, making my days so special.

I want to offer my best regards and blessing to all those who supported me in any respect during the completion of my research. I would also like also to thank myself, for the hard work during the last years, and for always following my heart, for falling many times and always standing up stronger, for learning from my mistakes, and for trying to be a better person every day.

I am grateful to have Conchi, Tania, Ana, Irene, and Miriam in my life. Since childhood we have grown together, discovering the meaning of life and making the most of it. Thanks to all of them for extending their hands to catch me before I fall and if I fell, thank you for lifting me up.

Last but not least, I cannot finish without saying how grateful I am for my family. I wish to thank my mother, my sister and Lolito for their infinite love, support and encouragement throughout my whole life. I am what I am now because of them and for that, I love them so much. My special thanks go to my lovely father, who left us a few years ago to be in a better place. His brightness and smile guide me every day.

TABLE OF CONTENTS

ACRONYMS

AP	Atmospheric Pressure Plasma
BLT	Bond Line Thickness
BS	British Standard
CAP	Cold Atmospheric Pressure Plasma
CT	Computerised Tomography
EHS	Environmental Health & Safety
eV	Electron-volts
FRPs	Fibre Reinforced Polymers
GB	Grit Blasting
HOQ	House of Quality
ILSS	Interlaminar Shear Strenght
IPA	Isopropyl Alcohol
ISO	International Organization for Standardization
LSS	Lap Shear Strength
MA	Manual Abrasion
MEK	Methylethylketone
NDT	Non-Destructive Testing
PP	Peel Ply
PTFE	Polytetrafluoroethylene
QFD	Quality Function Deployment
SEM	Scanning Electron Microscope
UD	Unidirectional
XPS	X-ray photoelectron spectroscopy

LIST OF FIGURES

LIST OF TABLES

1 Introduction

1.1 Background

The necessity in automotive and aerospace industries to increase fuel efficiency is achievable by weight reduction. With the proper design, engineering polymers can offer greater properties than metals. Reinforced polymers are a type of composite material where the limitations of the polymer such as fatigue sensitivity, low strength and stiffness can be overcome by reinforcing it with fibres.

Fibre reinforced polymers (FRPs) have increasingly become attractive in recent decades for many applications in aerospace, automotive and marine industries due their superior specific strength (strength-to-weight ratio) and specific modulus (stiffness-to-weight ratio) compared to aluminium and steel [1, 2].

The fibres can be carbon, glass, aramid, basalt or polyethylene. Other lesser used fibres include wood or asbestos. The most common fibre reinforcements used in advanced composites applications, especially in aerospace, are carbon fibres. Glass fibres are commonly used for infrastructure and marine applications while aramid fibres are used in aerospace and military applications. In comparison to metals, FRPs are lighter and corrosion resistant.

Table 1 compares the strength and stiffness of these fibres against aluminium and steel.

Table 1 Properties of synthetic fibres; aluminium, steel and asbestos have been included for comparison [3]

Material	Density (g/cm^3)	Young's Modulus (GPa)	Tensile Strength (MPa)
Aluminium	2.70	69	77
Steel mild	7.86	210	460
Asbestos	2.56	160	3100
Carbon fibres (High Modulus)	1.86	380	2700
E-glass fibres	2.54	70	2200
Aramid fibres (Kevlar 49)	1.45	130	2900

Figure 1 shows the increasing use of composites in civil aircraft from the 80s to the present, where now more than 50% of the weight of both the A350 and 787 aircraft comes from composite material.

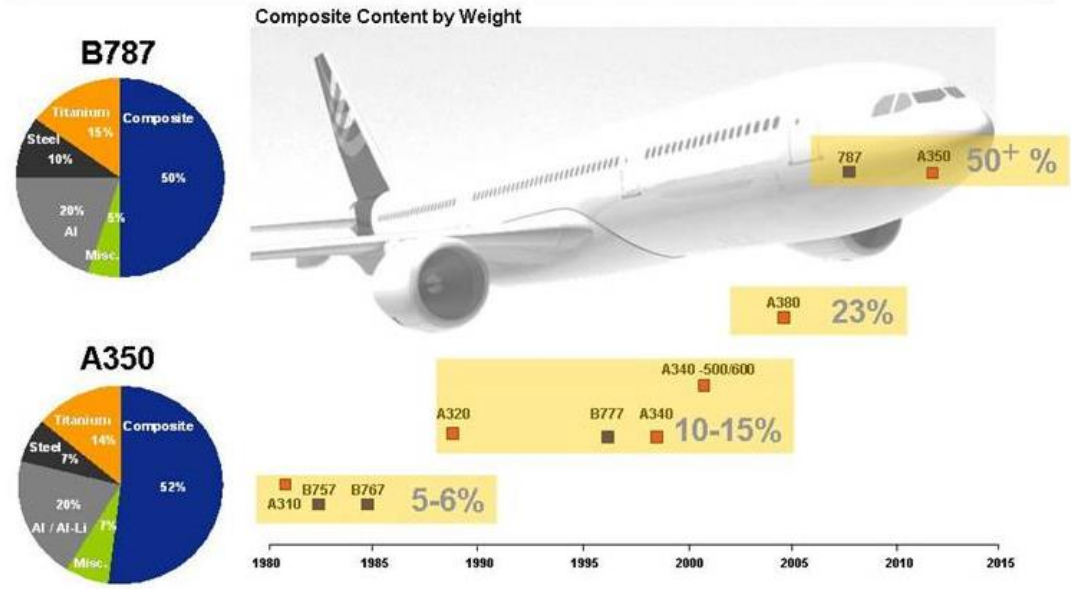

Figure 1 Commercial aerospace – composite penetration (courtesy of HEXCEL) [4].

Composite materials are formed by combining two or more materials in order to achieve properties that cannot be obtained using the original materials alone. These materials can be selected to achieve unique combinations of

stiffness, strength, weight, temperature resistance, corrosion resistance, hardness conductivity, etc. [5].

Although there are many types of composite materials, the following features can be distinguished within all of them:

- Reinforcement agent: a phase of discrete nature where its orientation is crucial to defining the mechanical properties of the material.
- Matrix: a continuous component which is responsible for the physical and chemical properties of the composite. It transmits load to the reinforcement agent. It also protects it and gives cohesion to the material.

Polymers can be divided into two categories: thermosets and thermoplastics. Thermoset polymers start as a liquid at low temperature but cure irreversibly with catalysis or heat by polymer cross-linking. This cross-linking transforms the material into a tightly bound three-dimensional network with high molecular weight. As these materials undergo an irreversible chemical change, they cannot be reformed or melted with the reintroduction of heat. Unlike thermoset polymers, thermoplastics can be re-melted and reformed with the reintroduction of heat, as there is no chemical bonding taking place during the curing process [6].

Joining of FRPs is an important step in the manufacturing of many composite structures, as simple parts can be joined together to produce complex components. In general, joining techniques can be categorized into mechanical fastening, adhesive bonding, and fusion bonding or welding.

Selecting the most suitable joining technique for a specific application requires careful consideration of different parameters, together with the knowledge of the service that the joint is expected to provide.

Adhesive bonding has been extensively used alongside mechanical fastening in the aerospace (in particular aircraft repair) and automotive industry, but not on its own in primary structures. The qualification of the adhesive bonding process (in terms of durability and bond strength) is still a concern that must

be investigated and solved before the aerospace authorities can allow the implementation of adhesive bonding in primary structures [7].

In secondary structures, adhesive bonding is common practice [8]. It offers the advantage of avoidance of stress concentrations and fibre cuts due to the introduction of fasteners. Adhesive bonding offers a continuous bond between the substrates, minimizes stress, and reduces the weight of the structure itself. Therefore, adhesive bonding is an excellent alternative to avoid the drawbacks coming from mechanical fastening and welding. Welding or fusion bonding is the process of joining materials (usually metals or thermoplastics) by melting the parts. Pressure and heat are necessary to produce the weld. Different energy sources can be employed to melt the parts either mechanically, electromagnetically or through external heat (hot gas, hot plate, extrusion, etc.). It is not possible to weld thermoset systems due to their interlocked chemical structure.

Mechanical fastening is a relatively fast and well established method. However, it can impose penalties in terms of mechanical integrity and weight, therefore the importance of adhesive bonding is significantly higher in the manufacturing of advanced composite structures.

The drawbacks of adhesive bonding when compared to welding and mechanical fastening are mainly the surface preparation of the components to be joined and also the cure time of the adhesive. In adhesive bonding, the parts to be joined are called adherents, and the joint is produced using an adhesive. Weak interfacial adhesion can lead to bond-line failure prior to the loads required to achieve cohesive failure within the adhesive.

Effective structural adhesive bonding relies on the creation of surfaces which are easily wetted by the adhesive and provide an appropriate topography and chemistry that promotes and maximises adhesion. These can be achieved through different surface pre-treatments prior to bonding the substrates.

1.2 Research need

The current methods for preparation of material surfaces prior to bonding are becoming progressively more constrained, due to environmental and health and safety (EHS) legislation. In addition, these pre-treatments use a considerable amount of time and energy. Therefore, there is a necessity for the industry to solve EHS issues and reduce overall process time.

The possibility of using dry, gas-phase processes (such as plasma) as a replacement for such pre-treatments could revolutionise many industries. Plasma pre-treatment offers significant cost and time savings, less energy consumption, application accuracy, no debris/dust generated during the process, and can be easily automated.

Many industry sectors (especially manufacturing and repair) have shown an interest in this technology, including aerospace, automotive and Formula 1, marine, and defence. Several companies are actively exploring plasma as an alternative to wet pre-treatments for titanium when bonding to carbon fibre reinforced polymers.

Plasma pre-treatment can offer the potential for the technology to be developed into a universal pre-treatment process.

1.3 Objectives

The main objective of this project is to analyse and evaluate the effect of plasma pre-treatment of the different surfaces of composite materials prior to adhesive bonding. These surfaces are the peel ply side of the composite and the side with no peel ply, called the bag side by industry.

This will be achieved by:

- Undertaking a detailed literature review to determine current state of the art.

- Carrying out a methodical study of the effects of different plasma parameters using both mechanical testing and analytical methods.
- Developing an understanding of the plasma technology for surface adhesion enhancement.

1.4 Contribution to knowledge

Benefits gained from this work are expected to be:

- A better understanding of plasma technology as there are different variable parameters involved during the process.
- Additional value to different market sectors interested in plasma pre-treatment such as aerospace, motorsports, medical, defence and electronics due to a lack of industrial awareness of this technology.
- The development of possible “recipes” to use the same technology for different substrates. These “recipes” could be used by the end users.

1.5 Scope of the thesis

The work of this thesis is presented in following order:

Chapter 1 Introduction

A description of the topic under investigation is presented with the main objectives of this study. Research need is also discussed followed by the contribution to knowledge of this work.

Chapter 2 Literature Review

This chapter discusses the current surface pre-treatments used by the aerospace industry. It focuses on the importance of replacing current methods with alternative ones that can reduce the dependence on current pre-treatments. Plasma pre-treatment is evaluated as an alternative to current

methods. A review of the current use of plasma pre-treatment for processing materials is also undertaken.

Chapter 3 Analysis of the Pre-treatments Discussed

This chapter analyses the different pre-treatments discussed in Chapter 2 to understand customer/industry needs or requirements, in order to choose the most appropriate pre-treatment.

Chapter 4 Methodology

This chapter describes the experimental methodology followed during this research, and materials and equipment used are listed. A detailed description of the different surface pre-treatments investigated is also provided.

Chapter 5 Results and Discussions

This chapter presents the data obtained for each pre-treated joint by the different methods investigated. It also discusses the most relevant data achieved during the investigation. An analysis of the results, in relation to the research questions, is given.

Chapter 6 Conclusions

This chapter summarises the findings of this investigation, highlighting the limitations of the material/technology under study.

At the end of the dissertation, different appendices are included showing the measurements of the samples and all experimental results from each joint tested.

2 Literature Review

There are several parameters which need to be considered for the assembly of components by adhesive bonding to ensure the reliability and the durability of the joint. Among these parameters, it will be necessary to select the most appropriate surface pre-treatment and adhesive, considering also the joint design. The performance of the joint will also be influenced by the chemical and physical properties of the substrate material.

For any adhesive to be successful during the bonding process, it has to wet the surface of the substrate. The capability of an adhesive to wet a solid surface can be quantified by the surface free energy of the substrate material. This concept will be discussed further in this thesis.

There are five main mechanisms for the adhesion between an adhesive and an adherent: mechanical interlocking, diffusion, electrostatic attraction, adsorption and chemisorption chemical bonding, and molecular forces and dipole interactions. These mechanisms can happen either alone or in combination to produce the adhesive bond [9].

Among the parameters under consideration, surface pre-treatment is the key factor to achieve strong and durable joints [10]. The work carried out by Matthews et al. [11] shows the importance of using the correct surface pre-treatment on the substrates before adhesive bonding or painting.

Therefore, surface pre-treatment during the joint assembly should be carefully carried out following the recommendations from the suppliers and industry. Best practice is covered in different standards (e.g. BS ISO 4588 or ASTM D2651 for surface preparation of metals and ISO 13895 or ASTM D2093 for plastics") [12]. These standards describe the usual procedures of surface preparation for metals/plastics adherents before adhesive bonding.

There is no specific standard available yet for the surface preparation of FRPs. However, some of the steps followed for surface pre-treatment of metals and polymers can be applied to FRPs. Subchapter 2.1 "Surface pre-treatments"

presents an overall overview of the different pre-treatments types used by the industry for FRPs.

2.1 Surface pre-treatments

Surface pre-treatments activate the surface of the adherents and this can lead to higher bond strengths. Through surface pre-treatments, surface free energy, surface roughness, and the chemical composition of the surfaces can be modified. Surface pre-treatments also prevent or remove contamination from the adherents. These concepts will be explained in more detail later on in this thesis.

Surface pre-treatments can be classified into five categories: cleaning, mechanical, chemical, energetic and use of priming or coupling agents. Selection of the most appropriate surface pre-treatment should be based on considerations such as cost, production, performance, compatibility, durability and EHS aspects.

Prior to any pre-treatment, cleaning is required, as it will remove the majority of contaminants (dust, oils, demoulding agents, etc.) from the surfaces of the substrates. This treatment is usually carried out using solvents, or through detergent wash and bonding cannot take place immediately as time is required for the volatiles to evaporate and/or the substrate to dry. The use of some chemicals for cleaning can give rise to environmental problems resulting in ongoing work to find effective replacements.

Methyl ethyl ketone, otherwise known as butanone or MEK, was commonly used as a solvent however, this solvent is toxic by all routes of exposure and many governmental regulations have now banned it, and less hazardous solvents have had to be considered [13]. Acetone and isopropyl alcohol (IPA) are now generally used for cleaning the substrates, offering fewer environmental issues than MEK.

The application of primers or coupling agents is usually the last step of the pre-treatment process. This final process will improve the pre-treated substrate by either creating a stable protective coating over the surface which is optimised for adhesive bonding (priming) or by enabling the pre-treated surface to be capable of directly reacting with the adhesive to form strong covalent bonds (coupling).

2.1.1 Mechanical pre-treatments

Current surface pre-treatments in the aerospace industry involve solvent cleaning, mechanical roughening, and peel ply removal (in the case of composites), either separately or in combination [14, 15].

Mechanical roughening techniques use abrasion to increase the roughness of the surfaces and remove contaminants from them.

Mechanical roughening includes manual abrasion and grit blasting. Manual abrasion is carried out using abrasive papers through rotary pads, followed by the cleaning of the composite structures using vacuum cleaning followed with a solvent wipe and then allowed to dry. Grit blasting is another form of mechanical abrasion, where a stream of abrasive material is expelled against a surface using compressed air to roughen the surface and remove contaminants.

Previous investigations on thermoset composites have shown that increasing the roughness of the surface by abrasion methods leads to mechanical interlocking, increasing the intrinsic adhesion, and therefore the strength of the assembly [16, 17]. However, the work carried out by Pocius and Wenz [18] determines that the critical factor for successful bonding is having contamination-free surfaces.

Abrasion methods are time-consuming, and generate debris and dust during the process (leading to health and safety issues). Another concern is inconsistency during surface preparation, as it depends on operator expertise,

giving variability during the process. Abrasion may also produce damage to the fibre matrix if not executed properly.

Peel ply is the other method broadly used for bonding the primary structures of the Boeing 787 and other commercial aircrafts [14]. Peel ply is a synthetic cloth (made from nylon or polyester), usually used during the manufacturing process of composite structures to prevent foreign materials from becoming integrated into the finished part [19]. Peel ply also textures the surface of composite laminates, reducing or eliminating the need for surface preparation, as shown in research carried out by Hollaway et al. [20] and Flinn et al. [21]. However, previous research has shown that stronger joints can be achieved using peel ply in combination with manual abrasion and cleaning of the surfaces prior to bonding [22].

When the composite part is cured, the peel ply can be peeled off just prior to bonding, achieving a consistent clean surface. After removing the peel ply, a solvent wipe is usually used to remove any possible contamination on the composite surface. However, it has been shown that fibres from the peel ply can be left behind during removal, and therefore can contaminate the bond area [23, 24].

One of the disadvantages of peel ply is that it can lead to damage of the underlying composite if the removal is not done properly. In addition, resin rich ridges can be found after the removal of the peel ply. These areas must be removed from the composite as they don’t have any reinforcing fibres in them, making these regions weaker and the resulting bond will not be so strong.

The fracture possibilities upon peel ply removal are shown in Figure 2.

Fracture possibilities upon peel ply removal

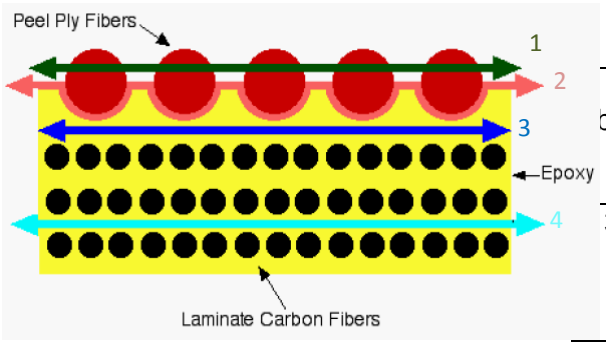

1. Green arrow: Peel ply fibre fracture (contamination of the composite surface)

2.Pink arrow: Interfacial fracture between the peel ply fabric and the epoxy matrix

3.Dark blue arrow: Fracture of the epoxy between the peel ply and carbon fibres

4.Turquoise arrow: Interlaminar failure (within the composite itself)

Figure 2 Fracture possibilities upon peel ply removal [21, 25].

The “dark blue arrow condition” shown in Figure 2 represents the fracture of the epoxy between the peel ply and carbon fibres. This will create a fresh and chemically active fractured resin surface, which will enhance the adhesion between the adhesive and the substrates [21, 26].

The main reason to use peel ply by the industry is to provide a clean roughened surface which is chemically (as it is a fresh resin surface) and physically (due to roughness) consistent, enhancing the adhesion between the adhesive and the substrates.

2.1.2 Chemical pre-treatments

Chemical treatments are quite versatile, as they can produce different surface finishes. They have been extensively used in industry, especially for painting and bonding of metals. Generally, these methods use strong acids or bases, which require specialist waste disposal and extensive rinsing with distilled water. Due to the hazardous nature of these substances, these treatments are becoming more tightly controlled, due to EHS legislation.

Chemical treatments are not used for surface pre-treatment of FRPs and therefore they will not be covered in this thesis.

2.1.3 Energetic pre-treatments

The other category of surface pre-treatments involves methods such as plasma, flame, laser, etc. These physical pre-treatments cause a change in the surface chemistry of the adherents, brought about by the interaction of highly energetic species with the adherent surface.

These energetic processes have the advantages of not requiring contact with the surface and by being dry.

Plasma is an excited gas containing molecules, free radicals, electrons, and ions. It is also called the fourth state of matter [27]. The four common states or phases of matter in the Universe (solid, liquid, gas and plasma) are illustrated in Figure 3.

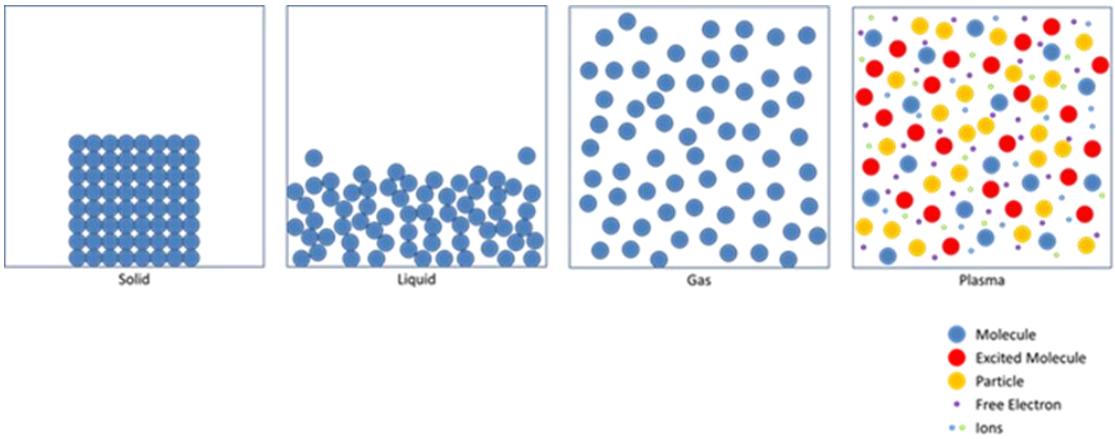

Figure 3 States of matter.

Plasma can be generated by heating a gas, or exposing it to a strong electromagnetic field. The latter can be achieved with a laser or microwave generator.

By applying an electromagnetic field electric field to a gas, the electrons transform the energy of the field into kinetic energy. If an electron has enough energy, it will not just bounce off an atom; it can disturb the electrons orbiting the atom and inelastic collisions can occur. This will produce the ionisation of neutral species and the generation of free electrons that will have the ability to conduct electricity. In the ionisation process, atoms or molecules obtain a positive or negative charge (by gaining or losing electrons) to form ions [28, 29].

Plasmas can be classified as either thermal (hot plasmas) or non-thermal (cold plasmas). Thermal plasmas are nearly fully ionised and they are characterized by an equilibrium (or near equality) among the temperature of the electrons (T_e), ions (T_i) and neutral species (T_n) (i.e., $T_e \approx T_i \approx T_n$) [28]. Temperatures of several thousand degrees are not unusual in hot plasmas. These plasmas are not suitable for most materials processing applications due their destructive nature. They are usually used in waste treatment and sintering. High temperature flames are an example of hot plasma [30].

The other possibility is that only a small fraction of the gas molecules a

re ionised (only 1-10%, the rest of the gas remains as neutral atoms or molecules). In this case, the plasma is classified as non-thermal plasma or cold plasma. Ions and neutral species are at much lower temperature than the electrons ($T_{e>>}T_i \approx T_n$). Due the large temperature values, it is more convenient to express the temperature in electron-volts (eV). Electrons can reach temperatures of 1-10 eV (1 eV = 11,600K). The temperature of the ions and the neutral species vary between 323 and 573K, much lower compared to the temperature of the electrons. This difference in temperature makes possible the creation of chemical reactions at relatively low temperatures. An example of cold plasma is the Aurora Borealis [28]. The low temperatures typical of non-thermal plasmas make them suitable for material processing applications.

In fact, cold plasma technology has been used since the late 1960s by the electronics industry for the deposition of thin film materials and for plasma etching of semiconductors, metals, and polymers [31].

The use of plasma treatment for processing of materials is quite broad. Apart from deposition of thin films, it is also used for sterilisation, where pathogens are chemically destroyed, and also for decontamination of chemical and biological weapons.

Different physical processes can be observed on the substrates pre-treated through plasma prior to bonding. These processes involve surface cleaning (removal of contaminants from the substrates) and ablation/etching of material from the surface (removal of weak boundary layers). These weak boundary layers could be formed during component manufacturing and must be removed to improve the adhesion. The difference between ablation and etching lies in the amount of material that is removed during the treatment. Ablation implies cleaning by removing of low molecular weight organic contaminants; and etching affects the surface morphology of the substrate [14].

The other two physical processes that are possible during plasma pre-treatment are the chemical modification of the surfaces (surface activation), and crosslinking. Regarding surface activation, plasma creates reactive polar functional groups at the surface which can intensely increase the surface free energy of the substrate, improving the wettability of the substrate by the adhesive and thus enhancing the adhesion. Surface free energy is a parameter used to quantify the wettability of a solid surface. Through surface pre-treatments the surface energy of the materials can be modified; and therefore the strength of the joint can be enhanced. Surface free energy can be measured using a contact angle analyser, which measures surface energies by measuring the contact angles of different liquids. Figure 4 shows the three possible scenarios.

If the contact angle formed by a liquid when placed in contact with a solid surface is higher than 90°, the surfaces are called hydrophobic, and they present a low surface free energy. These surfaces will be characterised by poor wetting and therefore poor adhesiveness (Figure 4a). If the contact angle is below 90° the surfaces are hydrophilic. They possess higher surface energy, providing better wetting and therefore better adhesiveness [32, 33] (Figure

4b). Figure 4c shows the ideal situation where the adhesive completely wets the surface (spreading).

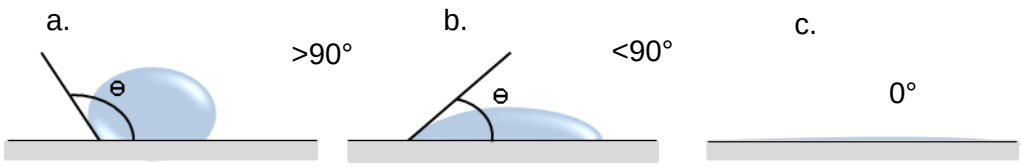

Figure 4 a. hydrophobic surface; **b.** hydrophilic surface; **c.** adhesive completely wets the surface.

As mentioned before, the ability of the adherents to be bonded depends on their chemical and physical properties. For example, adhesive joining of some thermoplastics (e.g. polyolefins, fluorohydrocarbons) is more challenging than for thermosets, due to their low surface energy [32, 34].

Through plasma, possible oxidation and nitrogenation of the substrates will occur. These two processes will produce chemical changes on the surface of the substrate potentially creating polar moieties such as ether, carboxyl, hydroxyl, carbonyl, imine, amine, etc. Such groups are capable of interacting with the applied adhesive enhancing adhesion.

Depending on the substrate material and the application, other gases can be used during the plasma process. For example plasma can be used for surface fluorination to create hydrophobic surfaces (eg waterproof textiles) [31].

The other detectable physical process during plasma pre-treatment is crosslinking. Exposing surfaces to noble gas plasma (such as He or Ar) produces the creation of new free radicals. These free radicals (uncharged molecules) are very unstable and hence highly reactive. Therefore, the free radicals can react with other free radicals or with other chains in chain-transfer reactions to gain stability. As a result, through crosslinking the surface of the adherents may become cross-linked, preventing the creation of weak boundary layers [31].

Current plasma technology available

Plasma pre-treatment of different materials can be executed at low pressure and at atmospheric pressure. One of the drawbacks of low pressure plasma systems is that the substrates to be treated must be placed inside a vacuum chamber, which limits the size of the components, and they cannot be treated in a continuous process, as pre-treatment of batches is then only option. Another disadvantage is that the power consumption required is quite high, and this makes the process relatively expensive.

In low pressure plasma technology, the plasma is generated using a high frequency generator. This technology is highly controllable in terms of gas/plasma composition, power, duration of the treatment, etc. When the process is complete and the chamber is back to atmospheric pressure, the door can be opened and the samples removed from the chamber.

Unlike low pressure plasma systems, atmospheric pressure plasmas (AP) can treat substrates in a continuous way at high speed, achieving processing cost savings [35]. AP has the potential to be automated with relatively low power consumption.

In AP technology, the plasma is generated with a high tension generator. The gas used to generate the plasma can come from different sources. It is a less controllable system than low pressure plasma technology. Figure 5 shows the main components of the AP system used in this research.

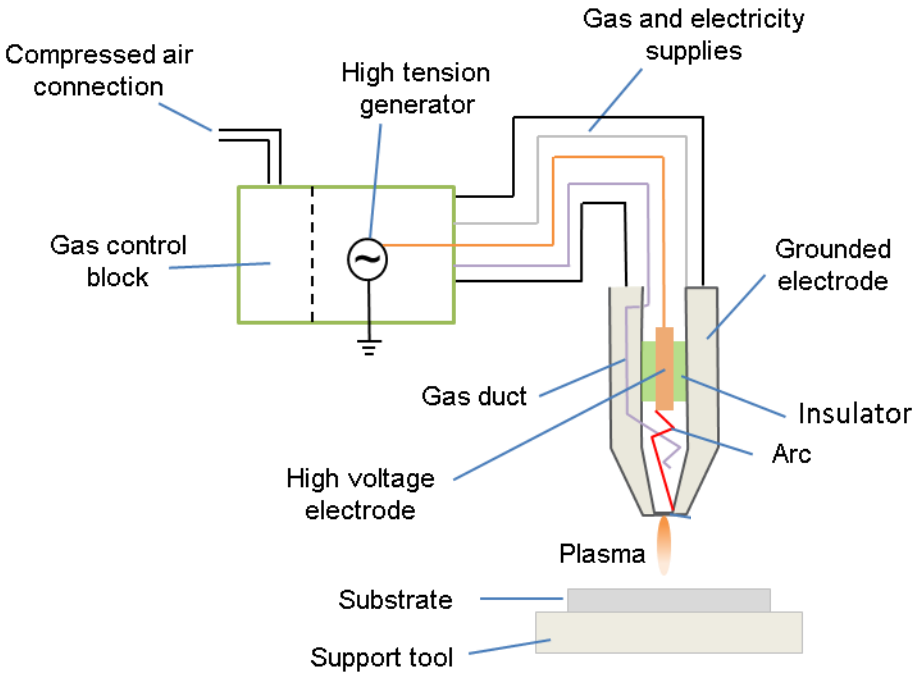

Figure 5 Components of an atmospheric pressure plasma system.

AP systems are quite versatile, as it is possible to integrate into them several non-rotating plasma jets. Rotating nozzles can also be incorporated into AP jet systems. Rotating nozzles can treat a large area of material in a single pass with less treatment intensity than static nozzles [36].

AP pre-treatment prior to structural bonding has shown promising results. This technology is already installed in some automated industrial process [37]. However, more research needs to be carried out in order for it to be implemented into production in the aerospace industry [15].

AP has been investigated in different materials under controlled process conditions, demonstrating an improvement of the adhesive bonding strength on polymers [38-41], and composites [42-46].

The work carried out by Zaldivar et al. [45] compared different pre-treatments on a cyanate ester composite. Lap shear strength values indicated an increase of 30% for the bond strength, compared with solvent wiping, peel ply and

plasma (Helium plus O_2) vs manual abrasion. The relative bond strength improvement of these pre-treatments is shown in Figure 6.

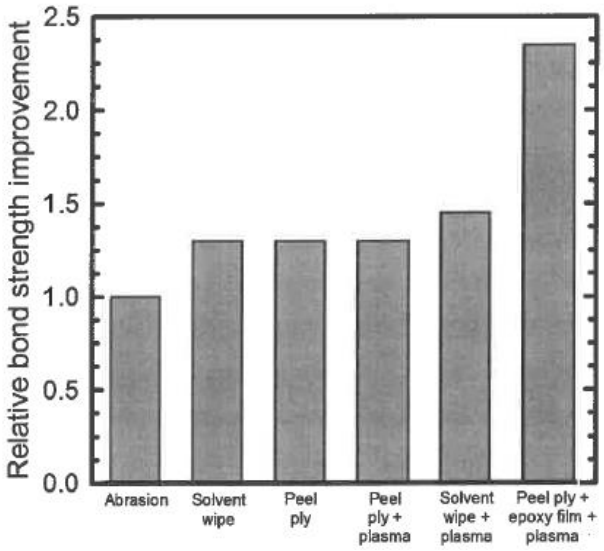

Figure 6 Relative bond strength improvement of a cyanate ester composite bonded with a room temperature cured adhesive [45].

Compared to polymers and composites, less work has been done for metals (Al, Ti, steel, etc.). Williams [29] studied the surface modification by AP of different materials (stainless steel 410, aluminium alloy 2024, and carbon fibre epoxy) achieving an improvement in the lap shear strength of the bonds.

Figure 7 shows lap shear strength values of bonded 410 stainless steel using different surface pre-treatments**.**

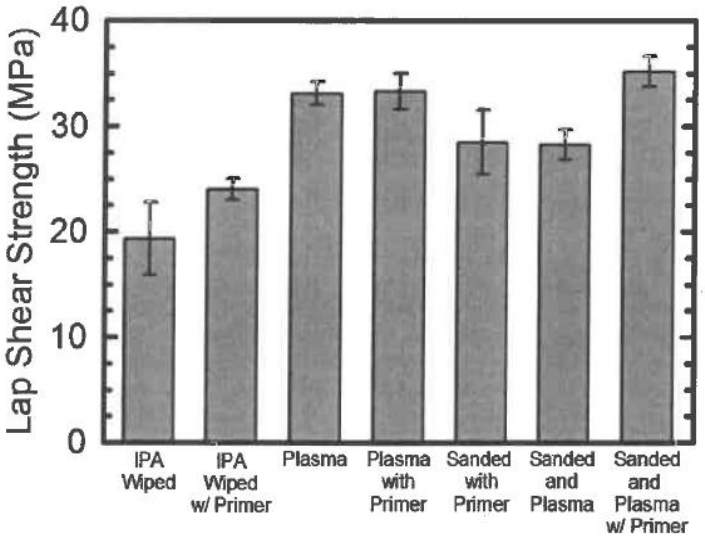

Figure 7 Lap shear strength values of bonded 410 stainless steel of different surface pre-treatments [29].

Figure 7 confirms that plasma treatment increases the bond strength to its maximum value. A value of 24±1MPa was achieved by cleaning the samples with IPA (using primer), compared with the 35±1MPa obtained treating the samples through manual abrasion and plasma activation (also using primer).

Different parameters will influence the plasma process. Among these parameters, it is important to highlight duration (speed of process and number of passes), power, flow rate of gas (combination of gases), and distance treatment. For each application and each substrate, these parameters need to be defined as the interaction between the plasma, and the surface depends intensely on the material properties [36].

The research carried out by Baghery et al. [47] of unsized carbon fibres using low pressure plasma shows the effects of different plasma process parameters (power, duration, and flow rate of oxygen gas) on the interfacial adhesion behaviour between the fibres and the resin. It could be, though, that longer treatment will improve the adhesion between the fibres and the matrix. However, it is shown in the investigation by Baghery that long exposure

treatment times decrease the bulk properties of carbon fibres, and therefore the interlaminar shear strength (ILSS) of treated fibre composites. The same effect was observed using high values of power.

The same effect can be observed in the investigation by Palleiro et al. [36]. High values of power showed degradation of the polymer surface leading to lower strenght of the joint. This indicated an overtreatment of the material.

Therefore, it is important to find out the processing window for each type of material treated. Processing window means the combination of the parameters involved in the plasma process, which improve the adhesion behaviour instead of damaging the materials and therefore reducing their properties.

There are different atmospheric plasma sources which can be classified depending on the excitation mode. Different groups can be listed [48, 49]:

- Direct current and low frequency discharges (1kHz-100kHz). Some examples within this group are corona discharge and dielectric barrier discharge.
- Radio frequency discharges: these operate in the frequency range of 1-100MHz.
- Microwave discharges: in this case, typical frequency is 2.45GHz.

Another energetic pre-treatment that oxidises the substrates is flame. This process consists of passing a flame over the surface. This will create polar groups at the surface, which will enhance the wettability of the adhesive, and therefore the strength of the bond. Flame temperature, and the distance between the adherent and the flame, should be carefully chosen [50].

Other types of surface pre-treatments are ultraviolet, laser, ion beams, and X-ray. These treatments are defined as closed systems, as the material under treatment has to be placed inside a chamber [34, 51].

2.2 Adhesive selection

The selection of the most appropriate adhesive for a specific application is another important parameter to consider in the bonding process. This task can be challenging due to the very wide range of commercial products available. However, the choice can be simplified by considering simple rules such as knowing which family of adhesives meet the requirements of the assembly. Figure 8 lists some of the parameters which need to be considered during the selection process of the most suitable adhesive.

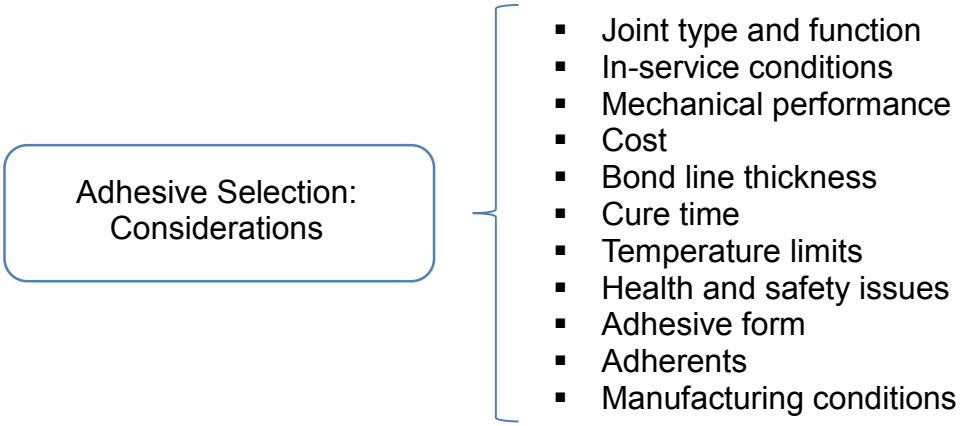

Figure 8 Adhesive selection: considerations.

Depending on the overall functionality of the assembly the selection of the adhesive will be completely different. For structural purposes, the selection will be made between thermosetting adhesives (e.g. acrylates, epoxies, and polyurethanes).

Epoxy adhesives are widely used in aerospace and other industries due to their excellent mechanical performance [52]. These materials have high strength, chemical resistance, and low shrinkage. Therefore, they form strong and durable bonds with most materials in well-designed joints. The form in which epoxy adhesives are available varies widely, from low viscosity liquids to solid pastes and films. Film adhesives are preferred for high precision engineering applications. These films can be cut into desired shapes.

Within the same chemical family there are often a number of different formulations and forms available from each supplier which can make the

selection process even more difficult. However, using the rules cited above in addition to different sources of assistance (suppliers, consultants, and software selection systems) can help to reduce the effort of choosing the most suitable adhesive.

One important parameter that will affect the strength of the final joint is the adhesive bond line thickness (BLT). A very thin BLT will create weak bonds and lead to premature failure, as there is not sufficient adhesive in the bond line to perform properly in demanding situations. Thin BLT will create poor wetted areas. Ideally the surface of the adherents should be fully wetted by the adhesive to achieve maximum strength of the joint.

The opposite scenario is to have very thick BLT. Thick BLT will cause offset loads and high stress concentration at the edges of the joints reducing the strength of the bond. This thick BLT will create an “extra” layer of material within the joint which is not desirable.

Depending on the type of adhesive, the BLT can vary significantly. For example, the BLT for epoxies varies between 50-300μm, for acrylics between 100-500μm, and for polyurethanes between 500-5000μm [53]. Adhesive suppliers can guide the end user in this area.

Adhesives should be applied in the proper controlled thickness. There are different ways to control the BLT of the adhesive. Glass beads, carrier films, wires, fillers, etc. can be added to the adhesive for this purpose. Other possibilities include tooling modification, adding external shims, considering joint design, etc. For example, some of the film adhesives have a carrier material incorporated in them, which offers a highly controlled bond-line thickness [53].

Another important parameter to consider is the type of defects in the adhesive layer. Voids can appear due to volatiles in the adhesive or air entrapment. Incorrect curing can be caused due incorrect mixing of the adhesive or contaminants. In some cases it is possible to observe cracks in the adhesive

layer due thermal shrinkage or curing. These defects could have an impact in the final strength of the joint.

In order to detect these defects at the bond line, different non-destructive methods can be used, such as ultrasound or computerised tomography (CT) scans.

2.3 Joint design

As cited before, one of the advantages of adhesive bonding is the better distribution of the stresses through the joint. The loading modes experienced by adhesive joints can be compression, shear, peel, cleavage, and tension. Adhesive bonded joints can experience several of these loading modes at the same time.

Adhesives should preferably be loaded in compression or shear as bonded joints are strongest under these loading modes. Peel, tension and cleavage forces must be avoided or minimised as these stresses are too severe for FRPs [54]. This can be achieved by applying the principles of well-designed joints [53].

Among the loads cited above to which the assembly is submitted, shear loading is the desirable mode. Therefore, the joint will be designed to be mostly restricted in the shear direction [52]. Single lap shear joints will be considered in this research as they are the simplest joint geometry where the shear stresses are achieved by traction on the two substrates, as shown in Figure 9. In this type of joint geometry, peel stresses will still appear.

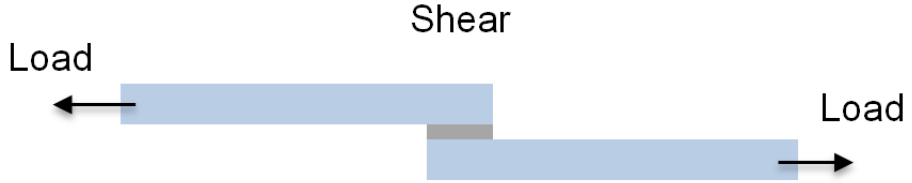

Figure 9 Single lap shear joint design.

In single lap joints, initial loading is carried in shear along the line of the bonded adherents. As load increases, peel forces start appearing at the ends of the overlap of the joint. In addition to this, tensile loads become important across the joint and failure can occur due to [55]:

- Failure of the adhesive - *cohesive failure*.
- Failure at the interface between the adhesive and the adherent - *adhesive failure.*
- Failure of one of the adherents - *parent material failure*.

The failure modes and the relation to bond strength are shown in Figure 10.

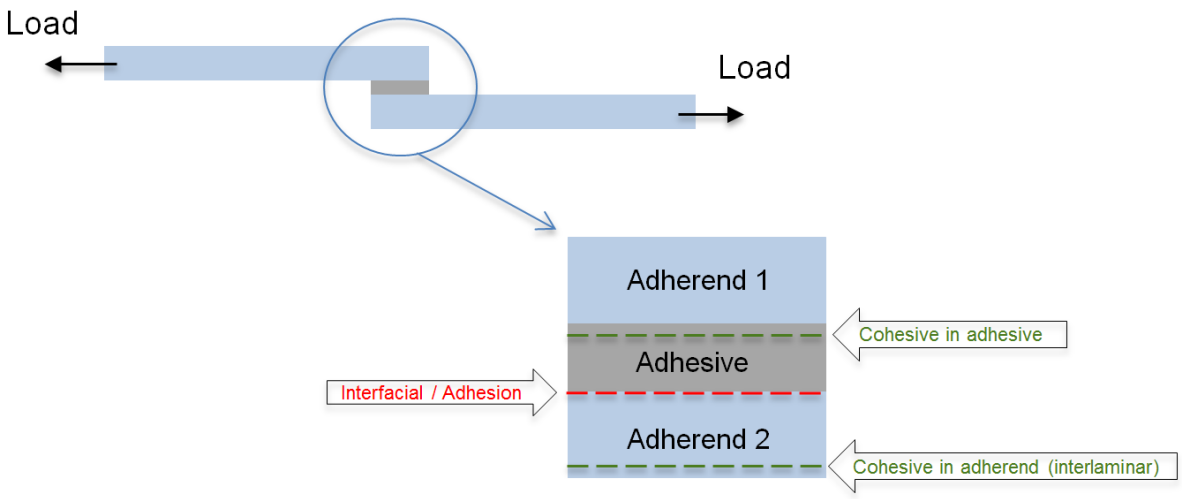

Figure 10 Failure modes for adhesive bonding.

Adhesive failure is the failure of the adhesive at the surface of one of the joined adherents (red line in Figure 10). It is considered to be the result of a weak bond and must be avoided (it is unacceptable by the aerospace industry). This type of failure can occur due to an inadequate or poor surface preparation or material mismatch [56].

Cohesive failure can occur either in the adhesive or in the adherents. Cohesive failure in the adhesive (top green line in Figure 10) happens when the load

exceeds the adhesive strength, providing a bond as strong as the adhesive itself. This type of failure can occur due to an inappropriate design or void content. Cohesive failure in the adherent (also called parent material failure or interlaminar failure in the case of composites, bottom green line in Figure 10) provides a bond as strong as the laminate itself.

Cohesive failure (either in the adhesive or in the adherent) is the acceptable type of failure for adhesive bonds [57].

In some cases, cohesive and adhesive failure can happen in the same bond.

As mentioned previously, failure along the adhesive and composite interface must be avoided, achieving cohesive failures of the joint. For example, Williams et al. [58] pre-treated steel samples through plasma and it was observed that cohesive failure of the treated samples increased to be 97% of the failure surface compared to 30% achieved for untreated samples.

The quality of the joints can be evaluated through mechanical testing (destructive methods) and non-destructive testing (NDT). Likewise, study of the fracture surface of the specimens through fractography (also visually) will provide a better understanding of the different failure modes. Standard BS ISO 10365 [59] describes the main type of failure patterns of bonded assemblies (regardless of the nature of the adherents and adhesive of the assembly).

Summary of literature review

This chapter has reviewed the different parameters involved during the adhesive bonding process, highlighting the importance of surface pre-treatments prior to bonding to achieve successful and durable joints.

Different aspects must be considered before creating adhesive bonds. The following diagram illustrates some of these important aspects:

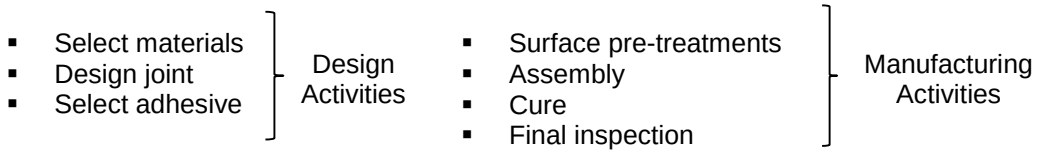

An assessment of the different surface pre-treatments used by the industry for FRPs has been conducted and a comparison of these methods has been carried out emphasizing the advantages and disadvantages of each one. The capability of the adherents to be bonded depends on their chemical and physical properties. Plasma pre-treatment has been shown to have the potential to replace conventional methods used in the aerospace industry as this method can create new chemical functionalities which are capable of interacting with the adhesives added to the substrates, thus enhancing the adhesion.

3 Considerations upon the technology requirements using QFD analysis

In this chapter, a Quality Function Deployment (QFD) analysis of the pre-treatments discussed in Chapter 2 was carried out. QFD is a useful tool that defines customer/industry needs or requirements which can then be translated into specific plans to produce products or develop technologies.

Through this tool a common understanding of the customer/industry needs is promoted and therefore a more reliable decision can be taken. The use of QFD tool can produce improvement in respect to cost, quality and development time.

Technologies and customer needs are rapidly changing. The QFD charts are ideal to reflect new facts and market conditions [60].

As previously discussed, the aim of this project is to investigate the possibility of replacing current methods for preparation of material surfaces prior to bonding. Therefore, an industrial analysis of the current pre-treatments was carried out in Chapter 2 to evaluate the existing methods and consider alternatives.

The aerospace industry uses peel ply, in combination with either manual abrasion or grit blasting, for the pre-treatment of composite surfaces prior to bonding. These two methods are both time and energy consuming and therefore, there is a necessity for industry to find pre-treatments that can be easily automated to reduce overall process time and increase efficiency. In addition, it is important to highlight that manual abrasion and grit blasting cause debris and dust to be generated, resulting in EHS issues. These processes may also damage the fibres if they are not executed properly, and they are highly dependent on the expertise of the operator.

Energetic pre-treatments, such as flame and plasma, were also evaluated. The flame method was dismissed, due to the high temperatures involved in the process, which would lead to the degradation of the material under study

(matrix of the composite). Plasma pre-treatment appears as a promising technique, as it offers cost and time savings, and no debris or dust is generated during operation. Plasma provides consistency, as it does not depend on the expertise of the operator and it has the potential to replace the chemical pre-treatments used for metals. This will be extremely interesting for joining hybrid materials (e.g. titanium to carbon fibre reinforced polymers).

Ultraviolet, laser, and x-ray pre-treatments were also considered however, the power consumption of these treatments is relatively high, making the processes quite expensive.

QFD analysis

QFD analysis was carried out by taking into account different criteria that a surface pre-treatment may be required to meet. From an industrial point of view, the preferred pre-treatment will be the one which reduces processing time and energy consumption. As the geometry of industrial components is becoming more complex, the favoured pre-treatment should possess the potential for industrialisation, making the operation relatively straightforward and consistent. Consistency during industrial operations is essential for reliable performance of the final component. The performance will also be affected by the selected process parameters. Choosing the incorrect parameters could lead to damage to the substrates, and therefore affect the strength of the final assembly. As already mentioned, current methods are becoming more constrained, due to EHS issues, and the selected process should be environmentally and operationally friendly.

The different criteria analysed during the QFD analysis are collated in Table 2 (processing time, cost, potential for industrialisation, process variability, EHS issues, and damage material).

Table 2 represents the interrelationship analysis that compares criteria against each other, in order to rank them in terms of importance in the industrialisation of a surface pre-treatment.

The rating system selected to compare criteria was 1:3:9, where 1 is “important”, 3 is “more important” and 9 is “much more important” [61]. The ranking for each of the criteria is calculated by dividing the raw total (rating scores added for each raw) by the grand total.

According to the ranking obtained in Table 2, “damage material” is the highest ranked criterion. The selected surface pre-treatment must be completely reliable, without damaging the material under treatment, as this will affect the final performance of the joint. Process variability is ranked second. For the implementation of an industrial process, it is important to achieve consistency in results to guarantee the success of the final product.

The third ranked criterion, EHS issues, is related to the importance of implementing pre-treatments that are friendly to the environment, and not harmful for the operators. Manufacturers are trying to be eco-friendly, which is the reason why this criterion ranked as more important than cost. Customers interested in this type of friendly pre-treatment are not afraid to invest in these technologies, which is why cost was understandably the lowest ranked.

From Table 2, it can be observed that the preferred pre-treatment that met most of the variables included in this analysis was plasma (cost and time savings, no debris or dust generated, potential for industrialisation, consistency). Different parameters will influence the plasma process. Among them, it is important to highlight the speed of the process, the number of times that the surface is pre-treated (number of passes), power, flow rate of gas, the types of gas, and distance treatment.

Table 2 Interrelationships analysis: criterion vs criterion

	Cost	Damage material	Process variability	Potential for industrialisation	EHS issues	Process time	Raw total	Relative	Ranking
Cost		1/9	1/3	1/3	1/3	1	2.11	0.041	6
Damage material	9		1	3	1	3	17.0	0.332	1
Process variability	3	1		1	3	3	11.0	0.215	2
Potential for industrialisation	3	1	1		1/3	3	8.33	0.163	4
EHS issues	3	1	1/3	3		3	10.33	0.202	3
Process time	1	1/3	1/3	1/3	1/3		2.33	0.045	5
						Grand total	51.1		

1/9 much less important
1/3 less important
1 important
3 more important
9 much more important

Table 3 Decision matrix (ranking parameters)

Pre-treatment parameters / Industry requirements	Weight	Type of gas		Gas flow		Number passes		Distance		Speed		Power	
		R	W	R	W	R	W	R	W	R	W	R	W
Damage material	0.332	1	0.332	3	0.996	3	0.996	1	0.332	1	0.332	3	0.996
Process variability	0.215	1	0.215	3	0.645	1	0.215	3	0.645	3	0.645	3	0.645
EHS issues	0.202	3	0.606	1	0.202	1	0.202	1	0.202	1	0.202	1	0.202
Potential for industrialisation	0.163	1	0.163	1	0.163	1	0.163	1	0.163	1	0.163	1	0.163
Process time	0.045	1	0.045	3	0.135	9	0.405	1	0.045	9	0.405	1	0.045
Cost	0.041	9	0.369	3	0.123	3	0.123	1	0.041	3	0.123	3	0.123
Total	1		1.730		2.264		2.104		1.428		1.87		2.174

R= Ranked, W= Weighted

Table 3 shows the decision matrix which maps the criteria assessed in Table 2 against the different parameters involved in the plasma pre-treatment. This matrix is a diagram which helps in determining how a product or technology meets the customer or industry needs. It is an important step in the pre-design phase, as this will reveal which aspects should be worked on more than others through numerical representation.

Figure 11 shows the rankings of each engineering characteristic with their respective weighting (taken from Table 3). Glass flow, power, and number of passes are the top three among the engineering characteristics described in Table 3.

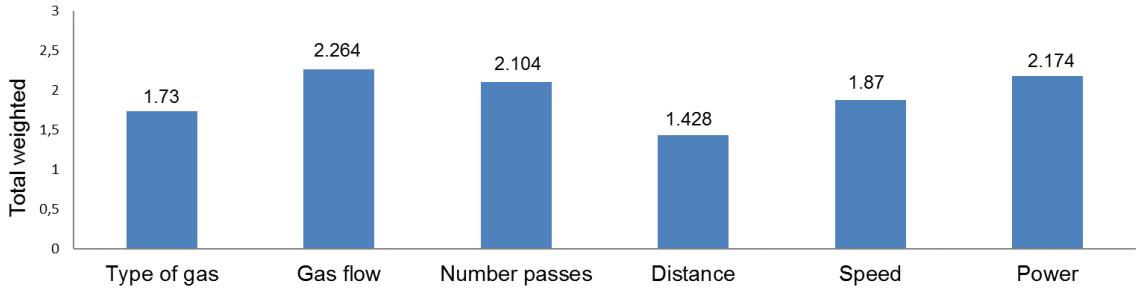

Figure 11 Rankings of each engineering characteristic with their respective weightings.

The description of the plasma equipment used during this research is explained in Chapter 4 (Section 4.3.4). The gas flow and the power used will be fixed at the maximum capacity of the equipment. The number of passes and the speed of the process will be modified during the research in order to evaluate the influence of these two process parameters, while the distance will be fixed at a constant value.

Different type of gasses can be used during the pre-treatment (argon, helium, fluorine, etc). The control unit available can use either argon or helium. Argon will be used as the primary gas instead of helium (argon is cheaper than helium).

4 Methodology

4.1 Materials

4.1.1 Adherents

The material used in this research was an epoxy resin, reinforced with carbon fibres. This material was supplied by HEXCEL Composites, Duxford (Cambridge, UK), in the form of prepreg.

Prepregs consist of a combination of a matrix (resin) and fibre reinforcement. They are ready to use in the component manufacturing process. Prepregs need to be stored at -18°C to hinder the curing of the resin [62]. The resin cures at high temperature, undergoing a chemical reaction that transforms the prepreg into a solid structural material that is exceptionally stiff, lightweight, temperature resistant, and highly durable.

Prepregs are available in two forms: unidirectional (UD) or woven fabric. In UD form, the fibres run in only one direction. Unlike UD fabrics, woven fabrics consist of at least two threads which are woven together (the warp and the weft direction). Performance and cost are the two main factors that influence the selection of the prepreg.

A UD prepreg was selected for this research, as it presents a stronger mechanical performance in the direction of the fibres compared with that of woven fabrics. Unlike woven fabrics, fibres in UD preform do not have a crimp (i.e. they are straight).

The specific material chosen was HexPly8552, a certified high performance, tough epoxy matrix used in primary aerospace structures. Table 4 provides the information for this prepreg.

Table 4 HexPly 8552 prepreg [63]

Product Description	Reinforcement	Matrix	Form	Volume Fibre (%)
HexPly8552	Carbon Fibres	Epoxy	UD Prepreg	58
Characteristics HexPly 8552	-Excellent mechanical properties -Elevated temperature performance, service temperature (121°C)			

4.1.2 Adhesives

The family of adhesive chosen was epoxy, as they are widely used in the aerospace industry due their excellent mechanical properties. They also present excellent wetting properties [58].

From the different epoxy adhesives available on the market, Redux 312 was selected. Redux 312 is a high strength 120°C curing film adhesive, suitable for metal to metal bonding, sandwich constructions and composite to composite bonding. Some versions (such as Redux 312/5) are supported with a woven nylon carrier for bond line thickness control purposes. Redux 312 was supplied by HEXCEL.

Table 5 Film adhesive Redux 312 [64]

Product Description	Form	Cure cycle	Characteristics
Redux 312	Film adhesive without carrier	30 minutes at 120°C	- Good mechanical performance up to 100°C - Low volatile content

4.1.3 Glass beads

A pinch of ballotini beads (glass beads) were added on top of the adhesive film Redux 312 (version without carrier) for bond line thickness control. The material was purchased from Sigma Life Sciences with a diameter range of 212-300µm [65].

4.2 Manufacturing composite laminates

Five prepreg laminates were manufactured at HEXCEL using an autoclave (four laminates of nominal size 600 x 600mm and a smaller laminate of 620 x 300mm). Each laminate had 16 layers of carbon fibre/epoxy with a final thickness of approximately 3mm.

The first step of the manufacturing process was to remove the prepreg from the freezer while it was still in the sealed bag. Once the prepreg reached room temperature, it was ready to be used.

Afterwards, 80 layers of HexPly8552 were cut. In order to manufacture one laminate, 16 plies were stacked. However, this was carried out first by stacking four plies, and then debulking them for five minutes under vacuum (pressure conditions: 0.95-1bar).

Debulking is an important step during the manufacturing process of composite parts. The objective is to compact or squeeze the air out from among plies, ensuring the seating of the plies on the tool and preventing wrinkles.

Another four plies were placed on top of the previous four plies, debulked again. The same procedure was applied until 16 plies were stacked. It was extremely important that each additional ply had full contact with the previous ply, avoiding gaps among plies. Finally, the whole laminate (16 plies) was debulked for five minutes.

After the plies of the five laminates were stacked together, the next step was the vacuum bagging of the laminates before their cure in the autoclave.

Vacuum bagging plays a significant role in the manufacturing of composite components. This process allows the application of compaction pressure to consolidate plies, as well as the extraction of moisture and volatiles from curing composites.

In order to achieve high quality composite components, great care must be taken when using different sequencing materials during the vacuum bagging

stage. The prepregs and vacuum bagging materials were placed on top of a flat aluminium tool and the first layer added was a polytetrafluoroethylene (PTFE) film. It was used as a release film to prevent the prepregs from adhering onto the mould surface during the curing phase. The next layer added was a peel ply of polyester. This peel ply was used to texture the surface of the composite laminates. The next step was to place the uncured laminates on top of the peel ply. Glass tape was added along the edges of the prepregs in order to create a continuous air path, followed by the addition of another layer of release film. Several glass fibre filaments were used to create a path for the air to be expelled. In addition, two layers of glass fibre cloth were added to release the air, as well as two layers of breather. These last two layers were used to keep a “breather” path through the bag to the vacuum source. This allowed the air and volatiles to escape, so that continuous pressure could be applied to the laminates.

Finally, the bag film was sealed at the edges of the aluminium tool. Three vacuum valves were located above the tool’s surface. A piece of breather was added between the valves and the tool in order to provide breather continuity. A leak test was carried out using a vacuum gauge to detect if there were any leaks.

The peel ply used to texture the surface of the composite laminates was a specific product from HEXCEL. The fibre type was polyester with a maximum use temperature of 204°C and a thickness of 0.101mm (dry peel ply).

Figure 12 shows the materials sequence during the vacuum bagging.

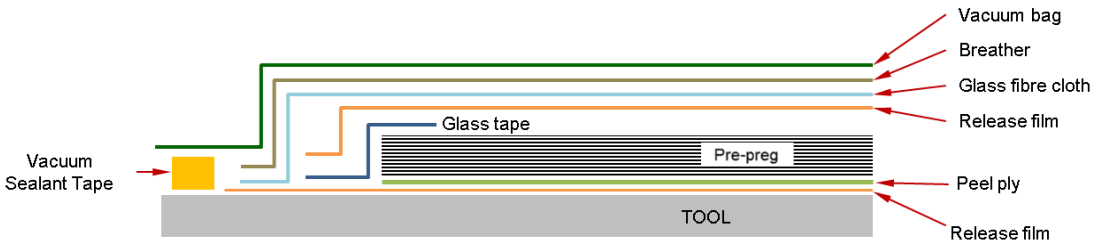

Figure 12 Schematic of the vacuum bagging.

At this point, the prepregs were ready to be cured in the autoclave. During the curing, two thermocouples were used to check the temperature.

Table 6 summarises the steps followed during the manufacturing of the composite laminates.

Table 6 Manufacturing composite laminates

#	Step	Description
1	Removing material from the freezer	Material could be used when room temperature was reached
2	Cutting material	80 plies were needed to manufacture 5 laminates
3	Piling plies up	- Debulking for 5 minutes after every 4 plies - Once 16 plies were piled up, debulking the whole laminate for another 5 minutes
4	Vacuum bagging and leak test	→ Sequence vacuum bagging: - PTFE film - Peel ply - Prepregs - Glass tape - Release film and glass fibre filaments - Glass fibre cloth - Breather - Bagging film and sealant tape → Leak test
5	Prepregs ready for autoclave	Check Table 7 for processing conditions

The temperature, pressure and vacuum profiles in the autoclave are shown in Table 7.

Table 7 Temperature, pressure and vacuum profiles autoclave

Temperature Profile				Pressure Profile				Vacuum Profile			
SP Type	**Ramp Rate (°C/min)**	**Target Press (°C)**	**Time**	**SP Type**	**Ramp Rate (bar/min)**	**Target Press (bar)**	**Time**	**SP Type**	**Ramp Rate (bar/min)**	**Target Vac. (bar)**	**Time**
Dwell	N/C	25	1′	Dwell	N/C	0	1′	Step	N/C	-0.80	N/C
Ramp	0.9	80	N/C	Ramp	0.10	6	N/C	Dwell	N/C	-0.80	1′
Ramp	0.9	180	N/C	Dwell	N/C	6	N/C	Step	N/C	-0.30	N/C
Dwell	N/C	180	2h	Dwell	N/C	6	10′	Dwell	N/C	-0.30	10′
Ramp	2.5	60	N/C	Dwell	N/C	6	10′	Dwell	N/C	-0.30	10′
Ramp	2.5	40	N/C	Ramp	0.50	0	N/C	Dwell	N/C	-0.30	5′

N/C: Not Controlled. Ramp Rate Temperature: °C/min, Ramp Rate Pressure: bar/min, Ramp Rate Vacuum: bar/min

Figure 13 shows the cure cycle of the laminates.

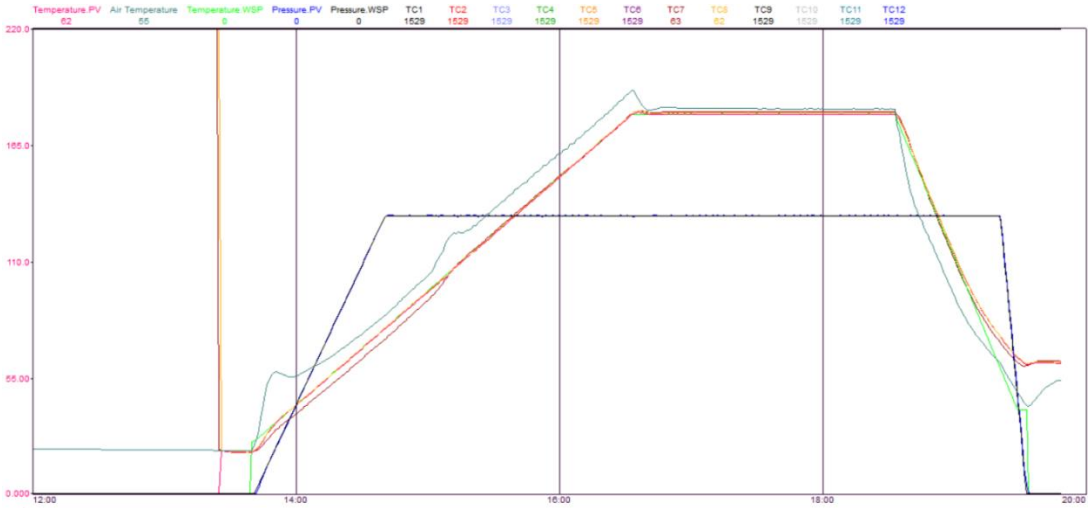

Figure 13 Curing cycle composite panels.

Table 8 summarises the information of the prepreg laminates manufactured:

Table 8 Summary manufactured prepregs

Product Description	Number of Laminates	Size	Lay up	Characteristic
HexPly8552 (Carbon fibre/epoxy)	4	600 x 600mm	$[0]_{16}$	Peel ply incorporated during the manufacturing process to texture the composite surface
	1	620 x 300mm		

4.2.1 Specimen cutting

Waterjet cutting was the method used to cut the composites laminates into small coupons. A waterjet uses a high pressure stream of water or a mixture of water and abrasive substance to erode a narrow line in the material to be cut. Waterjet cutting offers fast cutting. Due its precision and ability to cut almost any material, this technique is extremely versatile. It is the preferred method when the material being cut is sensitive to the high temperatures generated by the other cutting methods.

A mixture of water and abrasive garnet was used for cutting the composite laminates. An Australian garnet 80mesh was used (industry standard) and the cutting pressure applied was 60,000psi [66].

Through waterjet cutting, the composites laminates were cut into small coupons of 100mm length and 25mm width. These dimensions were chosen based on standard BS ISO 4587 [67] (more information about the joint assessment can be found in Chapter 4.5).

An individual specimen-naming system was devised to guarantee traceability to the original panels, treatment type, and joining conditions. Each specimen was named using the following code “Sxxx”; where “xxx” is the reference number from which panel the coupons were cut and also their position in the panel. Figure 14 shows a sketch of the specimens obtained per panel.

Each panel of 600 x 600mm was cut into 95 specimens. From the smallest laminate (620 x 300mm), 38 composite coupons were obtained. In total, 418 specimens were cut from the five composite panels manufactured. Measurements of the samples can be found in Appendix A.

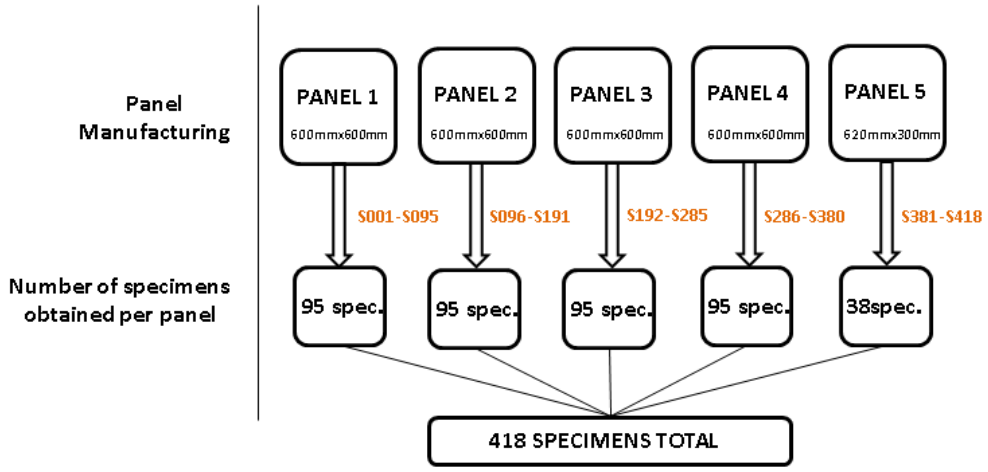

Figure 14 Panels and specimens obtained per panel**.**

4.3 Surface preparation

Different surface pre-treatments have been investigated in this research. The combinations of the pre-treatments carried out in the adherents are presented in Table 9.

After the peel ply was removed from the adherents, the surfaces were cleaned with acetone and pre-treated by manual abrasion, grit blasting and plasma. Each pre-treatment is discussed in more detail in the following subchapters.

Table 9 Surface pre-treatment combination

Surface pre-treatments combination				
Peel ply	Manual abrasion	Grit blasting	Plasma	
X	X			→ Base Line Industry
X		X		
X				→ Reference Line
X			X	

4.3.1 Pre-treatment peel ply plus manual abrasion

As cited in Chapter 1, peel ply is broadly used for bonding primary aerospace structures. It is added during the manufacturing process to prevent contamination and texture the surface of the composites, reducing or eliminating the need for abrasion.

As the aerospace industry conventionally uses abrasion and grit blasting for surface preparation, these methods will be used as the base line industry for comparison purposes. After the peel ply was removed from the samples, they were lightly manually abraded with medium-grit emery paper (p150 grit sand paper was used) [68-70]. The surfaces of the samples were abraded until the reflective surfaces turned dull grey (firstly in the direction of the fibres for ten seconds, afterwards in the opposite direction of the fibres for another ten seconds more and finally circular movements along the surface for 5 seconds).

Abrasion pre-treatment should be carried out in such a way that damage to the reinforcing fibres is avoided or minimised. It should always be followed by solvent cleaning to ensure the removal of loose particles. Therefore, all the samples were cleaned with acetone and left to dry (15 minutes) before the adhesive film was added. In an industrial environment, before cleaning the samples with the solvent, it may be necessary to use a vacuum system to remove much of the dust generated.

4.3.2 Pre-treatment peel ply plus grit blasting

Grit blasting was also investigated in order to compare the results obtained against manual abrasion.

A Guyson 400 syphon blasting system was used to grit blast the surfaces of the substrates. This system uses compressed air to propel blast media directly at the component through an exclusively designed blast nozzle.

Different run pressure values were investigated (35, 40 and 45psi) before blasting the real batches of samples. Images of grit blasted samples were

taken using scanning electron microscope (SEM) to look for evidence of resin on the surface and also fibre fracture. Experience has shown that resin/fibre exposure have an influence on adhesive bonding [72].

A scanning electron microscope produces images of a sample by scanning the surface with a focussed beam of electrons. A Zeiss 1455EP environmental scanning electron microscope with an EDAX Genesis 2000 EDX system was used.

Through grit blasting the original shiny texture of the surface must be eliminated to ensure the sample is correctly blasted (rather than underblasted). The samples treated at 40 and 45psi were shown to be over blasted with signs of carbon fibres being removed or damaged. This was not observed with the sample treated at 35psi.

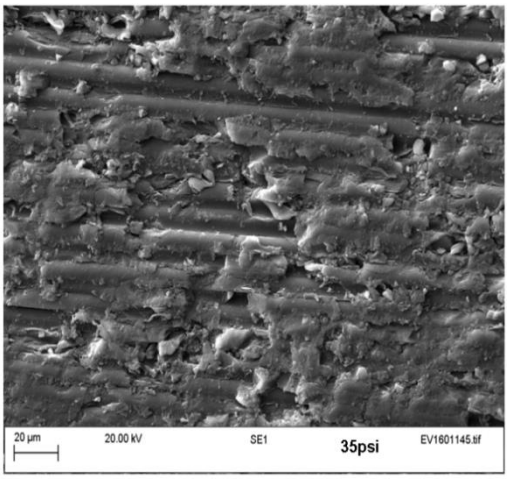

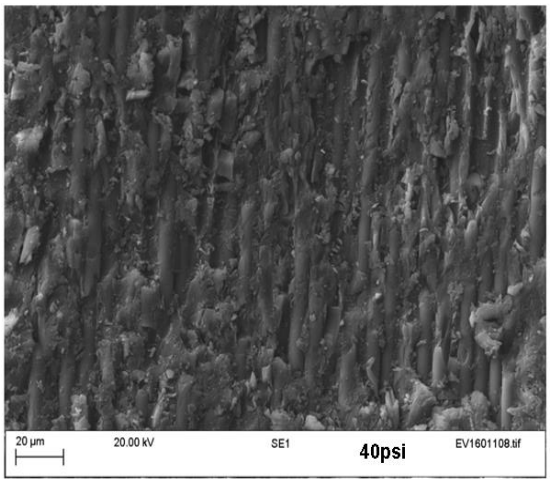

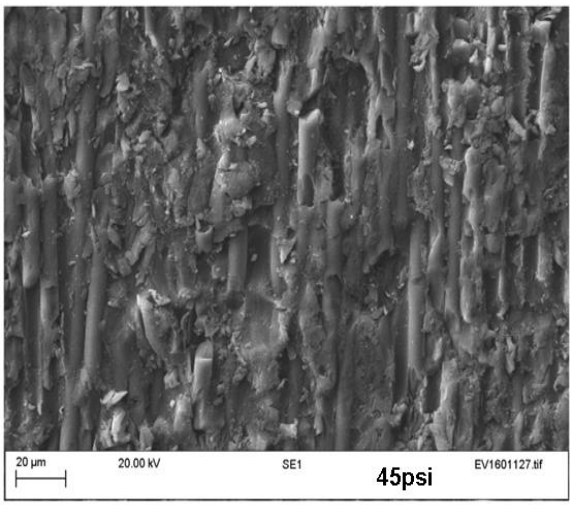

Figure 15 SEM images grit blasted samples: top left (35psi), top right (40psi) and bottom (45psi).

Table 10 presents information about the grit blasting machine used and the run pressure used during the process.

Table 10 Type and conditions grit blasting experiments

Description	
Equipment	Guyson 400 syphon blasting system
Grit	Saftigrit 100 mesh alumina
Nozzle	Airjet 2.8mm bore
Run pressure	35psi
Time	20 seconds

4.3.3 Pre-treatment peel ply

Peel ply (PP) was removed from another batch of samples. This method was used as a reference line to compare the strength of the joints against manual abrasion, grit blasting and plasma.

Initiation of the peel ply removal was done using a razor blade; the rest could be removed by hand.

4.3.4 Pre-treatment peel ply plus plasma

The following batches of samples were treated using a cold atmospheric pressure plasma (CAP) system. A PlasmaTact Atmospheric Device was used for the pre-treatment of the substrates, purchased from Adtec Europe Limited. The model of the equipment was a PM01-15AR0, intended for surface treatment for bonding or adhesion and cleaning for different materials.

This device generates plasma which uses microwave low-temperature atmospheric pressure plasma. The main part of the equipment consists of a

power supply and gas control. Argon or Helium plasma is generated by means of a plasma generator called a “mini-plasma torch”.

The device is connected to XYZ stage and parameters such as speed, distance between the plasma and the substrate, gas composition and flow rate can be changed and controlled.

The plasma equipment used in this research is shown in Figure 16. Table 11 summarizes the specifications of the system.

Table 11 Specifications plasma equipment

Specifications	
Model	PM01-15AR0
Plasma generation method	Microwave atmospheric pressure streamer plasma generation
Plasma generator	Mini-plasma torch
Plasma gas	-Primary gas: Argon or Helium purity ≥ 99.9% -Possible secondary gases:N_2, O_2, functional gases (CH_4,CF_4)
Flow rate gas	Primary gas: 10l/min* Secondary gas: 5l/min*
Microwave Amplifier	Maximum Output: 15W solid-state system Frequency: 2.45GHz fixed
Control	Manual Operation

*maximum values

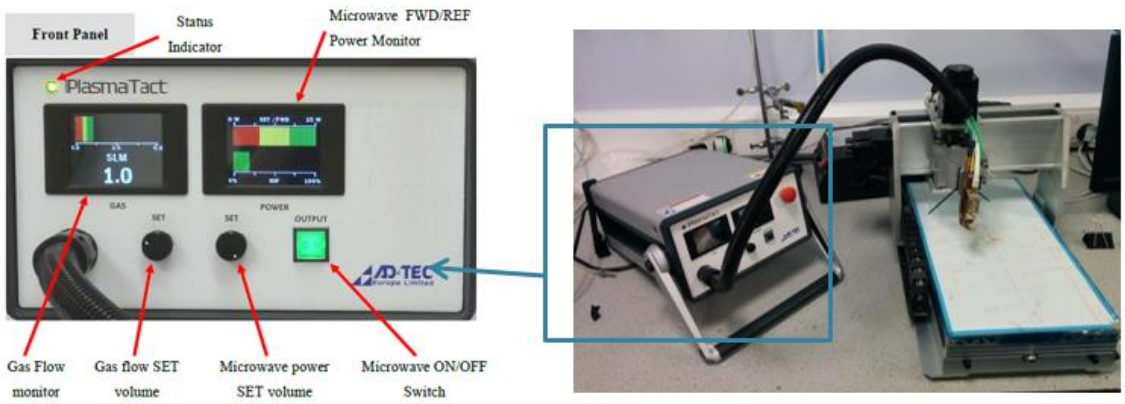

Figure 16 Plasma equipment.

This control unit can use argon or helium gases as the carrier, and oxygen and nitrogen as the active gases.

As explained in Chapter 2, different parameters can be considered while pre-treating substrates through plasma.

The type of gas used during this research was argon as primary gas, combined with 20% of air as secondary gas. Plasma conditions were fixed at 15W of radio frequency (2.45GHz) power. The plasma exposure was defined by the number of passes of the plasma jet over the substrate. Table 12 presents the values of different parameters considered during the surface pre-treatment of the samples [71].

Table 12 Parameters and values used plasma treatment

Parameter	Step	Value
Type of gas	Fixed	Argon: primary gas Air: secondary gas
Gas Flow	Fixed	Primary gas: 8l/min Secondary gas: 0.2l/min
Power	Fixed	15W
Distance (between the nozzle and the substrate)	Fixed	4mm
Speed	Variable	100, 300 and 500mm/min
Number of passes	Variable	1, 3 and 5

The variable parameters (speed and number of passes) defined the test matrix (Figure 17) used for the experiments.

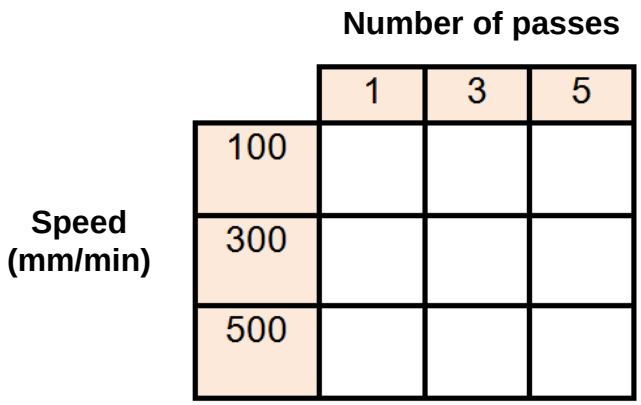

Figure 17 Test matrix for plasma pre-treatment.

Once the peel ply was removed from the samples, the substrates were cleaned with acetone and dried for 10 minutes. The substrates were then ready to be pre-treated by plasma using the values listed in Table 12.

Mach3 G-code software was used to programme the number of passes of the plasma nozzle, the speed, the distance of the plasma to the substrates and the path that the plasma should follow to treat the substrates. The area treated in the composite coupons through plasma was fixed to 12.5mm which corresponds with the overlap length value required according to BS ISO 4587 standard.

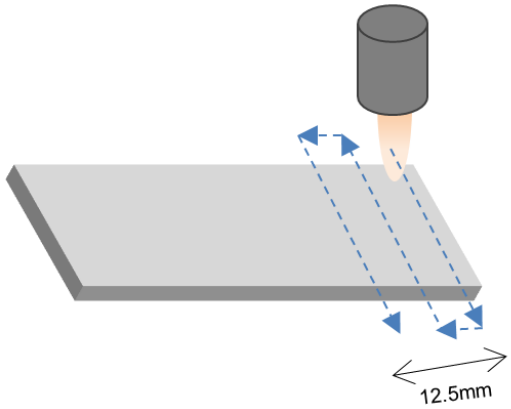

Figure 18 Path of the plasma nozzle during the treatment.

A fibre optic temperature sensor from Optocon was used to check the temperature of the CAP system. Figure 19 represents the evolution of the plasma temperature at the nozzle exit, varying the distance of the nozzle from the support tool (Figure 5, temperature sensor was placed on the support tool).

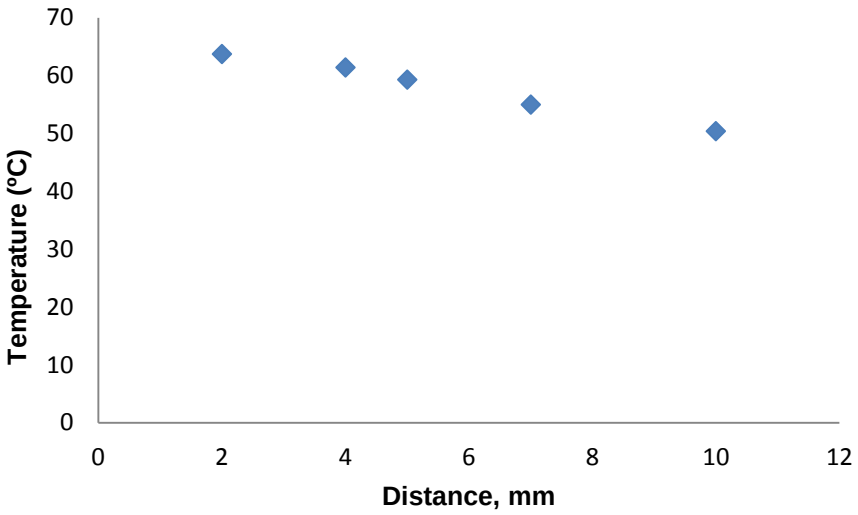

Figure 19 Plasma temperature evolution varying the distance of the nozzle from the support tool.

4.3.5 No pre-treatment: samples as received

For comparison purposes, the side of the substrates with no peel ply, called bag side (Figure 20), was also studied to investigate variances between bonding these two different sides of the substrates. The bag side was also pre-treated through manual abrasion, girt blasting and plasma using the parameters defined in Table 12.

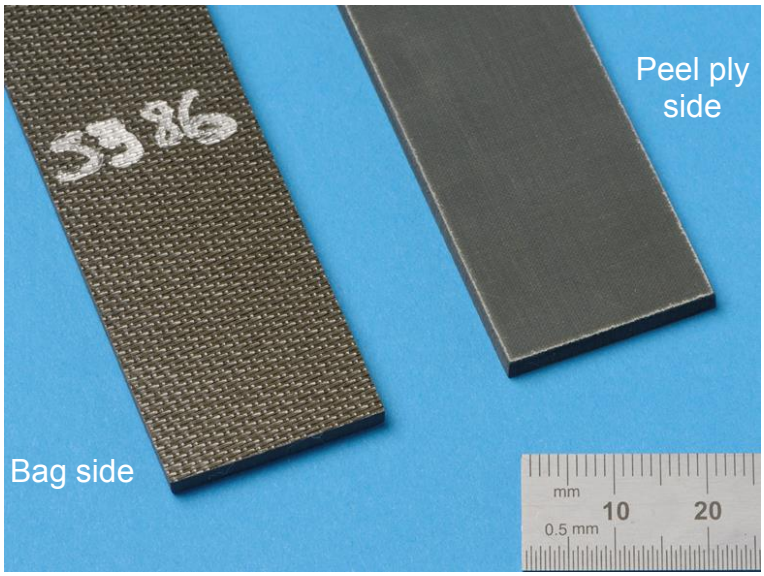

Figure 20 Bag side on the left and peel ply side on the right.

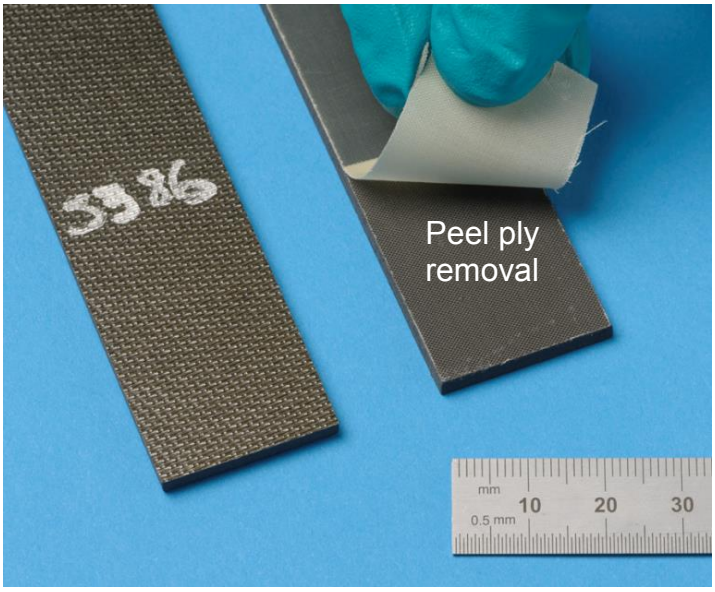

Figure 21 Peel ply removal.

4.3.6 Summary of pre-treatment types

Table 13 summarises the different pre-treatments types explored during this research.

Table 13 Pre-treatment types: peel ply side and bag side

Pre-treatment type				
Peel Ply	Manual Abrasion	Plasma	Grit blasting	Bag side
×	×			
×			×	
×				
×		×		
		×		×
	×			×
			×	×
No Pre-treatment: samples as received				
				×

4.4 Joint assembly

Once the substrates had been pre-treated through the different methods (peel ply, manual abrasion, grit blasting and plasma), the adherents were ready to be bonded.

In order to achieve reproducible and high quality joints, the bonding process was aided using further assembly equipment. For this purpose, the jig shown in Figure 22 was designed and manufactured, providing two additional benefits during the bonding process. Firstly, the correct position of the substrates will be guaranteed since the components will not be able to move. Secondly, a consistent overlap length of 12.5mm will be ensured for all the joints during the bonding process.

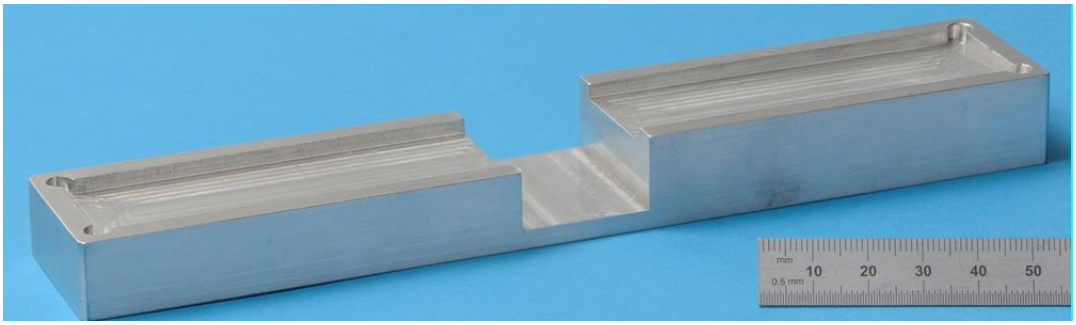

Figure 22 Jig manufactured for assembly of the joints.

One of the substrates was placed in the jig and the adhesive film added on top of it (Figure 23a.) A pinch of ballotini beads were added on top of the adhesive film for thickness control. The next step was to place the other substrate in the jig to complete the joint assembly. Pressure was required during the bonding process to make sure that the bond will occur. For this product, cure pressures of 100-350kPa are recommended during cure [64]. For this purpose, foldback clips were used (Figure 23b).

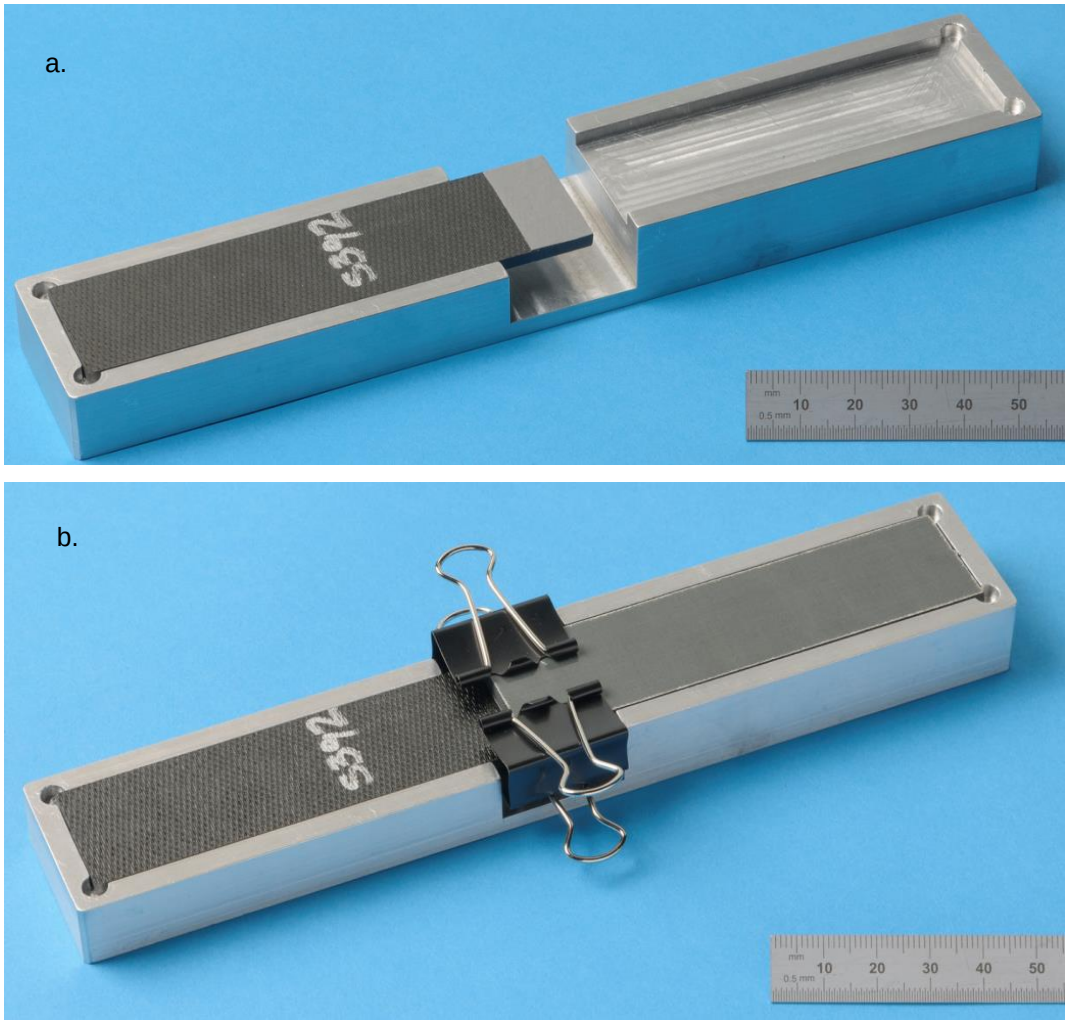

Figure 23 Joint assembly: **a.** positioning first adherent and adhesive film, **b.** positioning second adherent and foldback clips.

At this stage, the joint was ready to be placed in the oven for curing the adhesive at 120°C for 30 minutes. In order to cure the adhesive, a Binder M240 high performance temperature chamber was used. This chamber can operate in a temperature range from 5°C ambient temperature up to 300°C.

After the curing of the adhesive, the joints were cooled to below 70°C before releasing the pressure (recommendation from the resin supplier).

Tables 14 to 21 summarise the steps followed for all the surface pre-treatments applied during this researched for both sides of the substrates, peel ply and bag side.

Table 14 Pre-treatment: peel ply plus manual abrasion

Pre-treatment type	Steps pre-treatment
Peel ply plus abrasion (Base line industry)	- Removing peel ply - Abrasion of the substrates - Wiping substrates acetone and dry - Place adhesive film onto one of the substrates - Add ballotini beads - Completion the joint assembly - Measurement bond line thickness before curing - Curing at 120°C for 30 minutes - Cooling down below 70°C before removing clamps - Measurement bond line thickness after curing

Table 15 Pre-treatment: peel ply plus grit blasting

Pre-treatment type	Steps pre-treatment
Peel ply plus grit blasting (Base line industry)	- Removing peel ply - Wiping substrates acetone and dry - Grit blasting pre-treatment - Wiping again substrates acetone and dry - Place adhesive film onto one of the substrates - Add ballotini beads - Completion the joint assembly - Measurement bond line thickness before curing - Curing at 120°C for 30 minutes - Cooling down below 70°C before removing clamps - Measurement bond line thickness after curing

Table 16 Pre-treatment: peel ply

Pre-treatment type	Steps pre-treatment
Peel ply (Reference line)	- Removing peel ply - Wiping substrates acetone and dry - Place adhesive film onto one of the substrates - Add ballotini beads - Completion the joint assembly - Measurement bond line thickness before curing - Curing at 120°C for 30 minutes - Cooling down below 70°C before removing clamps - Measurement bond line thickness after curing

Table 17 Pre-treatment: peel ply plus plasma

Pre-treatment type	Steps pre-treatment
Peel ply plus plasma	- Removing peel ply - Wiping substrates acetone and dry - Plasma pre-treatment of the substrates, changing the speed and number of passes - Place adhesive film onto one of the substrates - Add ballotini beads - Completion the joint assembly - Measurement bond line thickness before curing - Curing at 120°C for 30 minutes - Cooling down below 70°C before removing clamps - Measurement bond line thickness after curing

Table 18 Pre-treatment: plasma on bag side of the substrates

Pre-treatment type	Steps pre-treatment
Plasma on bag side	- Wiping substrates acetone and dry - Plasma pre-treatment of the substrates, changing the speed and number of passes - Place adhesive film onto one of the substrates - Add ballotini beads - Completion the joint assembly - Measurement bond line thickness before curing - Curing at 120°C for 30 minutes - Cooling down below 70°C before removing clamps - Measurement bond line thickness after curing

Table 19 Pre-treatment: manual abrasion on bag side of the substrates

Pre-treatment type	Steps pre-treatment
Manual abrasion on bag side	- Wiping substrates acetone and dry - Abrasion of the substrates - Wiping substrates acetone and dry - Place adhesive film onto one of the substrates - Add ballotini beads - Completion the joint assembly - Measurement bond line thickness before curing - Curing at 120°C for 30 minutes - Cooling down below 70°C before removing clamps - Measurement bond line thickness after curing

Table 20 Pre-treatment: grit blasting on bag side of the substrates

Pre-treatment type	Steps pre-treatment
Grit blasting on bag side	- Wiping substrates acetone and dry - Grit blasting pre-treatment - Wiping substrates acetone and dry - Place adhesive film onto one of the substrates - Add ballotini beads - Completion the joint assembly - Measurement bond line thickness before curing - Curing at 120°C for 30 minutes - Cooling down below 70°C before removing clamps - Measurement bond line thickness after curing

Table 21 No pre-treatment, bag side: samples as received

Pre-treatment type	Steps pre-treatment
No pre-treatment *Bag side, samples as received*	- Wiping substrates acetone and dry - Place adhesive film onto one of the substrates - Add ballotini beads - Completion the joint assembly - Measurement bond line thickness before curing - Curing at 120°C for 30 minutes - Cooling down below 70°C before removing clamps - Measurement bond line thickness after curing

4.5 Joint assessment

Once the joint was assembled, the quality of the joints was assessed through mechanical testing. The mechanical test was based on BS ISO 4587 “Adhesive – Determination of tensile lap-shear strength of rigid-to-rigid bonded assemblies” (Figure 24) [72]. The machine used to carry out the static test was a Zwick 100kN tensile machine.

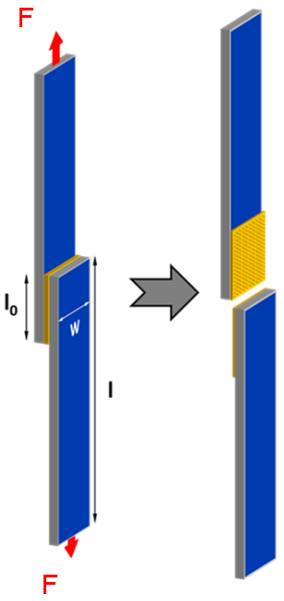

Figure 24 Specimen under tensile lap shear test.

According to standard BS ISO 4587, the length of each coupon should be 100mm and the width 25mm. The length of the overlap shall be 12.5mm. The tests were carried out at a constant speed so that the average joint will break in a period of 65s ± 20s (0.5mm/min). Five specimens per pre-treatment were tested [72]. The dimensions of the joints and their tolerances are shown in Figure 25.

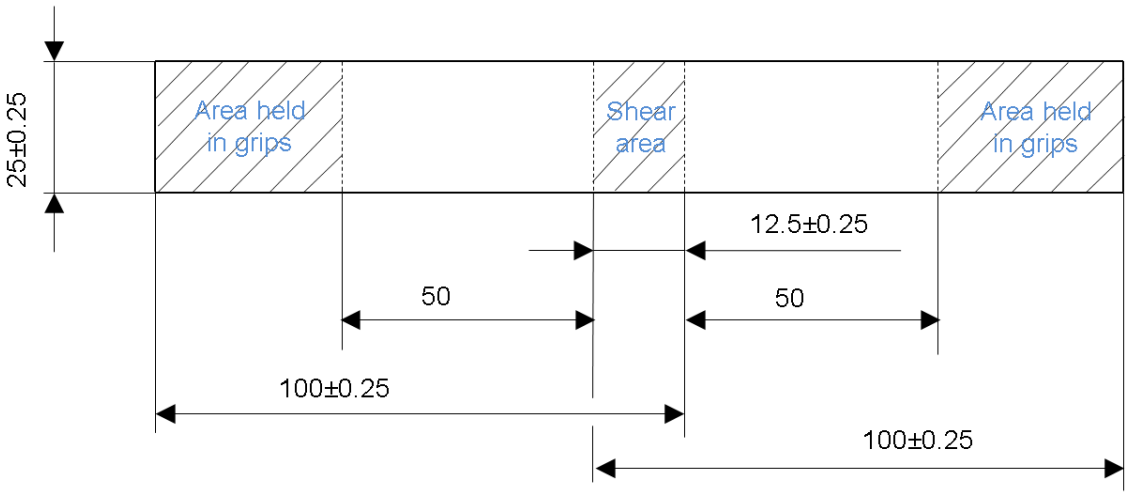

Figure 25 Dimensions and tolerances of joint (mm).

Aluminium tabs were added to the specimens to avoid slipping during the mechanical testing. The tabs were added to the specimens at the location of the grips (see Figure 25). Therefore, the dimensions of each tab were 25mm width and 50mm length.

Tabs were bonded using an adhesive that cures at or below the panel cure temperature, and also below the curing temperature of the adhesive film used to make the lap shear joint. This is to avoid adding undesirable postcure to the panel and any effects in the film adhesive.

The adhesive used to bond the tabs onto the substrates was DP490, supplied by 3M. DP490 is a two component epoxy adhesive that provides high quality bonding performance. This adhesive cures at 80°C for one hour. Before adding the tabs, each one was wiped with acetone to remove loosely attached surface films as oils, dusts, mill-scale and all other surface contaminants.

5 Results and Discussion

The bonded joints were assessed using tensile lap shear tests, according to the BS ISO 4587 standard [72] (detailed in subchapter 4.5). An assessment of the different pre-treatments was carried out using lap shear strength (LSS) values alongside a surface characterisation of the substrates (surface roughness, surface tension measurements and analysis of potential chemical changes).

The full data from LSS experiments are provided in Appendix B. These values are shown in tables with the corresponding representation of load values versus displacement.

This chapter presents a summary of the data obtained for joints which were pre-treated using different methods followed by a discussion of the findings for this investigation.

5.1 Joint assessment

Table 22 shows the different pre-treatments investigated in this research for both sides of the composite coupons (peel ply side and bag side).

Table 22 Summary of Table 13: pre-treatment types

Pre-treatment type
Peel Ply + Manual Abrasion (Base line industry)
Peel Ply (Reference line)
Peel Ply + Plasma (Argon + Air)
Peel Ply + Grit Blasting (Base line industry)
Bag side + Plasma (Argon + Air)
Bag side + Manual Abrasion
Bag side + Grit Blasting
No pre-treatment
Bag side

5.1.1 Joint assessment, peel ply side

LSS values for peel ply, peel ply plus manual abrasion, peel ply plus plasma and peel ply plus grit blasting pre-treatments are shown in Table 23. LSS values are the result of the average of testing five specimens per treatment/combination as established in the BS ISO 4587 standard. Values for standard deviation (SD), which quantifies the amount of variation of a set of data, and coefficient of variation (COV), the ratio of the SD to the mean, are also presented.

For peel ply plus plasma pre-treatment, different joints were first bonded using the extreme corners of the test matrix (Figure 26). The LSS values did not vary significantly using these four different conditions (1pass-100mm/min, 5passes-100mm/min, 1pass-500mm/min and 5passes-500mm/min, shaded in light green in Figure 26a). Therefore, the number of passes was increased to 10 passes, and the speed of the process to 1000mm/min, resulting in a new test matrix (Figure 26b).

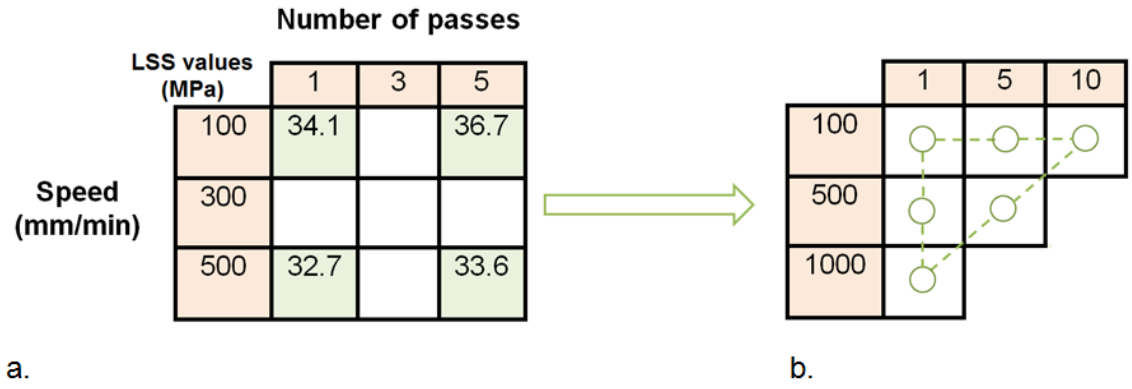

Figure 26 a. Test matrix plasma pre-treatment, **b.** New test matrix plasma pre-treatment.

Table 23 LSS values peel ply side using different pre-treatments

Peel Ply Side				
Pre-treatment type	**LSS (MPa)**	**SD (MPa)**	**COV(%)**	**Failure mode**
Peel ply + manual abrasion	38.4	1.1	3.0	Cohesive Adhesive
Peel ply	33.3	0.9	2.7	Cohesive
Peel ply + grit blasting	39.9	1.4	3.5	Cohesive
Peel ply + plasma. Conditions:				
1pass, 100mm/min	34.1	1.3	3.8	
1pass, 500mm/min	35.1	0.7	1.9	
1pass, 1000mm/min	32.7	0.7	2.1	Cohesive
5passes, 100mm/min	36.7	0.8	2.1	
5passes, 500mm/min	33.6	0.8	2.3	
10 passes, 100mm/min	35.3	0.5	1.4	

Figure 27 represents the LSS values achieved treating the peel ply side of the composite through the different pre-treatments.

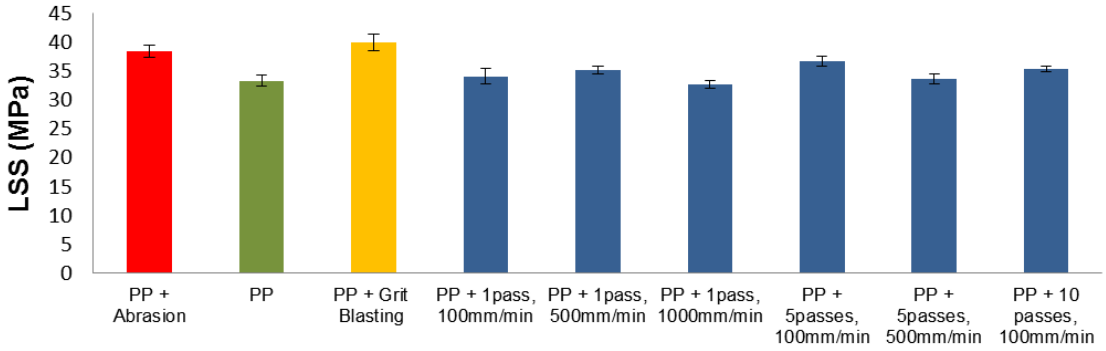

Figure 27 LSS values versus pre-treatment type, peel ply side.

Before the discussion of results, Figures 28 to 31 illustrate some examples of the failure mode of the different pre-treatments.

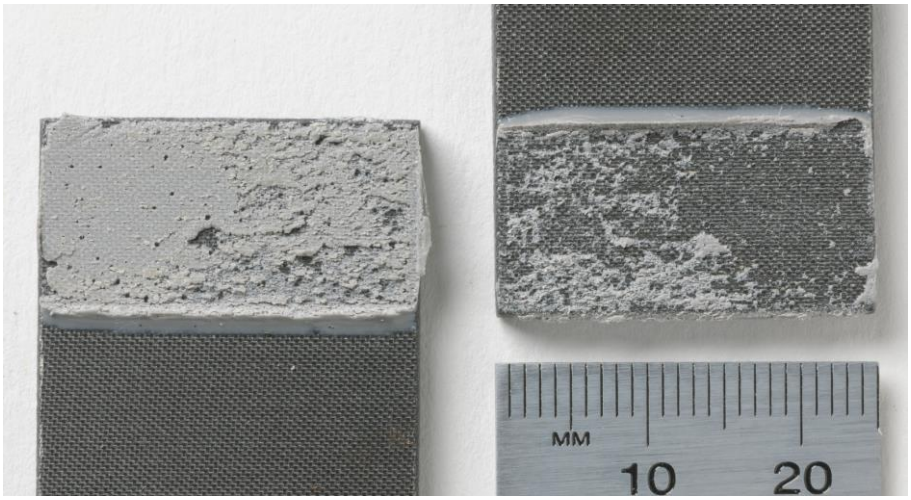

Figure 28 Failure of bonded sample S203-S204: peel ply side as received. Cohesive failure.

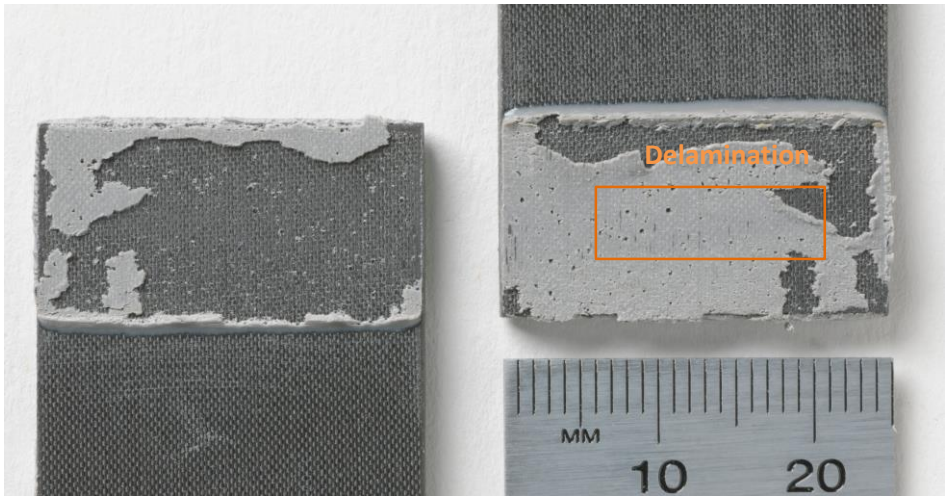

Figure 29 Failure of bonded sample S186-S187: peel ply side pre-treated through manual abrasion. Cohesive plus adhesive failure (slight delamination).

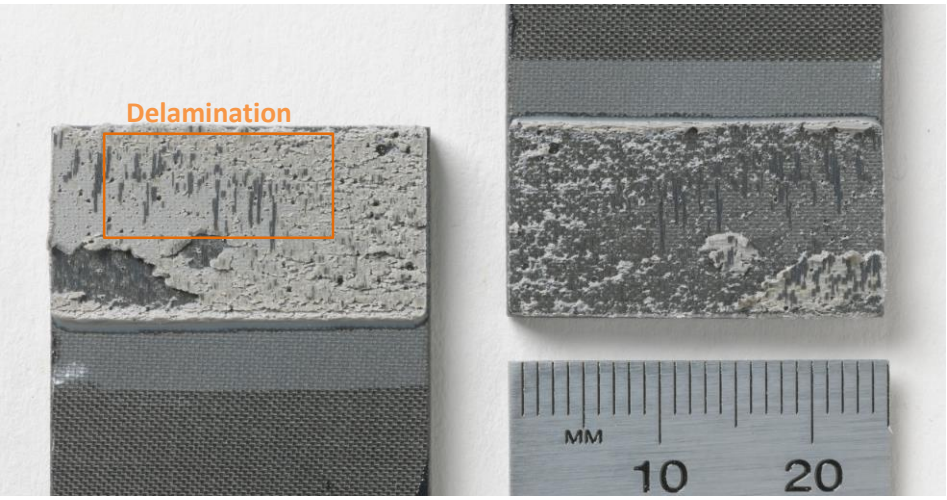

Figure 30 Failure of bonded sample S210-S209: peel ply side pre-treated through grit blasting. Cohesive failure plus delamination.

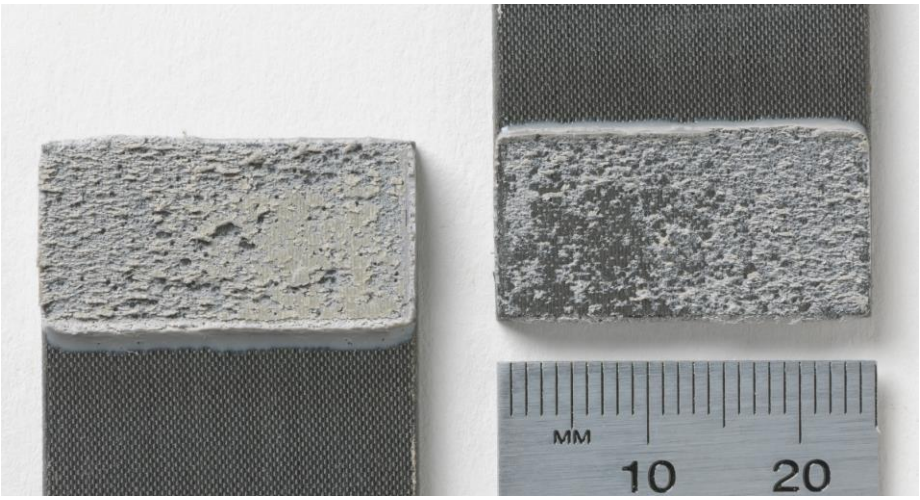

Figure 31 Failure of bonded sample S153-S154: peel ply side pre-treated through plasma (conditions: 10 passes, 100mm/min). Cohesive failure.

Figure 27 shows that treating the peel ply surface of the samples using manual abrasion (38.4MPa) and grit blasting (39.9MPa) produces an improvement of 15% and 20% respectively in the strength of the joints, compared to those just with peel ply (33.3MPa).

During the removal of the peel ply, some synthetic peel ply cloth can remain on the substrates. Through manual abrasion and grit blasting, these residues

can be eliminated. In addition, through these processes, more resin in the substrates is removed, and therefore the underlying composite fibres will be highly exposed, leading to an improvement of the strength of the final joint. The fibre exposure can be observed in Figure 29 (manual abrasion), and, more noticeably, in Figure 30 (grit blasting).

Through grit blasting, the strength value was higher than for manual abrasion. This is due to the nature of the process. During grit blasting, a gun is used to propel blast media directly at the component, ensuring that the whole area will be treated. Through manual abrasion, an even treatment over the whole area is more difficult, due to the inconsistent manual nature of the process. It is also important to highlight that through manual abrasion, the possible contamination left after removing the peel ply may transfer to the abrasive paper, and therefore it could be transferred to other areas on the surface, rather than being removed.

The highest strength achieved using plasma pre-treatment was with 5 passes at 100mm/min (36.7 ± 0.8 MPa), and the lowest value was reached at 1 pass at 1000mm/min (32.7 ± 0.7 MPa). In all cases, it was noticed that the adhesive always failed cohesively.

It is known that plasma pre-treatment is an excellent method for removing contaminants from substrates prior to bonding. Comparing the strength values achieved through pre-treating the samples with plasma against no pre-treatment (ie just peel ply), there is no significant change in the LSS values. This shows that the addition of peel ply during the manufacturing of the composite part is very effective for preventing contaminants from being integrated into the finished part.

Comparing manual abrasion against plasma, there is a slight improvement of LSS when pre-treating the samples using manual abrasion. Due the nature of the process, it is high likely that manual abrasion introduced a slight modification at the end of the joint where the edges become rounded (Figure 32a). However, through plasma, the shape of the edges of the joints remained the same as the original ones after the pre-treatment (Figure 32b).

An example to support this theory would be the modification of window profiles in aircraft. In the past, the shape of aircraft windows was rectangular. However, the shape was changed to oval, as it was proved that this shape had less stress concentration around the edges of the windows and, therefore, offered greater structural integrity [73].

This rounded or oval effect at the edges of the joints that were pre-treated through manual abrasion (visible to the naked eye) could reduce the local load stresses around the edges, resulting in a slight increase in the strength, as observed in Table 23. However, this is just a possibility, and further analysis should be carried out, as the SD of the samples that were pre-treated through manual abrasion was slightly higher than those pre-treated through plasma.

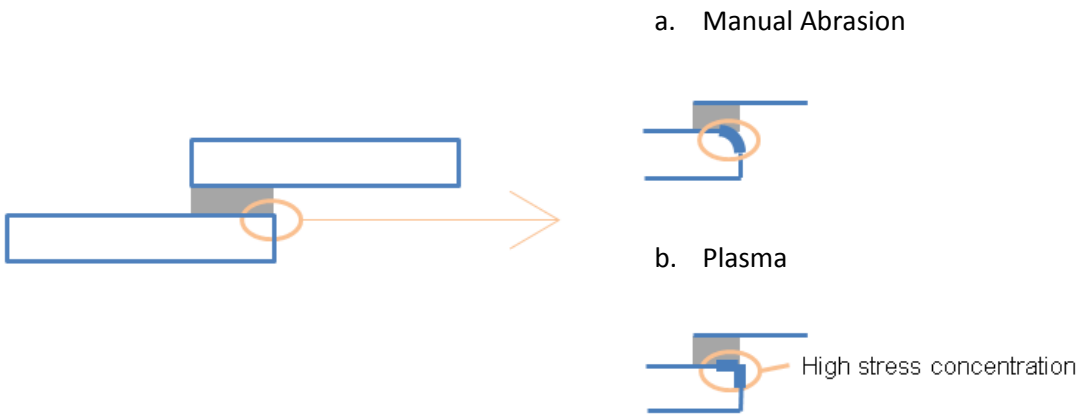

Figure 32 a. Shape of the end of the joint through manual abrasion pre-treatment (slightly rounded); **b.** Shape of the end of the joint through plasma pre-treatment.

As discussed in Chapter 2, the adhesive bond line thickness (BLT) will have an influence on joint strength. Therefore, the BLT was calculated by measuring the thickness of the lap shear joints before and after curing the adhesive, using a digital (Mitutoyo) micrometre (accuracy of ±2μm).

The general effect of increasing the BLT of an adhesive in single lap joints is shown in Figure 33. It is noticeable that shear strength decreases if the layer of the adhesive is thick. If the BLT is too thin, there will be a risk of incomplete

filling of the joint due to contact between high points on the joint substrates. The shape of the curve will be affected by the type of adhesive. This curve is characterised by an optimum BLT area. For each adhesive, the values within this area will vary. In the case of epoxies, the optimum BLT area often varies between 50-250μm [53].

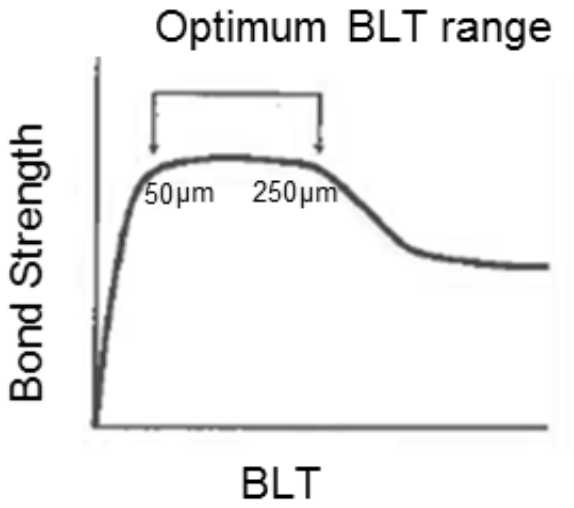

Figure 33 Shear strength versus bond line thickness [53].

Table 24 shows the BLT of the specimens when pre-treating the peel ply side with the different pre-treatments. BLT values are given by taking the average measurements of five specimens. Figure 34 illustrates the influence of the thickness of the film adhesive (ballotini beads added) on the joint strength.

Table 24 BLT lap shear joints peel ply side

Peel Ply Side			
Pre-treatment type	**BLT (mm)**	**SD BLT* (mm)**	**LSS (MPa)**
Peel Ply + Manual Abrasion	0.105	0.045	38.4
Peel Ply	0.195	0.025	33.3
Peel Ply + Grit Blasting	0.142	0.055	39.9
Peel Ply + Plasma. Conditions:			
1pass, 100mm/min	0.245	0.024	34.1
1pass, 1000mm/min	0.181	0.025	35.3
5passes, 100mm/min	0.247	0.029	32.7
5passes, 500mm/min	0.267	0.025	33.6
10passes, 100mm/min	0.211	0.009	36.7

*The SD deviation is illustrated in Figure 34. However, some SD values are so small that cannot be noticeable due the markers on the graphic.

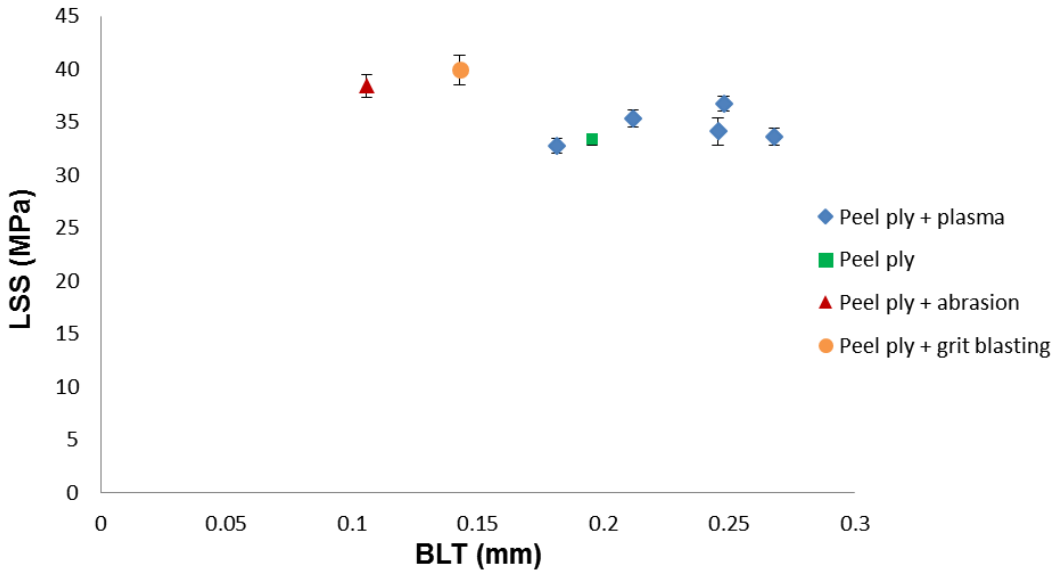

Figure 34 Influence of film adhesive thickness on LSS – peel ply side.

Figure 34 shows that the drop in strength occurs somewhere between 0.142 and 0.181mm. In thicknesses greater than 0.19mm, shear strength is roughly constant.

5.1.2 Joint assessment, bag side

As mentioned in Subchapter 4.3.5, the bag side of the substrates was also pre-treated and investigated. LSS values are given in Table 25.

Table 25 LSS values bag side using different pre-treatments

Bag Side				
Pre-treatment type	**LSS (MPa)**	**SD (MPa)**	**COV(%)**	**Failure mode**
Bag side + Plasma. Conditions:				
1pass, 100mm/min	39.4	1.0	2.5	
1pass, 500mm/min	34.4	1.9	5.5	Cohesive
1pass, 1000mm/min	38.0	1.3	3.5	Adhesive
5passes, 100mm/min	42.8	1.9	4.4	
5passes, 500mm/min	36.8	1.8	4.8	
10passes, 100mm/min	41.1	1.9	4.6	
Bag side + Manual Abrasion	34.7	1.7	4.8	Cohesive Adhesive
Bag side + Grit Blasting	40.8	0.5	0.5	Cohesive Adhesive
No pre-treatment				
Bag side	17.4	1.4	8.1	Adhesive

Figure 35 represents the LSS values achieved when pre-treating the bag side of the composite with the different pre-treatments.

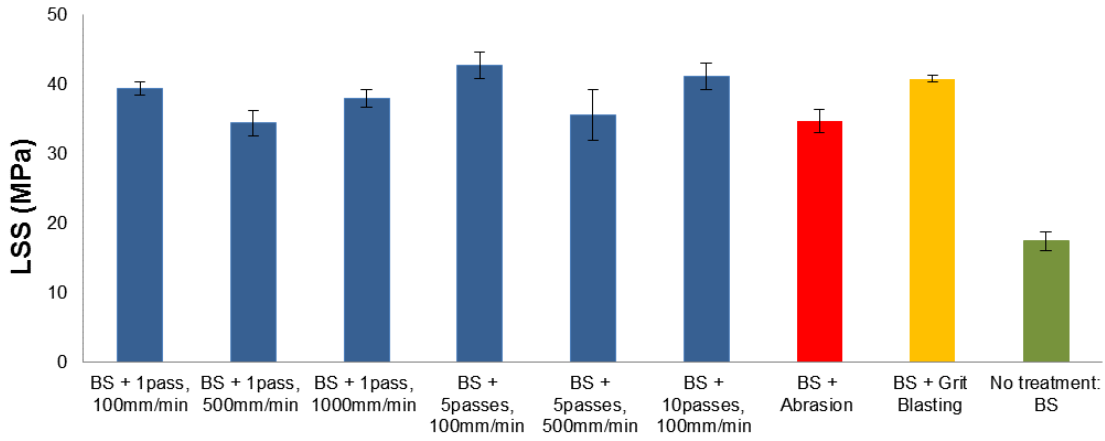

Figure 35 LSS values versus pre-treatment type, bag side.

Figure 36 shows that the failure mode observed for the bag side with no pre-treatment was adhesive in type. This means that the failure happened at the interface between the adhesive and the adherent. This type of failure must be avoided, as it is considered the result of a weak bond. This is the reason why the value of LSS achieved was very low, reaching only 17MPa. Also, it is possible to observe a significant number of voids at the failure interface, making the joint relatively weak. The cause of these voids is unknown, but it could be due to air entrapment during the bonding process.

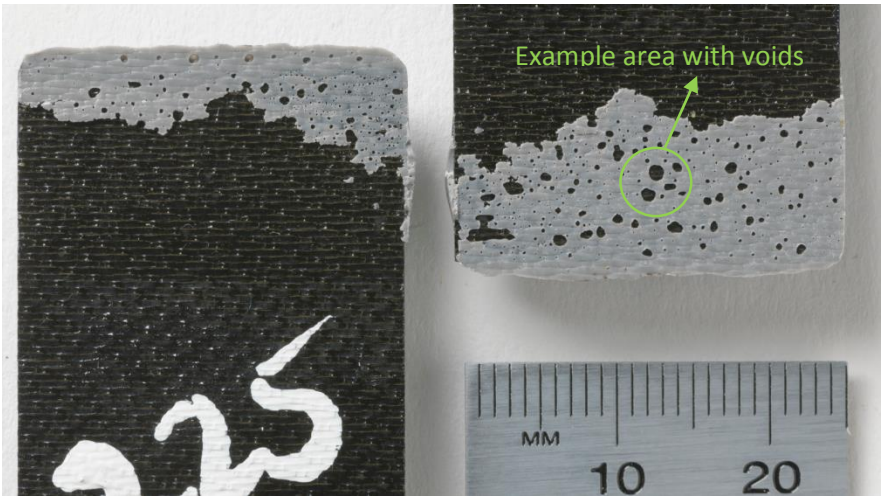

Figure 36 Failure of bonded sample S225-S226: bag side, no pre-treatment. Adhesive failure.

As mentioned in Section 2.3, in some cases cohesive and adhesive failures can happen in the same bond. This mixed-mode failure was experienced by the samples that were pre-treated using grit blasting and manual abrasion. Examples of this type of failure are shown in Figures 37 and 38.

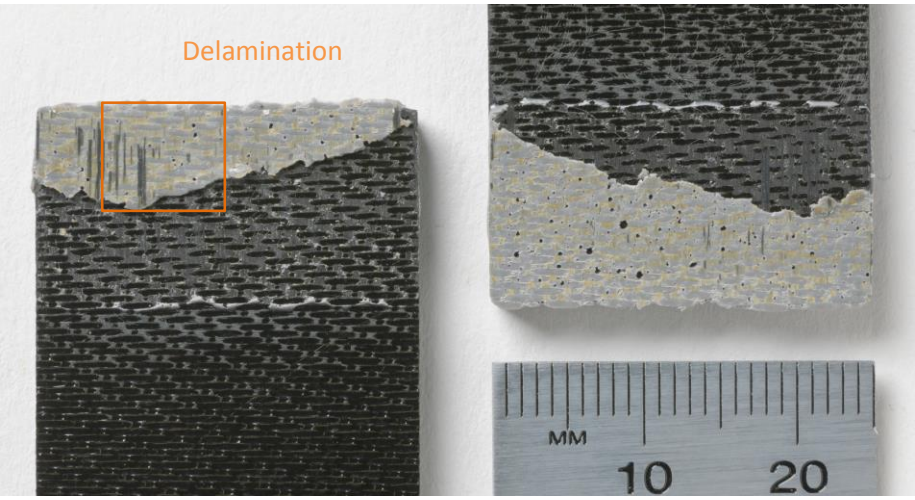

Figure 37 Failure of bonded sample S282-S283: bag side pre-treated through manual abrasion. Cohesive failure plus delamination (also adhesive failure but in much less proportion that the other failure modes).

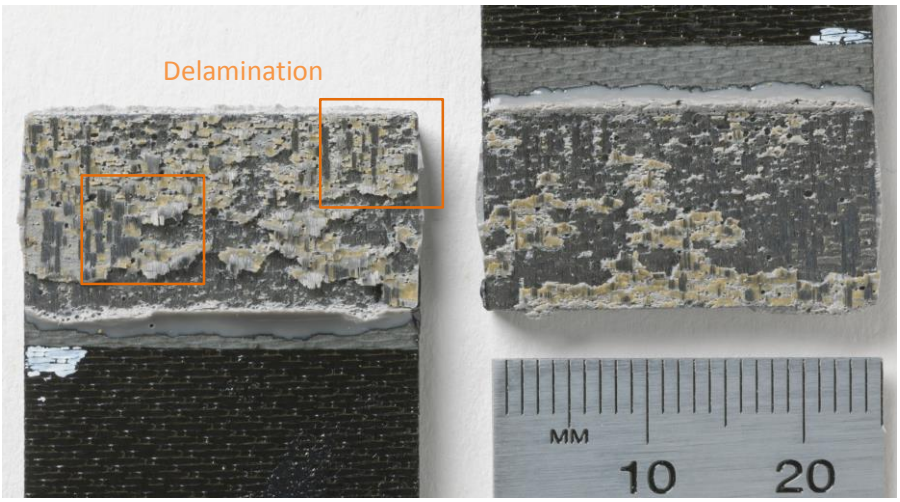

Figure 38 Failure of bonded sample S216-S217: bag side treated through grit blasting. Cohesive failure and delamination.

The LSS value achieved for grit blasting was higher (40.8MPa) than for manual abrasion (34.7MPa). As explained before, this could be due to the nature of the process. Grit blasting provides more consistency than manual abrasion. This fact can also be explained by comparing the SD of both processes, which was 0.5MPa for grit blasting, and 1.7MPa for manual abrasion.

Delamination appears when pre-treating the bag side of the coupons using manual abrasion and grit blasting (delamination is boxed in orange on Figures 37 and 38). Comparing this against bag side without any pre-treatment (Figure 36), two different colours are noticeable in Figures 37 and 38 at the failure interface. Light grey could represent the cohesive failure through the adhesive, while yellow could indicate adhesive plus the epoxy of the composite (adhesive pulls some of the resin off). The amount of resin on the bag side of the laminates is higher than on the peel ply side. This could be the reason why the yellow colour is only noticeable at the failure interface on the bag side of the samples (pre-treating them through manual abrasion, grit blasting, and plasma).

Samples treated with plasma showed a very real improvement, achieving the highest strength of 42.8MPa when treating the samples with plasma at 100mm/min and 5 passes (same conditions that the highest value was obtained when treating the peel ply side of the material). Samples treated with plasma also presented a mixed-mode failure. An example is shown in Figure 39.

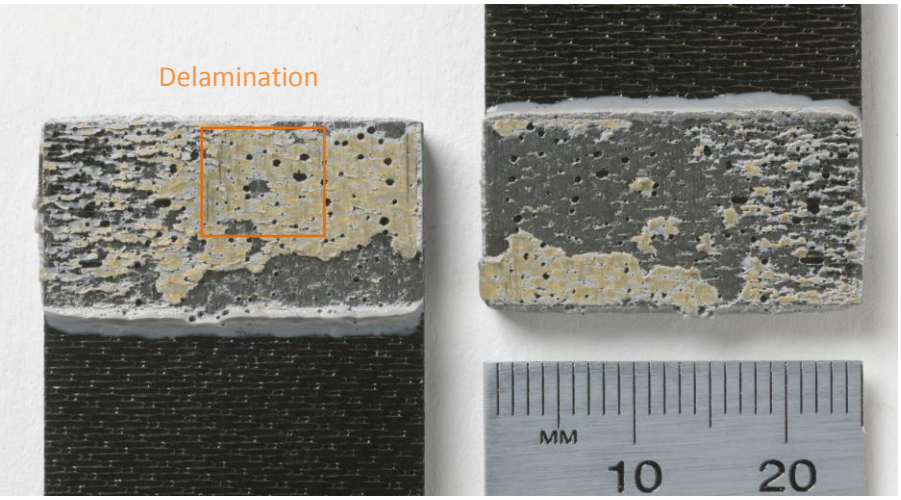

Figure 39 Failure of bonded sample S264-S263: bag side treated through plasma (conditions: 10passes, 100mm/min). Cohesive failure plus slight delamination.

This improvement by treating the bag side of the samples (17.4MPa) with plasma (highest achieved value 42.8MPa) shows the effectiveness of the plasma pre-treatment as a preparation method. During the manufacturing of composite laminates, the bag side was covered by a layer of release film, as shown in Figure 12 (Chapter 4). This means that the bag side of the laminate was not protected from contamination during the manufacturing process. Therefore, the possibility of the laminate being contaminated appears during the manufacturing process, and increases during the storage period of the laminate prior to bonding. The thicker, “less stiff” layer of resin and adhesive on the bag side of the samples could also be another explanation for this improvement, as this layer has greater capacity to take up more strain.

Table 26 shows the BLT of the specimens when treating the bag side using the different pre-treatments. Figure 40 represents the influence of the thickness of the film adhesive (ballotini beads added) on the joint strength. As observed in this figure, all the BLT measurements are between 0.05-0.12mm and therefore, it is difficult to observe a clear trend. BLT measurements for the peel ply side (Figure 34) shows a clearer trend as the measurements area is wider (~0.3mm).

Table 26 BLT lap shear joints bag side

Bag Side			
Pre-treatment type	**BTL (mm)**	**SD BLT* (mm)**	**LSS (MPa)**
Bag side + Plasma.			
Conditions:	0.101	0.025	39.4
1pass, 100mm/min	0.066	0.018	42.8
1pass, 500mm/min	0.081	0.021	41.1
1pass, 1000mm/min	0.051	0.019	34.4
5passes, 100mm/min	0.074	0.021	36.8
5passes, 500mm/min	0.097	0.041	38.0
10passes, 100mm/min			
Bag side + Manual Abrasion	0.113	0.027	34.7
Bag side + Grit Blasting	0.128	0.010	40.8
Bag side	0.070	0.015	17.4

*The SD deviation is illustrated in Figure 40. However, some SD values are so small that cannot be noticeable due the markers on the graphic.

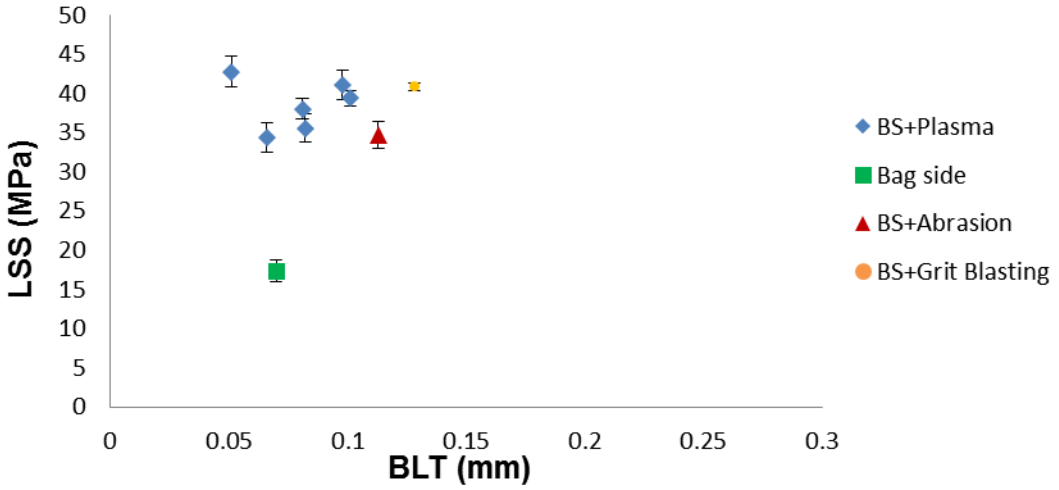

Figure 40 Influence of film adhesive thickness on LSS – bag side.

5.2 Surface characterization

The pre-treatment effects in the joints were assessed in terms of mechanical performance (LSS values) and also by using three different surface characterization methods. The methods employed were roughness assessment, X-ray photoelectron spectroscopy analysis and wettability study.

These techniques are discussed in more detail in the following subchapters.

5.2.1 Roughness assessment

Surface texture of the samples was measured using a calibrated Taylor Hobson Form Talysurf Intra 50 Surface Profilometer. The profilometer is housed on a granite slab to dampen vibrations. A Gaussian filter was applied to separate waviness and roughness profiles.

One of the most common parameters used to measure surface roughness is the arithmetic average roughness (R_a). R_a represents the average value of individual heights and peaks in a surface topology, from the mean line, recorded within the sampling length. Figure 41 illustrates an example of the roughness profile taken from one of the samples studied in this research.

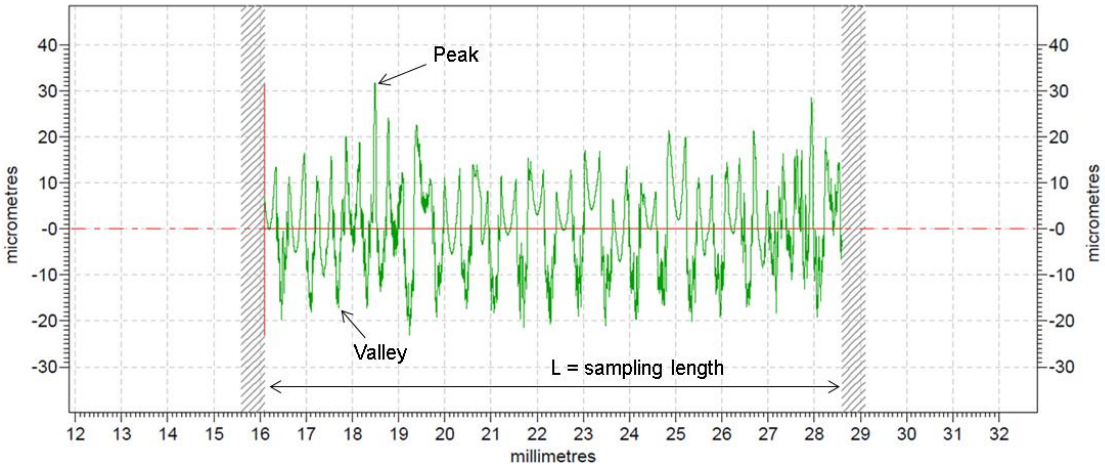

Figure 41 Surface roughness profile of sample without peel ply and no pre-treatment.

Evaluation lengths were selected based on the surface R_a values according to BS ISO 4288-1996 [74] .The sampling length (l_r) was 2.5mm and the number of sampling lengths was five, making this a total of 12.5mm roughness evaluation length (l_n). Three different roughness measurements were taken per sample.

Table 27 gives, and Figure 42 represents, the average R_a values obtained after the roughness assessment of the different pre-treatments for the peel ply side of the adherents.

Table 27 R_a values, peel ply side, different pre-treatments

Peel Ply Side			
Pre-treatment type	**R_a (µm)**	**SD (µm)**	**COV (%)**
Peel Ply	7.465	0.262	3.51
Peel Ply + Manual Abrasion	4.253	1.153	27.11
Peel Ply + Grit Blasting	7.653	0.263	3.43
Peel Ply + Plasma. Conditions:			
1pass, 100mm/min	7.918	0.286	3.61
1pass, 500mm/min	7.804	0.303	3.88
1pass, 1000mm/min	8.175	0.891	10.89
5passes, 100mm/min	7.753	0.975	12.57
5passes, 500mm/min	7.203	0.492	6.83
10passes, 100mm/min	7.871	0.122	1.55

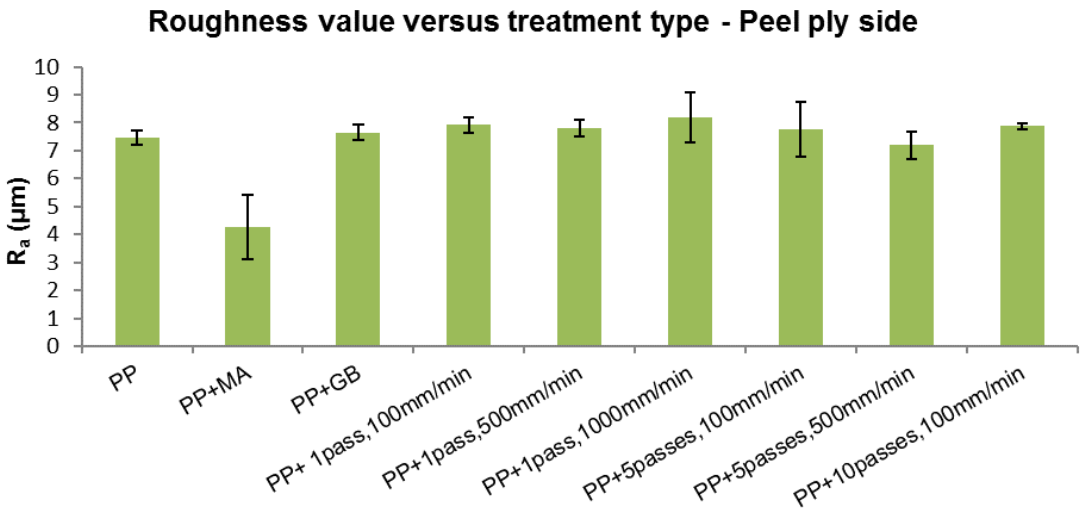

Figure 42 Average roughness R_a of different pre-treatments on peel ply side.

Figure 43 compares the R_a values obtained for each pre-treatment type against the results of the shear strength for the peel ply side. Figure 43 shows that the lowest shear strength value (32.7MPa for treatment using plasma 1 pass and 1000mm/min) was achieved with the highest roughness value, R_a =8.1µm. The higher shear strength (39.9MPa for treatment using peel ply plus grit blasting) was obtained with a roughness of R_a = 7.653µm. The second highest shear strength value (38.4MPa for manual abrasion) was obtained with the lowest roughness value R_a = 4.2µm.

The work carried out by Matienzo et al. [16] and Wingfield et al. [17] showed that increasing the roughness of the surface led to stronger joints. However, the investigations done by Boutar et al. [75] showed that by increasing the roughness of the adherents, a decrease in the lap shear strength occurs. Boutar et al. found that specimens abraded with P1000 abrasive paper, which gave a roughness of 0.6µm, were much stronger than the ones abraded with P500, which gave a roughness of 3µm (material used in this investigation was an aluminium-copper alloy).

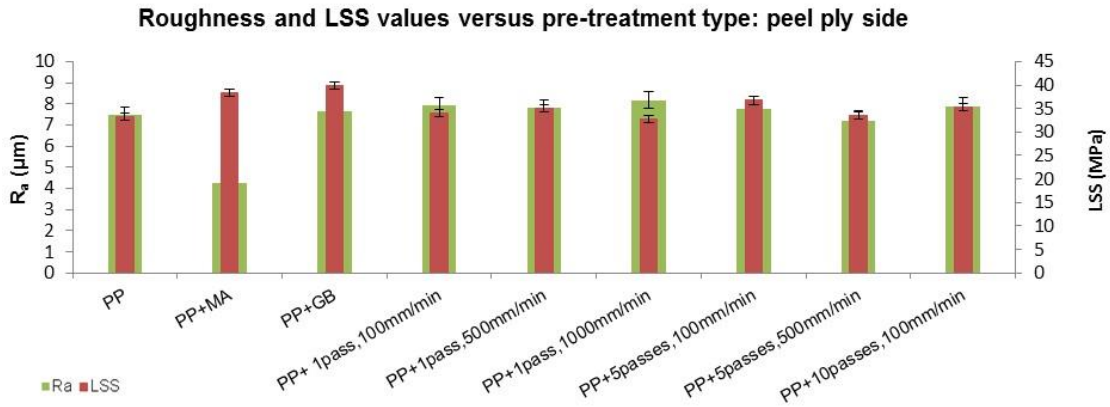

Figure 43 Average roughness R_a of different pre-treatments on peel ply side compared to LSS values (standard deviation for LSS is shown).

For the pre-treatments and combination conditions for the peel ply side of the substrates under study in this research, the effect of roughness measured did not have a major impact on the strength. Looking at the LSS values, the adhesive used in this research was very good at wetting the surfaces, regardless of roughness.

The same roughness assessment was carried out for the bag side of the adherents. Table 28 and Figure 44 represent the average R_a values obtained after the roughness assessment of the different treatments.

Table 28 R_a values bag side different pre-treatments

Bag Side			
Pre-treatment type	**R_a (µm)**	**SD (µm)**	**COV (%)**
Bag side + Manual Abrasion	4.192	0.481	11.47
Bag side + Grit Blasting	8.556	0.364	4.25
Bag side + Plasma. Conditions:			
1pass, 100mm/min	7.605	0.336	4.41
1pass, 500mm/min	7.252	0.589	8.12
1pass, 1000mm/min	7.861	0.543	6.91
5passes, 100mm/min	7.427	0.541	7.28
5passes, 500mm/min	7.583	0.396	5.22
10passes, 100mm/min	7.979	0.206	2.58
Bag side	7.842	0.563	7.17

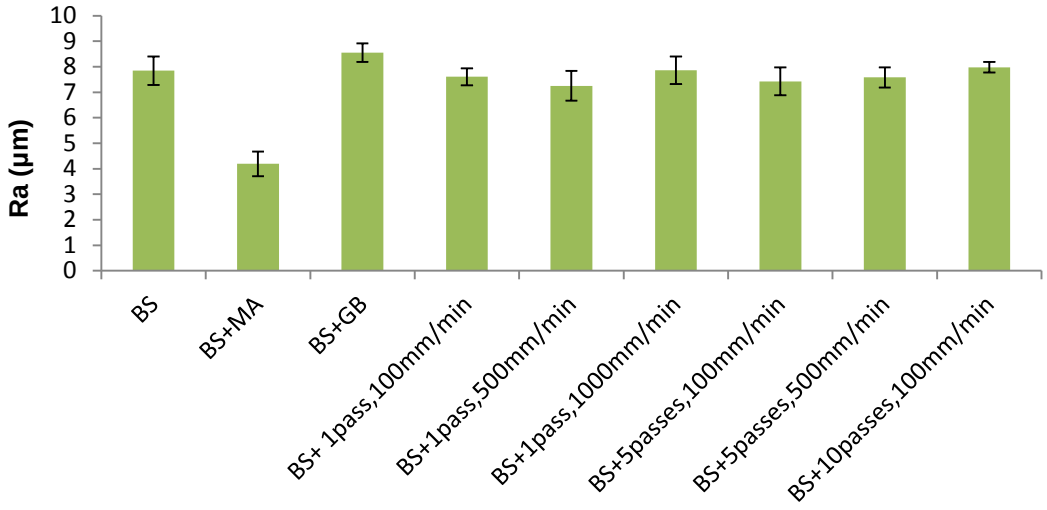

Figure 44 Average roughness R_a of different pre-treatments on bag side.

Figure 45 compares the R_a values obtained for each treatment type against the results of the shear strength for the bag side of the substrates.

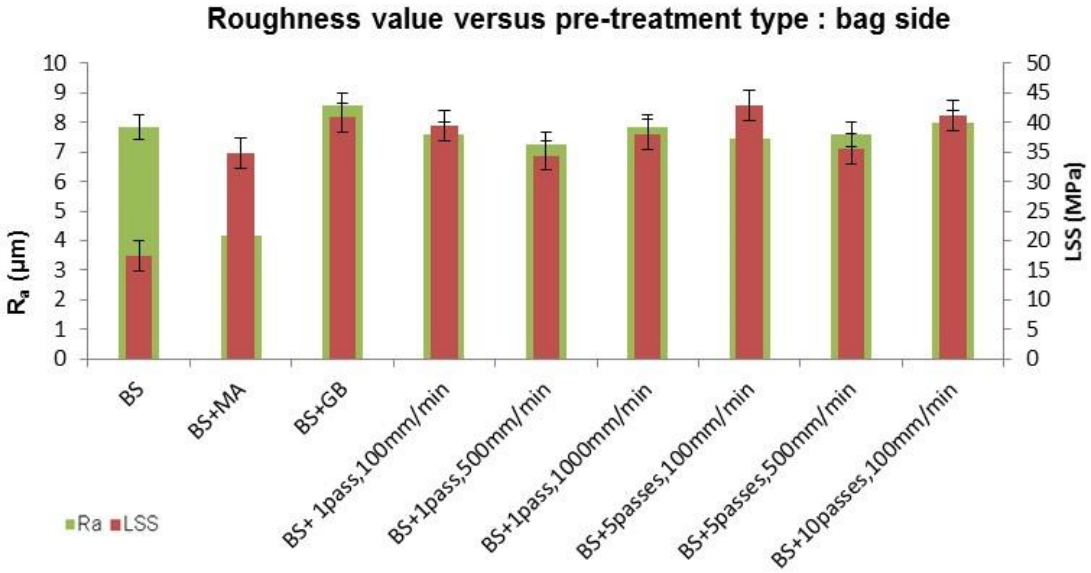

Figure 45 Average roughness R_a of different pre-treatments on peel ply side compared to LSS values (standard deviation for LSS is shown).

Figure 45 shows that the lowest shear strength value (17.4MPa for bag side without any treatment) was achieved with a roughness value of R_a = 7.842µm. In contrast, the higher shear strength value (42.8MPa for treatment using

plasma 5passes and 100mm/min) was obtained with a roughness of R_a = 7.427µm.

The same outcome found on the peel ply side was observed for the bag side of the substrates, where the effect of roughness measured did not have a major impact on LSS strength.

When comparing both sides of the composite, it is possible to highlight that manually abrading the surfaces produces a decrease in the original roughness of both sides. R_a for the peel ply side has an average of 7.465µm, and after manual abrasion the R_a decreases to 4.253µm. The same effect was observed for the bag side of the composite, where R_a is 7.842µm, and this value dropped to 4.192µm after manual abrasion. The drop in the R_a values is due to the manual operation, which reduces the height of the original peaks.

Comparing the R_a values for all the pre-treatments for both sides, it is noticeable that the values for each pre-treatment/composite side are quite similar. However, checking the surface roughness profile for both sides, the pattern is different for each side. An example is illustrated in Figure 46.

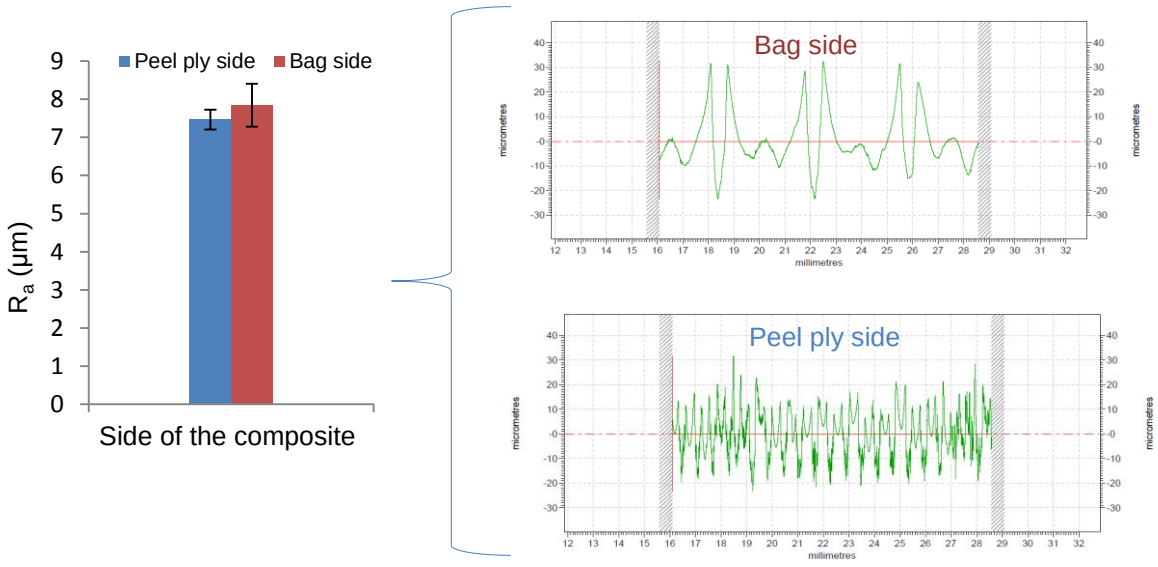

Figure 46 R_a values (left) and surface roughness profile for bag side (no pre-treatment involved) and peel ply side (right).

The R_a value for the peel ply side of the composite is 7.465µm with a LSS value of 33.3MPa. The bag side, without any pre-treatment, has a Ra value of 7.842µm; however, its LSS value is quite low (17.MPa) compared to the 33.3MPa achieved for the peel ply side.

R_a values only give information about the roughness deviation from the centre line. However, they do not give any information on how that deviation is distributed. The mean spacing at the mean line roughness parameter (R_{Sm}) expresses the mean of the width of the profile curve elements in a sampling length. Looking at Figure 46, the surface roughness profile of the bag side has a few large peaks, so the R_{Sm} value is higher (1768.42µm) than the value obtained for the peel ply side (486.91µm), which has small peaks. R_{sm} essentially means peak spacing, so the higher the value the few the number of peaks (and vice versa). This parameter explains why the surface roughness profile of these two sides is different.

5.2.2 X-ray photoelectron spectroscopy (XPS) analysis

XPS is a technique that measures the elemental composition of the elements that exist at the surface in a material. It is an excellent way to analyse the changes in surface chemistry after exposing substrates to a treatment.

XPS spectra are generated by bombarding the surface of a material with a beam of X-rays. As the X-rays hit the surface, it emits electrons and kinetic energy, which can be measured to create the spectrum. Emission of electrons occurs over a range of different electron kinetic energies which can be recorded to produce a photoelectron spectrum. Each peak represents electrons off a particular characteristic energy emitted from the atoms. Each element has specific binding energy (BE), is the energy required to remove an electron from the atom or molecule. The energies and intensity of the photoelectron peaks enable identification and quantification of all surface elements (except hydrogen) [50, 76].

Chemical changes of the substrates were analysed using a VG Scientific ESCALAB MkII fitted with a Thermo Scientific Alpha 110 analyser and a Thermo Scientific XR3 digital X-ray source. Spot analysis on the samples was performed using an X-ray spot size of 3mm. The methodology employed in this analysis consisted of a low resolution survey scan with a pass energy of 300eV and 5 scans followed by a series of high resolution scans spanning each element detected in the survey with pass energies of between 20 and 80eV depending on element intensity.

The chemical composition of the pre-treated samples for both surfaces, peel ply and bag side, is presented in Table 29 and 30.

In these tables the calculation of hydrogen does not appear as XPS does not detect hydrogen as it does not possess core electrons [77].

Figure 47 and Figure 48 illustrates the X-ray photoelectron spectroscopy spectra of the surfaces treated (LSS values are also included in the table for comparison purposes). Appendix C collects the individual spectrum of each treatment, with their corresponding binding every value and the atomic concentrations.

Table 29 LSS values and XPS atomic concentrations of surface pre-treated peel ply side

Peel ply side							
Pre-treatment type	**LSS (MPa)**	**Atomic concentration (%)**					
		C	**O**	**N**	**S**	**Si**	**Zn**
PP	33.3	75.66	13.14	-	2.34	1.39	1.15
PP+Grit blast	39.9	61.81	22.41	8.91	2.76	0.72	0.17
PP+Plasma 5passes,100mm/min	36.7	37.90	36.71	12.84	6.30	1.03	-
PP+Plasma 1pass,1000mm/min	32.7	51.50	30.21	4.61	0.91	0.44	0.22

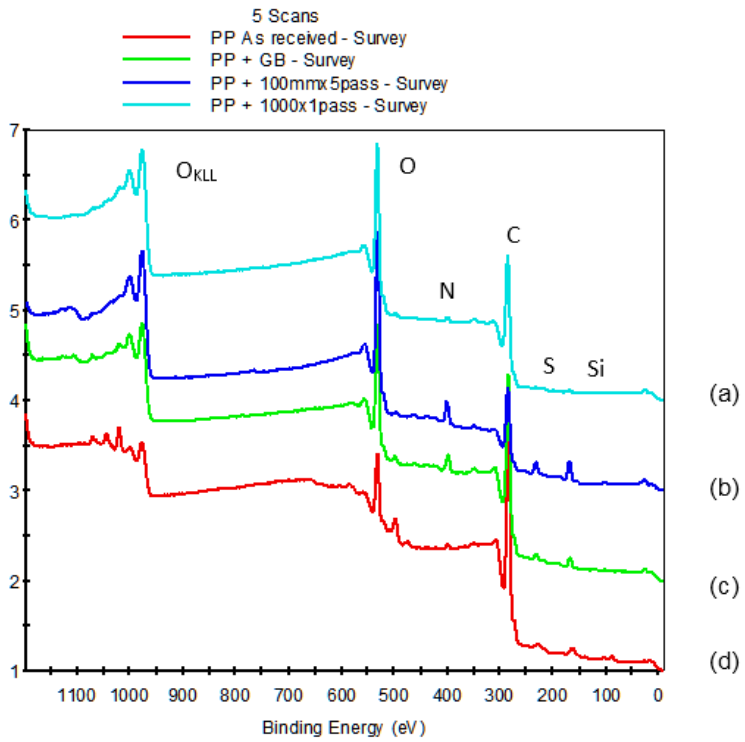

Figure 47 XPS spectra of surface pre-treated peel ply side: (a) peel ply+plasma, 1pass-1000mm/min; (b) peel ply+plasma, 5pass-100mm/min; (c) peel ply + grist blasting; (d) peel ply as received.

Carbon, oxygen, nitrogen and sulphur are elements expected to be present in epoxy composite resin. Small traces of silicon and zinc were also found in the peel ply surface. The concentration of these elements (Si and Zn) dropped after pre-treating the samples through grit blasting and plasma.

Through plasma pre-treatment is possible to see the oxidation effect as the surface oxygen concentration increased from 13% to 37%.

Table 30 XPS atomic concentrations of surface pre-treated bag side

Bag side							
Pre-treatment type	**LSS (MPa)**	**Atomic concentration (%)**					
		C	**O**	**N**	**F**	**S**	**Si**
As received	17.4	55.43	14.57	6.77	20.03	1.59	1.61
BS+Grit blast	40.8	66.77	21.96	7.49	-	2.74	1.04
BS+Plasma 5passes,100mm/min	42.8	35.45	32.79	13.11	9.77	7.03	1.85
BS+Plasma 1pass,1000mm/min	38	39.77	18.43	8.98	29.32	1.75	1.75

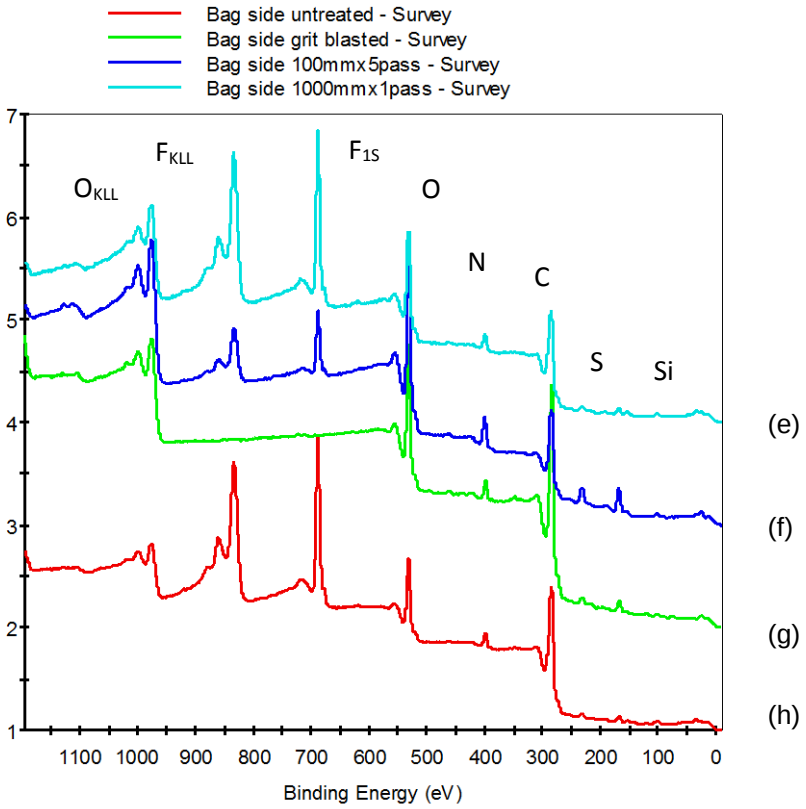

Figure 48 XPS spectra of surface pre-treated bag side: (e) bag side+plasma, 1pass-1000mm/min; (f) bag side+plasma, 5pass-100mm/min; (g) bag side+grist blasting; (h) bag side untreated.

For the bag side of the samples (before any pre-treatment) a measurable concentration of fluorine (F) was identified on the surfaces (20%). This fluorine is attributed to fluoropolymer from the release film used during the manufacturing of the composite laminates. This finding has been reported by other researchers in the field [78].

Checking Table 29 it was not possible to observe fluorine on the surfaces pre-treated through peel ply as the use of peel ply (as discussed several time along this thesis) prevents the occurrence of initial contamination.

Grit blasting pre-treatment was also successful in removing the fluorine. For the pre-treating of the surfaces using plasma, two conditions were analysed: the fastest pre-treatment (1pass, 1000mm/min) and the slowest one (5passes, 100mm/min). For the fastest period, the plasma did not have any effect for the removal of fluorine. In fact, the value of fluorine was higher (29.3%) than the one obtained for the bag side of the samples without any pre-treatment (20%).

In contrast, pre-treating the samples at lower speed (100mm/min) and increasing the number of passes from one to five produced a decrease in the fluorine concentration from 20% (no pre-treatment) to 10%. This fact shows again the efficiency of plasma as a surface cleaning method.

5.2.3 Wettability study

As explained in subchapter 2.1.3, the wettability is the capability of a liquid to wet and spread on a solid surface. This characteristic can be quantified measuring the contact angle formed by a liquid when is placed in a solid surface.

Young's equation [Formula 1] shows that there is a relationship between the contact angle (Θ), the surface free energy of the liquid (γ_l) and of the solid (γ_s) and the interfacial tension between the liquid and the solid (γ_{sl}) [32].

$$\gamma s = \gamma sl + \gamma l \times cos\theta \quad \text{[Formula 1]}$$

Contact angles were measured using a Drop Shape Analyser DSA100 from Kruss. Two solvents were employed to calculate the contact angles; water and di-iodomethane. As shown in Figure 4, when a liquid is applied and does not spread, a drop with a specific contact angle on the surface will be created.

Calculation of the contact angles was made measuring three different points on the samples with each solvent. Through the contact angles, the surface free energies were calculated using the Fowkes method in which surface free energy can be expressed by two components, the dispersive energy and the polar energy. The dispersive energy can be related to the surface roughness or topography; while the polar energy can be associated to the chemistry of the surface.

Table 31 and Figure 49 collect and represent respectively the values of the dispersive and polar components and the total surface free energy for the peel ply side (Table 31 also shows the LSS values for comparison purposes).

Table 31 Dispersive and polar components, and surface free energy values peel ply side with LSS values

Peel Ply Side				
Pre-treatment type	**Surface energy (mN/m)**			**LSS (MPa)**
	γ^d *	**γ^p ***	**γ ***	
Peel Ply + Manual Abrasion	45.62	0.78	46.40	38.4
Peel Ply	16.39	3.63	20.02	33.3
Peel Ply + Plasma.				
Conditions:	37.63	23.53	61.16	34.1
1pass, 100mm/min	38.26	21.67	59.93	35.1
1pass, 500mm/min	24.19	27.17	51.36	32.7
1pass, 1000mm/min	33.45	15.81	49.26	36.7
5passes, 100mm/min	33.62	19.26	52.88	33.6
5passes, 500mm/min	33.12	23.29	56.41	35.3
10passes, 100mm/min				
Peel Ply + Grit Blasting	43.25	4.13	47.38	39.9

*γ^d: dispersive component; γ^p: polar component; γ: surface free energy

The SD deviation is not illustrated in Figure 49 as only one measurement per pre-treatment was taken.

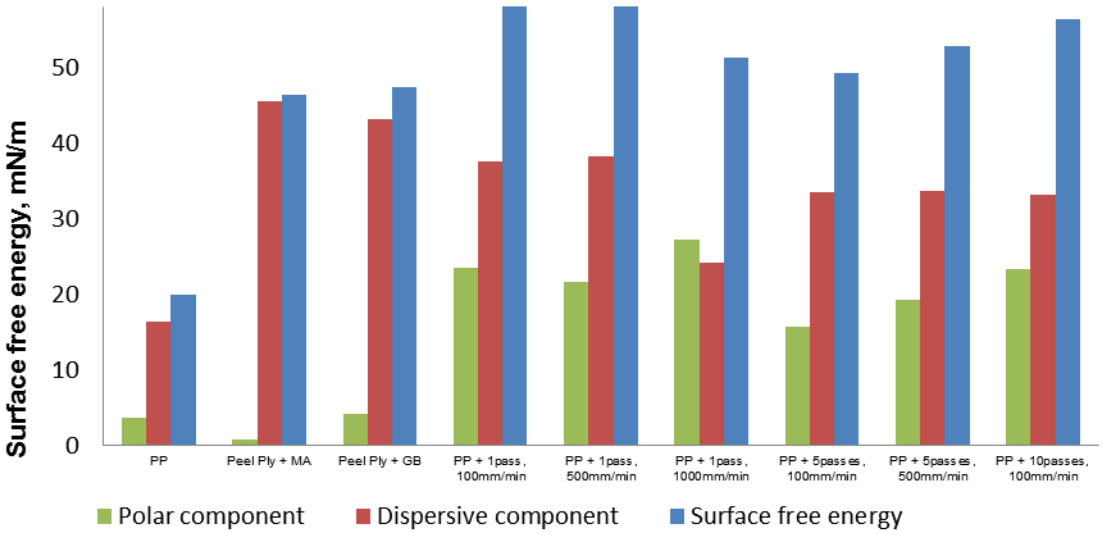

Figure 49 Comparison of surface free energy of the different pre-treatments on the peel ply side.

Looking at Figure 49, little polar contribution was found for grit blasted and manual abraded samples. These pre-treatments presented significantly higher surface free energy when compared with the peel ply samples (this is due to the improvement of the dispersive component in both pre-treatments).

In the samples that were pre-treated through plasma, a significant improvement in the surface free energy was observed. This is mostly through an increase in the polar component of the surface. This could imply two possible mechanisms; either the dispersive component (nonpolar) is being removed by plasma, or it is being functionalised by active species in the plasma.

Compared to the other pre-treatments, peel ply presented the lowest surface free energy (~20mN/m). However, the LSS value for the peel ply samples was similar to the LSS values obtained when pre-treating the samples through plasma (where the highest surface free energies were obtained). The surface free energy values did not have a direct impact in the strength of the joints. This indicates that once the surface possesses good wetting capability for the adhesive, there is no real relationship between bond strength and surface free energy.

The bag side of the adherents was also studied. Table 32 and Figure 50 display the values of the dispersive and polar components, and the total surface free energy for the bag side; Table 32 shows also the LSS values for comparison purposes.

Table 32 Dispersive and polar components, and surface free energy values bag side with LSS values

Bag Side				
Pre-treatment type	**Surface energy (mN/m)**			**LSS (MPa)**
	γ^d *	**γ^p ***	**γ ***	
Bag side + Plasma. Conditions:				
1pass, 100mm/min	20.89	33.83	54.71	39.4
1pass, 500mm/min	13.46	17.28	30.74	34.4
1pass, 1000mm/min	25.89	4.09	29.98	38.0
5passes, 100mm/min	33.31	7.85	41.16	42.8
5passes, 500mm/min	20.07	27.35	47.42	36.8
10passes, 100mm/min	31.18	22.24	53.42	41.1
Bag side + Manual Abrasion	30.97	3.37	34.34	34.7
Bag side + Grit Blasting	47.68	3.18	50.87	40.8
Bag side	19.97	0.52	20.50	17.4

*γ^d: dispersive component; γ^p: polar component; γ: surface free energy

The SD deviation is not illustrated in Figure 50 as only one measurement per pre-treatment was taken.

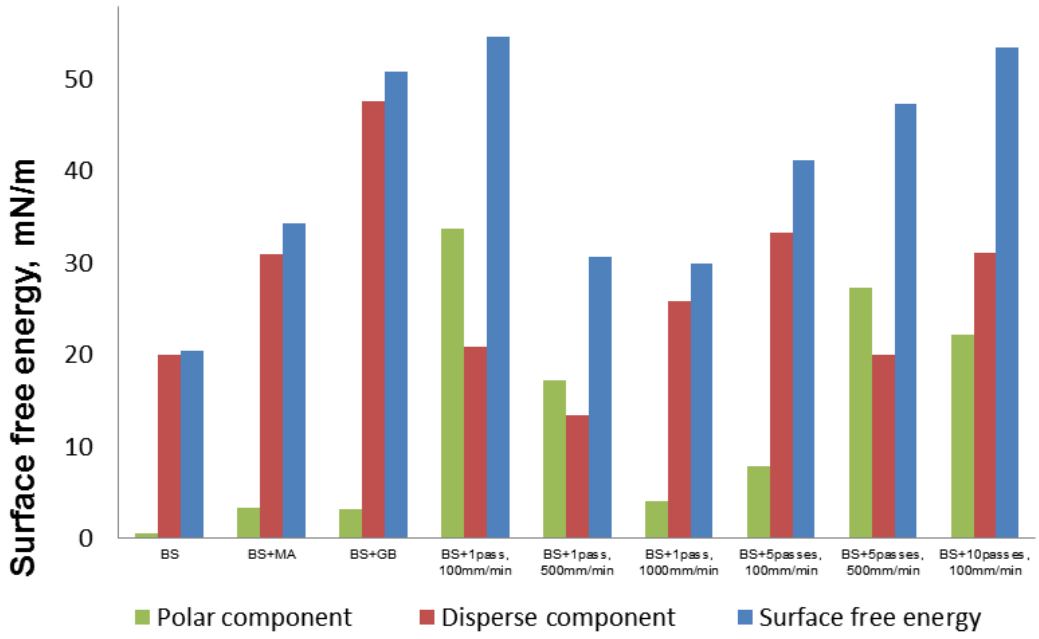

Figure 50 Comparison of surface free energy of the different pre-treatments on the bag side.

Figure 50 shows that both manually abraded and grit blasted samples exhibit higher total surface free energy compared to the samples without any pre-treatment. Comparing these pre-treatments (manual abrasion and grit blasting) against samples pre-treated through plasma, it is possible to observe an increase of the polar component and a decrease of the dispersive component. It is noticeable with the samples that were pre-treated with one plasma pass, that when decreasing the speed of the process, the polar component increases.

The lowest surface free energy value corresponded to the samples without any pre-treatment. These set of samples had the lowest LSS value due to contamination by fluorine found through XPS analysis, and the voids at the failure interface.

5.3 Adhesive void calculation

The void content at the joining interface may significantly affect the final strength of the joint. Computerised tomography (CT) was employed as non-destructive testing (NDT) technique to detect the voids at the bond line. This non-destructive test was carried out before the destructive testing (lap shear test).

CT imaging is a NDT technique which uses X-rays to create 2D and 3D sectional images of an object. These CT images can provide various characteristics about the internal structure of an object including defects, dimensions, shapes and density. This is achieved by passing an array of X-rays through an object and placing a series of detectors on the opposite side of the object which pick up the change in density or attenuation of these X-rays while they pass through the object.

Four samples were scanned to check the void content at the joining line. The equipment used was a HMXCT 225kV system from NIKON. This system possesses X-ray equipment that is capable of producing very small focal spots which are in the micro-focus range. This small focal spot size enables the

system to have high magnification levels which produce very high resolution CT scans.

Table 33 shows the samples scanned through CT and their void content. The void content was calculated through the software “Volume Graphics Software” (VGStudioMax 2.1) using the defect detection tool module to obtain the relevant information about voiding.

Table 33 Void content joint samples

Sample designation	Treatment Type	Void content (%)
S122-S123	Peel Ply side	7.09
S124-S125		8.04
S126-S127	Peel Ply side + plasma (5passes, 500mm/min)	8.01
S128-S129		9.55

Figure 51 shows an example of a CT scan of one of the joints assessed (S128-S129). In this figure, the white dots at the bonding area represent the ballotini beads added before the assembly of the joint. The black dots are the voids present at the bonding interface. It can be seen that the areas and size of the voids are not homogenous along the bonding interface.

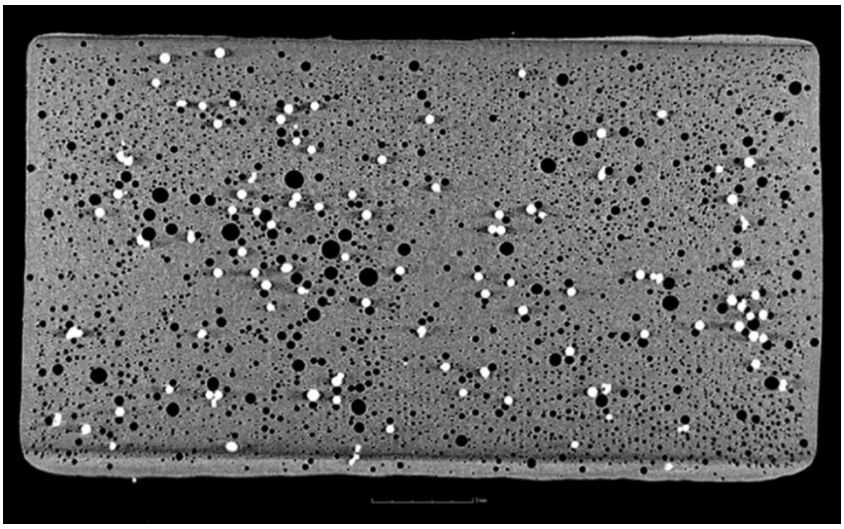

Figure 51 CT scan of the bonded area of sample S128-S129.

There is no specific standard that defines the allowed void content in components. The permitted porosity will depend on the component, its loading and the distribution of the porosity within the component. The aerospace industry is more restricted than the other industries in terms of void content; where more than 4% should be avoided (ideal situation would be 0%).

In this case, the samples assessed through CT had a void content in the range between 7-9.5%. In order to reduce the void concentration, a press to apply heat and pressure for the bonding can be used.

Figure 52 illustrates one of the images taken using VGStudioMax software.

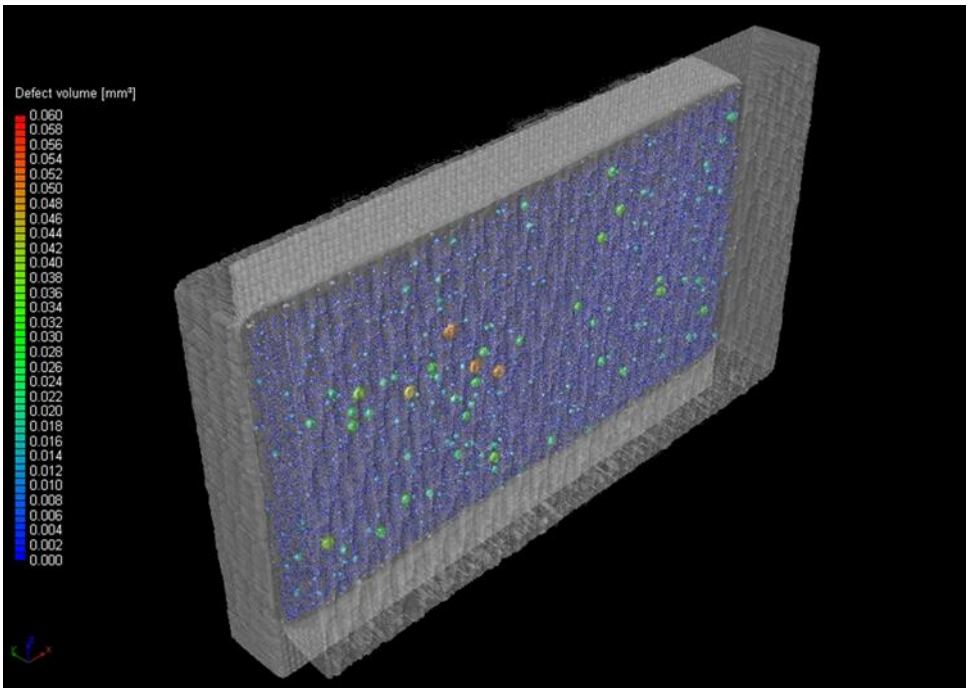

Figure 52 S128-S129 Void calculation using VGStudioMax 2.1.

6 Conclusions

The use of cold atmospheric plasma pre-treatment can be extended to new industrial areas of investigation, where different companies have already shown their interest, such as HEXCEL, Bombardier, and Rolls-Royce.

- It is known that the addition of the peel ply during the manufacturing process of composites protects the components from contamination. This has been proved by comparing the LSS values achieved for both sides of the composites. The bag side of the composites does not have the peel ply protection during the manufacturing process, and therefore this side is prone to contamination. This fact can be observed through the XPS analysis, where fluorine (coming from the release film used during the manufacturing process) is transferred to the composite side. Fluorine was not found in the peel ply side of the composite. The contamination of the bag side of the laminates (ie no peel ply) increases during the storage period of the composite components prior to bonding. Protecting the composite laminates with peel ply doubles the performance of the joint, making them 52% stronger.

- In the aerospace industry, the peel ply technique is widely used, either separately or in combination with mechanical roughening techniques (manual abrasion or grit blasting). This investigation has demonstrated that the strength of the joints is higher when combining peel ply with manual abrasion and grit blasting, rather than when using peel ply alone. Through these mechanical roughening techniques, the remains of the peel ply, coming from the removal of this ply, can be eliminated. Also, these techniques remove more resin from the substrates, and therefore, the underlying composite fibres will be highly exposed, leading to an improvement of the strength of the joint. When comparing grit blasting and manual abrasion, the strength value is higher for grit blasted samples than the abraded ones. This is due to the nature of the process. Through manual abrasion, an even treatment over the whole area is more difficult, due to

the inconsistent manual nature of the process. It is also important to highlight that through manual abrasion, the possible contamination left after removing the peel ply may transfer to the abrasive paper, and therefore could be transferred to other areas on the surface, rather than being removed.

- The strength of the bag side of the composites without any pre-treatment is increased by pre-treating the samples through manual abrasion, grit blasting, and plasma. It was observed that grit blasting and plasma pre-treatments (lowest speed process and 5 passes) were effective as cleaning methods, as there was no evidence of fluorine on the grit blasted samples, and the concentration of fluorine dropped considerably for the plasma pre-treated samples.

- The surface resulting from the tool can be characterised for the particular process used. However, this varies widely, and transfer levels change such that testing done on a tool surface is highly specific to the particular conditions used.

- Plasma pre-treatment of the peel ply side of the composite did not show a significant change in the LSS values compared with the samples just pre-treated with peel ply. Different plasma parameters have been varied in this research (number of passes and speed of the process). It was found that the highest LSS values for both sides of the composite material were achieved using the same conditions: five passes and 100mm/min (the lowest speed process selected for this research). For the peel ply side of the composite, the strength of the joints was improved by 10% compared with the samples with only peel ply. For the bag side of the composite, the strength of the joints without pre-treatment increased from 17.4MPa to 42.8MPa while pre-treating the bag side with plasma. This improvement is

essentially due to the effectiveness of the plasma as a cleaning method; as mentioned before, the bag side of the composite is prone to be contaminated as it is not protected prior to bonding. The key differentiator between both sides is their cleanliness.

- The effect of roughness measured did not have a major impact on the strength. The adhesive used in this research was very good at wetting the surfaces, regardless of roughness. For both sides, manual abrasion creates a surface that appears to be less rough than the substrate without pre-treatment. This is due to the nature of the process, as manual abrasion reduces the height of the original peaks.

- The surface free energy values did not have a direct impact on the strength of the joints. This indicates that once the surface possesses good wetting capability for the adhesive, there is no real relationship between bond strength and surface free energy.

- All the pre-treatments studied in this research have shown their effectiveness in removing contaminants. However, it is important to highlight that the failure mode in all the cases (except for the bag side of the samples without any pre-treatment) was cohesive, meaning that the adhesive failed. Therefore, it is difficult to understand the joint performance, as the adhesive is the limiting factor. More work will be carried out in the near future using a stronger adhesive which leads to failure at the interface between the adhesive and the adherent (adhesive failure).

References

[1] Soutis, C. (2005) ´Fibre Reinforced Composites in Aircraft Construction´, *Progress in Aerospace Sciences,* 41 (2), pp. 143-151.

[2] Park, S. Choi, W. Choi, H. Kwon, H. and Kim, H. (2010) ´Recent Trends in Surface Treatment Technologies for Airframe Adhesive Bonding Processing: A Review (1995-2008)´, *Journal of Adhesion,* 86 (2), pp. 192-221.

[3] Matthews, F. and Rawlings, R. ´Composites Materials: Engineering and Science´. London: Woodhead Publishing Limited, pp. 31.

[4] HEXCEL Composites (2008). Available at: http://www.hexcel.com

[5] Sharma, M. Gao, S. Mader, E. and Bijwe, J. (2014) ´Carbon Fiber Surfaces and Composite Interphases´, *Compos Sci Technol,* 102, pp. 35–50.

[6] Hull, D. and Clyne, T. (1996) ´An Introduction to Composite Materials´, *Cambridge Solid State Science Series*.

[7] HEXCEL Composites (2008). Available at: http://www.sec.gov/Archives/edgar/data/717605/000110465908021748/a08-9785_1defa14a.htm (Accessed: April 2008).

[8] Tserpes, I. and Pantelakis, S. (2013) ´Adhesive Bonding of Composite Aircraft Structures: Challenges and Recent Developments´, *Science China. Airworthiness and Fatigue*.

[9] Chang, T. (1998) ´Plasma Surface Treatment in Composites Manufacturing´, *Journal of Industrial Technology*, 15 (1).

[10] Gower, M. and Broughton B. ´Preparation and Testing of Adhesive Joints. Good Practice Guide No.47´, *Adhesive Design Toolkit*.

[11] Matthews, F. Kilty, P. and Godwin, E. (1982) ´A Review of the Strength of Joints in Fibre-Reinforced Plastics. Part 2. Adhesively Bonded Joints´, *Composites,* 13 (1), pp. 29-37.

[12] British Standard BS ISO 4588 and American Standard ASTM D2651 ´Adhesives – Guidelines for the surface preparation of metals´, and BS ISO 13895 or ASTM D2093 ´Adhesives – Guidelines for the surface preparation of plastics´.

[13] Molitor, P. Barron, V. and Young, T. (2001) ´Surface Treatment of Titanium for Adhesive Bonding to Polymer Composites: a Review´, *International Journal of Adhesion and Adhesives,* 21 (2), pp. 129-136.

[14] Zaldivar, R. Nokes, J. Steckel, G. Kim,H. and Morgan,B. (2010) ´The Effect of Atmospheric Plasma Treatment on the Chemistry, Morphology and resultant Bonding Behaviour of a PAN-based Carbon Fiber-Reinforced Epoxy Composite´, *Journal of Composite Materials,* 44 (2).

[15] Sanchez, J. Urena, A. Lazcano, S. and Blanco, T. (2015) ´New Approach to Surface Preparation for Adhesive Bonding of Aeronautical Composites: Atmospheric Pressure Plasma. Studies on the Pretreatment Lifetime and Durability of the Bondline´, *Composites Interfaces,* 22 (8), pp. 731-732.

[16] Matienzo, L. Venables, J, Fudge, J. and Velton, J. (1985) ´Surface Preparation for Bonding in Advanced Composites. Part I: Effect of peel ply materials and mold release agents on bond strenght´, *30th National Symposium*, pp.302.

[17] Wingfield, J. (1993) ´Treatment of Composite Surfaces for Adhesive Bonding´, *International Journal of Adhesion and Adhesives,* 13 (3), pp. 151-156.

[18] Wenz, R. and Pocius, A. (1985) ´Mechanical Surface Preparation of graphite-epoxy composites´, *SAMPE*, Sep/Oct:50.

[19] Hart-Smith, L. Redmond, G. and Davis, M. (1996) ´The Curse of Nylon Peel Ply´, *Douglas Aerospace and Royal Australian Air Force*, *41st SAMPE International SYMPOSIUM and Exhibition, California*. Available at: http://www.adhesionassociates.com/papers/35%201996%20Curse%20of%20Nylon%20Peel%20Ply,%20SAMPE%20(Anaheim)%20MDC%20950072.pdf.

[20] Head, P. and Hollaway, L. (2001) ´Advance Polymer Composites and Polymers in the Civil Infrastructure´, Oxford: Elsvier Science, First edition, pp. 121-123.

[21] Flinn, B. Clark, B. Satterwhite, J. and Van Voast, P. (2007) ´Influence of Peel Ply of type on Adhesive Bonding of Composites´, *SAMPE Annual Technical Conference (Baltimore)*.

[22] Kinloch, A. (1987) ´Adhesion and Adhesives´, *British Polymer Journal,* 20 (3), pp. 123-127.

[23] Waghorne, R. and Parker, B. (1982) ´Surface Treatment of Carbon Fibre Reinforced Composites for Adhesive Bonding´, *Composites,* 13 (3), pp. 280-288.

[24] Stone, M. (1981) ´Effect of the Degree of Abrasion of Composite Surfaces on the Strengths of Adhesively Bonded Joints´, *International Journal of Adhesion and Adhesives,* 1 (5), pp. 271-272.

[25] BTG Labs and Abaris Training , ´Webinar: Measuring Surface Energy in Manufacturing and Repair of Composites to Assure Quality of Bonded Interfaces´. Available at:

https://attendee.gotowebinar.com/recording/viewRecording/1519109828557636099/6105965576695229452/matthew.cleaver@hexcel.com.

[26] Hart-Smith, L. Redmond, L. and Davis, M. (1996) ´The Curse of the Nylon Peel Ply (Mc Donnell Douglas Aerospace and Royal Australian Air Force)´, *41st Sampe International Symposium and Exhibition*, (California).

[27] Eliezer, S. and Eliezer, Y. (1989) ´The Fourth State of Matter: An Introduction to the Physics of Plasma´, (Bristol and Philadelphia).

[28] Chang, J. and Chen, F. (2002) ´Principals of Plasma Processing´, Los Angeles: Plenum / Kuvler Publishers.

[29] Scott, W. (2013) ´PhD Thesis: Surface Modification by Atmospheric Pressure Plasma for Improved Bonding´, University of California.

[30] Selwyn, G. Herrmann, H. Park, J. and Henins, I. (2001) ´Materials Proccesing using an Atmospheric Pressure, RF-Generated, Plasma Source´, *Contributions to Plasma Physics,* 41 (6), pp. 610-619.

[31] Strobel, M. Lyons, C. and Mittal, K. (1994) ´Plasma Surface Modification of Polymers: Relevance to Adhesion´, (The Netherlands).

[32] Shaw, S. Comyn, J. and Mascia, L. (1996) ´Surface Treatment and Bonding of Thermoplastic Composites´, *83rd Meeting of the AGARD SMP on "Bolted/Bonded Joints in Polymeric Composites,* (Italy).

[33] Hart, R. ´Contact Angle Goniometers´. Available at: http://www.ramehart.com/contactangle.htm.

[34] Sato, C. Sekiguchi, Y. Okamoto, H. Shimamoto, K. Katano, M. Naito, K. Kuratani, Y. Okayama, T. Katano, A. Hamaguchi, Y. Kufumoto, T. and Furukawa, K. (2014) ´Evaluation of Surface Treatments for Adhesion of Thermoplastics Composites for Automotive Use´, *ECCM16-16th European Conference on Composite Materials*, (Spain).

[35] Kusano, Y. Mortensen, H. Stenum, B. Kingshott, P. Andersen, T. and Brondsted, P. (2007) ´Atmospheric Pressure Plasma Treatment of Glass Fibre Composite for Adhesion Improvement´, *Plasma Processes and Polymers,* vol. 4.

[36] Palleiro, C. Stepanov, S. Rodriguez-Senin, E. Wilken, R. and Ihde, J. (2015) ´Atmospheric Pressure Plasma Surface Treatment of Thermoplastic Composites for Bonded Joints´, *20th International Conference on Composite Materials*, (Denmark).

[37] Blackman, B. Kinloch, A. and Watts, J. (1994) ´The Plasma Treatment of Thermoplastic Fibre Composites for Adhesive Bonding´, *Composites,* 25 (5), pp. 332-341.

[38] Benedictus, R. Bhowmik, S. and Iqbal, H. (2010) ´Surface Modification of High Performance Polymers by Atmospheric Pressure Plasma and Failure Mechanism of Adhesive Bonded Joints´, *International Journal of Adhesion and Adhesives,* vol. 30, pp. 418-424.

[39] Noeske, M. Degenhardt, J. Strudthoff. S and Lommatzsch. U (2004) ´Plasma Jet Treatment of five Polymers at Atmospheric Pressure: Surface Modification and the Relevance for Adhesion´, *International Journal of Adhesion and Adhesives,* vol. 24, pp. 171-177.

[40] Zaldivar, R. Kim, H. Steckel, G. and Patel, D. (2011) ´Surface Preparation for Adhesive Bonding of Polycyanurate-based fiber-reinforced Composites using atmospheric plasma treatment´, *Journal of Applied Polymer Science,* vol. 120, pp. 921-931.

[41] Barankova, H. and Bardos, L. (2010) ´Cold atmospheric plasma: sources, process and applications´, *Thin Solid Films,* vol. 518, pp. 6705-6713.

[42] Sanchez, J. Urena, A. and Lazcano, S. (2011) ´Effects of Atmospheric Pressure Plasma as Surface Treatment for Adhesive Bonding of Aeronautical Epoxy/Carbon Fibre Composite Laminates´, (Spain: Costa, J. and Guemes, A. MatComp11).

[43] Sanchez, J. Urena, A. Lazcano, S. and Blanco, T. (2013) ´Evaluation of Atmospheric Plasma as Surface Pre-Treatment for Fibre-Reinforced Thermosets prior Structural Assembly by Adhesive Bonding´.

[44] Law, V. Mohan, J. O'Neil, F. and Ivankovic, A. (2014) ´Air based Atmospheric Pressure Plasma Jet Removal of Frekote 710-NC prio to Composite-Composite Adhesive Bonding´, *International Journal of Adhesion and Adhesives,* vol. 54, pp. 72-81.

[45] Zaldivar, R. Steckel, G. Morgan, B. Nokes, J. and Kim, H. (2012) ´Bonding Optimization on Composite Surfaces using Atmospheric Plasma Treatment´, *Adhesion and Adhesives,* vol. 26, pp. 381-401.

[46] O'Flynn, K. Dobbyn, P. and Dowling, D. (2015) ´Application of Atmospheric Plasma Treatments to Enhance the Mechanical Properties of Unsized Carbon/Fibre Epoxy Composites´, *20th International Conference on Composite Materials.*

[47] Baghery, M. Mousavi, A. Nosratian, E. and Haji, A. (2016) ´Influence of oxygen plasma treatment parameters on the properties of carbon fiber´, *Journal of Adhesion Science and Technology*.

[48] Tendero, C. Tixier, C. Tristant, P. Desmaison, J. and Leprince. P (2006) ´Atmospheric Pressure Plasmas: A Review´, *Spectrochimica Acta Part B,* 2 (30).

[49] Jõgi, I. (2011) PlasTEP ´Methods of plasma generation and plasma sources´Available at: http://www.plastep.eu/fileadmin /dateien/Events/ 2011/110725_ Summer_School /Joegi_SummerSchool_2011_Part1.pdf.

[50] Williams, D. (2013) ´Master Thesis: Flame Treatment of Polypropylene: A Study by Electron and Ion Soectroscopies´, University of Surrey.

[51] Kim, J. and Lee, D. (2003) ´Ultraviolet Surface Treatment for Adhesion Strenght Improvement of Carbon/Epoxy Composites´, *Adhesion Science and Technology´*, 17 (1), pp. 1523-1542.

[52] Lecomte, J. (1996) ´The Assembly of Thermoplastics by Adhesive Bonding: Process and Control´, *83rd Meeting of the AGARD SMP on "Bolted/Bonded Joints in Polymeric Composites*, (Italy).

[53] Adhesive Bonder Best Practice Guide (2013), *TWI Training School*, (Cambridge).

[54] Design Guidance - Joint Types. Adhesives Design Toolkit (TWI, NPL, ESR Technology and MERL). Available at: http://www.adhesivestoolkit.com/ Toolkits/ Design Guidance/ JointTypes.xtp.

[55] Bond, D. and Davis, M. (1999) ´The Importance of Failure Mode Identification in Adhesive Bonded Aircraft Structures and Repairs´, *Composites Materials*, (Paris).

[56] Davs, M. and McGregor, A. (2010) ´Assesing Adhesive Bond Failures: Mixed-Mode Bond Failures Explained´, in *ISASI, Australian Safety Seminar*, (Canberra).

[57] Flinn, B. Aubin, J. and Hickmott, C. ´Improving Adhesive Bonding of Composites through Surface Characterization, Role of Surface Preparation on Durability of Bonded Composite Joints´, (University of Washington).

[58] Williams, T. Yu, H. Yeh, P. Yang, J. and Hicks, R. (2014) ´Atmospheric Pressure Plasma Effects on the Adhesive Bonding Properties of Stainless Steel and Epoxy Composites´, *Journal of Composite Materials,* 48 (2), pp. 219-233.

[59] British Standard ISO 10365 ´Adhesives – Designation of Main Failure Patterns´.

[60] Atherton, M. and Jussel, R. ´Improve Product Development using QFD´, appeared in the first quarter edition of *Measuring Business Excellence*, 4 (1).

[61] Mares, C. (2016) ´Principles of Aircraft Design´. Brunel University.

[62] Hexcel Composites, ´HexPly Prepreg Technology (2013)´, Available at: http://www.hexcel.com/Resources/DataSheets/Brochure-Data-Sheets/Prepreg_Technology.pdf.

[63] Hexcel Composites, ´Product Data Sheet HexPly 8552´. Available at: http://www.hexcel.com/Resources/DataSheets/Prepreg-Data-Sheets/8552_us.pdf

[64] Hexcel Composites, ´Product Data Redux 312´, March 2015. Available at: http://www.hexcel.com/Resources/DataSheets/Adhesives-Data-Sheets/312_eu.pdf

[65] Sigma Life Sciences ´Product Data Sheet Glass Beads´. Available at: www.sigmaaldrich.com/catalog/product/sigma

[66] GMA Garnet Group, ´Optimum Setup for Waterjet Cutting´, Available at: http://www.garnetsales.com/wp-content/uploads/2014/05/GMA-Garnet%E2%84%A2-Waterjet-Cutting-2013.pdf.

[67] British standard BS ISO 4587 ´Adhesive – Determination of tensile lap-shear strength of rigid-to-rigid bonded assemblies´.

[68] Landrock, A. (1985) Adhesive Technology Handbook. Noyes Publications.

[69] Henkel Corporation, ´Hysol® Surface Preparation Guide´. Available at: http://www.loctite.ph/php/content_data/LT4536_TT_Aerospace_Surface_Preparation_Guide.pdf.

[70] Wegman, R. and Twisk, J. (2012) Surface Preparation Techniques for Adhesive Bonding, Second Edition, Elseiver.

[71] TWI Ltd, ´Unpublished TWI report´ (Cambridge, 2015).

[72] British Strandard ISO 4587: 2003, *´Adhesives - Determination of tensile lap-shear strenght of rigid-to-rigid bonded assemblies´*.

[73] Nield, D. (2016) Science Alert, ´There's a scientific reason for why plane windows are always round´. Available at: http://www.sciencealert.com/watch-there-s-a-scientific-reason-for-why-aeroplane-windows-are-always-round.

[74] British Strandard ISO 4288: 1998, ´Geometric Product Specification – Surface Texture – Profile Method: Rules and procedures for the assessment of surface texture, Table 1´.

[75] Boutar, Y. Naimi, S. Mezlini, S. Hamdaouui M. and Ali, M. (2016) ´Effect of Adhesive Thickness and Surface Roughness on the Shear Strenght of Aluminiun one-

component Polyurethane Adhesive single-lap Joints for Automotive Applications´. *Journal of Adhesion Science and Technology,* 30 (17), pp. 1913-1929.

[76] Thermo Scientific, ´XPS Simplified´. Available at: http://xpssimplified.com/whatisxps. php.

[77] Stojilovic, N. (2012) ´Why can't we see Hydrogen in X-Ray Photoelectron Spectroscopy?´, *Journal of Chemical Education,* 89 (10), pp. 1331-1332, 2012.

[78] Damico, D. Wilkinson, T. and Niks, S. (1994) ´Surface Pretreatment and Adhesive Bonding of Carbon Fiber-Reinforced Epoxy Composites´, *Composite Bonding* (USA).

Appendix A:

Measurements Samples

Table A1 Width and thickness of composite samples

Sample designation	Width (mm)	Thickness (mm)		Sample designation	Width (mm)	Thickness (mm)		Sample designation	Width (mm)	Thickness (mm)
S001	25.04	3.22		**S058**	24.99	3.25		**S115**	24.98	3.19
S002	25.10	3.15		**S059**	25.04	3.17		**S116**	25.01	3.16
S003	25.11	3.16		**S060**	24.99	3.18		**S117**	24.94	3.16
S004	25.07	3.14		**S061**	25.04	3.14		**S118**	25.03	3.15
S005	25.06	3.14		**S062**	24.97	3.14		**S119**	24.95	3.15
S006	25.06	3.15		**S063**	24.98	3.14		**S120**	24.99	3.15
S007	25.06	3.14		**S064**	24.95	3.14		**S121**	25.04	3.14
S008	25.10	3.14		**S065**	25.01	3.12		**S122**	25.00	3.13
S009	25.14	3.13		**S066**	25.02	3.15		**S123**	25.07	3.12
S010	25.06	3.13		**S067**	25.01	3.13		**S124**	25.00	3.13
S011	25.11	3.12		**S068**	25.00	3.13		**S125**	25.09	3.15
S012	25.16	3.12		**S069**	25.14	3.15		**S126**	25.11	3.14
S013	25.16	3.14		**S070**	25.02	3.14		**S127**	25.09	3.14
S014	25.12	3.14		**S071**	25.04	3.15		**S128**	25.06	3.15
S015	25.04	3.11		**S072**	25.01	3.13		**S129**	25.09	3.13
S016	25.13	3.14		**S073**	25.06	3.15		**S130**	25.07	3.15
S017	25.12	3.15		**S074**	25.14	3.16		**S131**	25.07	3.17
S018	25.18	3.15		**S075**	25.14	3.15		**S132**	25.13	3.19
S019	25.08	3.19		**S076**	25.04	3.16		**S133**	24.99	3.22
S020	25.05	3.20		**S077**	25.02	3.12		**S134**	24.81	3.19
S021	25.10	3.16		**S078**	25.04	3.04		**S135**	24.93	3.15
S022	25.01	3.18		**S079**	25.04	3.09		**S136**	24.86	3.16
S023	25.10	3.15		**S080**	25.05	3.00		**S137**	24.91	3.14
S024	24.99	3.15		**S081**	25.01	3.00		**S138**	24.83	3.14
S025	25.05	3.15		**S082**	25.08	3.05		**S139**	24.84	3.14
S026	25.10	3.15		**S083**	25.08	3.08		**S140**	24.80	3.14
S027	25.06	3.16		**S084**	25.16	3.11		**S141**	24.84	3.15
S028	25.17	3.14		**S085**	25.13	3.06		**S142**	24.86	3.12
S029	25.06	3.15		**S086**	25.16	3.05		**S143**	24.86	3.12

Sample designation	Width (mm)	Thickness (mm)		Sample designation	Width (mm)	Thickness (mm)		Sample designation	Width (mm)	Thickness (mm)
S030	25.14	3.18		**S087**	25.12	3.08		**S144**	24.94	3.13
S031	25.16	3.14		**S088**	25.10	3.07		**S145**	24.95	3.13
S032	25.18	3.15		**S089**	25.19	3.05		**S146**	24.94	3.15
S033	25.13	3.15		**S090**	25.13	3.04		**S147**	24.91	3.16
S034	25.07	3.15		**S091**	25.06	3.11		**S148**	24.94	3.15
S035	25.13	3.17		**S092**	25.18	3.04		**S149**	24.95	3.15
S036	25.11	3.17		**S093**	25.13	3.01		**S150**	24.92	3.15
S037	25.21	3.16		**S094**	25.21	3.02		**S151**	24.91	3.17
S038	25.10	3.21		**S095**	25.22	3.02		**S152**	24.92	3.21
S039	24.91	3.22		**S096**	24.95	3.22		**S153**	24.87	3.18
S040	25.04	3.19		**S097**	25.08	3.14		**S154**	24.96	3.16
S041	24.94	3.19		**S098**	25.04	3.16		**S155**	24.93	3.16
S042	24.99	3.14		**S099**	25.00	3.14		**S156**	24.97	3.14
S043	24.92	3.15		**S100**	24.99	3.14		**S157**	24.91	3.14
S044	24.91	3.16		**S101**	24.98	3.14		**S158**	24.91	3.12
S045	24.89	3.16		**S102**	24.98	3.13		**S159**	24.87	3.12
S046	24.95	3.15		**S103**	25.04	3.14		**S160**	24.93	3.13
S047	24.95	3.16		**S104**	25.07	3.14		**S161**	24.91	3.13
S048	24.97	3.15		**S105**	25.00	3.13		**S162**	24.92	3.14
S049	25.01	3.14		**S106**	25.04	3.13		**S163**	24.90	3.15
S050	25.02	3.13		**S107**	25.09	3.13		**S164**	24.99	3.14
S051	25.01	3.15		**S108**	25.09	3.14		**S165**	24.94	3.15
S052	24.99	3.13		**S109**	25.07	3.14		**S166**	24.97	3.15
S053	25.02	3.13		**S110**	24.98	3.15		**S167**	24.92	3.14
S054	25.05	3.15		**S111**	25.07	3.17		**S168**	24.97	3.16
S055	25.00	3.15		**S112**	25.03	3.17		**S169**	25.03	3.05
S056	25.01	3.17		**S113**	25.08	3.18		**S170**	25.04	3.07
S057	25.02	3.22		**S114**	25.01	3.25		**S171**	24.97	3.08
S172	24.96	2.96		**S229**	25.03	3.13		**S286**	25.21	3.13
S173	25.00	3.03		**S230**	25.04	3.12		**S287**	25.12	3.15
S174	25.01	3.03		**S231**	25.05	3.13		**S288**	25.10	3.15

Sample designation	Width (mm)	Thickness (mm)		Sample designation	Width (mm)	Thickness (mm)		Sample designation	Width (mm)	Thickness (mm)
S175	25.03	3.00		**S232**	25.07	3.12		**S289**	25.21	3.13
S176	25.01	3.02		**S233**	25.09	3.14		**S290**	25.17	3.13
S177	25.04	3.03		**S234**	25.07	3.14		**S291**	25.17	3.13
S178	25.03	3.05		**S235**	25.10	3.15		**S292**	25.11	3.13
S179	25.06	3.06		**S236**	25.05	3.13		**S293**	25.08	3.13
S180	25.04	3.05		**S237**	25.05	3.11		**S294**	25.11	3.13
S181	25.06	2.99		**S238**	25.08	3.12		**S295**	25.16	3.12
S182	25.03	3.00		**S239**	24.89	3.13		**S296**	25.06	3.13
S183	25.03	3.08		**S240**	24.91	3.13		**S297**	24.92	3.14
S184	25.09	3.03		**S241**	25.01	3.13		**S298**	25.05	3.15
S185	25.03	3.03		**S242**	25.02	3.14		**S299**	25.11	3.14
S186	24.99	3.05		**S243**	24.97	3.14		**S300**	25.06	3.15
S187	25.09	3.06		**S244**	24.97	3.13		**S301**	25.03	3.14
S188	25.04	3.05		**S245**	24.90	3.15		**S302**	24.95	3.15
S189	25.11	3.03		**S246**	24.89	3.15		**S303**	25.10	3.14
S190	25.13	3.08		**S247**	24.95	3.15		**S304**	25.07	3.13
S191	25.12	3.14		**S248**	25.01	3.12		**S305**	25.13	3.06
S192	25.03	3.15		**S249**	25.06	3.15		**S306**	25.21	3.10
S193	25.00	3.13		**S250**	25.05	3.14		**S307**	25.21	3.10
S194	25.08	3.13		**S251**	25.10	3.12		**S308**	25.29	3.09
S195	25.01	3.14		**S252**	25.06	3.13		**S309**	25.22	3.10
S196	25.07	3.13		**S253**	25.06	3.13		**S310**	25.24	3.09
S197	25.03	3.13		**S254**	25.04	3.11		**S311**	25.17	3.10
S198	24.94	3.13		**S255**	25.04	3.11		**S312**	25.24	3.10
S199	25.01	3.13		**S256**	25.04	3.10		**S313**	25.16	3.09
S200	25.05	3.12		**S257**	25.04	3.09		**S314**	25.17	3.10
S201	24.96	3.15		**S258**	25.00	3.12		**S315**	25.15	3.10
S202	24.84	3.15		**S259**	24.95	3.12		**S316**	25.07	3.10
S203	24.96	3.12		**S260**	24.98	3.13		**S317**	25.12	3.11
S204	25.02	3.13		**S261**	25.04	3.13		**S318**	25.20	3.11
S205	24.94	3.13		**S262**	25.03	3.12		**S319**	25.06	3.12

Sample designation	Width (mm)	Thickness (mm)		Sample designation	Width (mm)	Thickness (mm)		Sample designation	Width (mm)	Thickness (mm)
S206	24.91	3.16		**S263**	24.97	3.14		**S320**	25.08	3.13
S207	24.85	3.15		**S264**	24.83	3.15		**S321**	25.05	3.12
S208	24.99	3.15		**S265**	24.87	3.14		**S322**	25.07	3.11
S209	24.99	3.15		**S266**	24.92	3.15		**S323**	25.09	3.07
S210	25.04	3.13		**S267**	25.10	3.01		**S324**	25.11	3.10
S211	25.10	3.12		**S268**	25.16	3.08		**S325**	25.10	3.11
S212	25.09	3.13		**S269**	25.10	3.03		**S326**	25.11	3.14
S213	25.13	3.12		**S270**	25.14	3.05		**S327**	25.16	3.12
S214	25.15	3.14		**S271**	25.12	3.06		**S328**	25.18	3.12
S215	25.13	3.15		**S272**	25.13	3.07		**S329**	25.17	3.11
S216	25.05	3.14		**S273**	25.07	3.05		**S330**	25.20	3.13
S217	25.14	3.13		**S274**	25.06	3.03		**S331**	25.14	3.11
S218	25.06	3.13		**S275**	25.10	3.05		**S332**	25.15	3.13
S219	25.08	3.12		**S276**	25.05	3.06		**S333**	25.19	3.14
S220	25.03	3.11		**S277**	25.01	3.03		**S334**	25.01	3.12
S221	24.98	3.11		**S278**	24.95	3.01		**S335**	25.00	3.12
S222	25.06	3.14		**S279**	25.02	3.03		**S336**	25.09	3.13
S223	25.11	3.14		**S280**	25.03	3.05		**S337**	25.11	3.12
S224	25.00	3.13		**S281**	24.98	3.03		**S338**	25.05	3.12
S225	25.02	3.15		**S282**	24.92	3.02		**S339**	25.06	3.12
S226	25.00	3.16		**S283**	24.98	3.06		**S340**	25.01	3.12
S227	25.04	3.15		**S284**	25.02	3.06		**S341**	24.95	3.11
S228	25.05	3.15		**S285**	24.85	3.00		**S342**	25.00	3.13
S343	25.10	3.13		**S369**	25.17	2.97		**S395**	25.06	3.14
S344	25.19	3.14		**S370**	25.19	2.98		**S396**	25.07	3.13
S345	25.14	3.14		**S371**	25.18	2.94		**S397**	25.14	3.15
S346	25.20	3.12		**S372**	25.12	2.94		**S398**	25.21	3.15
S347	25.17	3.12		**S373**	25.07	3.05		**S399**	25.13	3.12
S348	25.16	3.12		**S374**	25.12	3.05		**S400**	25.02	3.06
S349	25.16	3.13		**S375**	25.14	3.06		**S401**	24.97	3.09
S350	25.15	3.13		**S376**	25.08	3.04		**S402**	24.90	3.10
S351	25.18	3.14		**S377**	25.01	3.09		**S403**	24.95	3.11

Sample designation	Width (mm)	Thickness (mm)		Sample designation	Width (mm)	Thickness (mm)		Sample designation	Width (mm)	Thickness (mm)
S352	25.16	3.13		**S378**	25.10	3.04		**S404**	24.95	3.08
S353	25.11	3.10		**S379**	25.10	3.08		**S405**	24.96	3.10
S354	25.05	3.12		**S380**	24.97	3.01		**S406**	24.94	3.09
S355	25.09	3.14		**S381**	24.94	3.13		**S407**	24.96	3.08
S356	25.14	3.13		**S382**	24.96	3.15		**S408**	24.90	3.08
S357	25.13	3.16		**S383**	24.97	3.15		**S409**	24.99	3.11
S358	25.08	3.14		**S384**	25.04	3.15		**S410**	24.92	3.09
S359	24.92	3.12		**S385**	25.00	3.14		**S411**	24.96	3.09
S360	24.97	3.14		**S386**	24.97	3.16		**S412**	25.04	3.06
S361	25.03	3.13		**S387**	24.90	3.14		**S413**	25.05	3.07
S362	25.20	2.99		**S388**	24.99	3.13		**S414**	25.07	3.05
S363	25.24	3.00		**S389**	24.99	3.12		**S415**	25.09	3.09
S364	25.19	3.01		**S390**	25.04	3.13		**S416**	25.11	3.11
S365	25.25	2.99		**S391**	24.91	3.11		**S417**	25.16	3.08
S366	25.22	3.01		**S392**	24.95	3.12		**S418**	25.09	3.05
S367	25.22	2.98		**S393**	25.06	3.13				
S368	25.18	2.99		**S394**	25.05	3.14				

Appendix B:

Experimental Results – LSS values

Table B1 LSS values and failure type: peel ply side plus grit blasting pre-treatment

OUTPUT: Mechanical Testing				
#	**Sample designation**	**Max. Load (kN)**	**LSS (MPa)**	**Failure Type**
1	S181-S182	12.9	41.2	Cohesive (Delamination)
2	S183-S184	12.5	39.9	
3	S185-S206	12.5	40.1	
4	S207-S208	12.9	41.4	
5	S209-S210	11.7	37.4	
			Mean: 39.9MPa Standard deviation: 1.4MPa COV (%): 3.5	

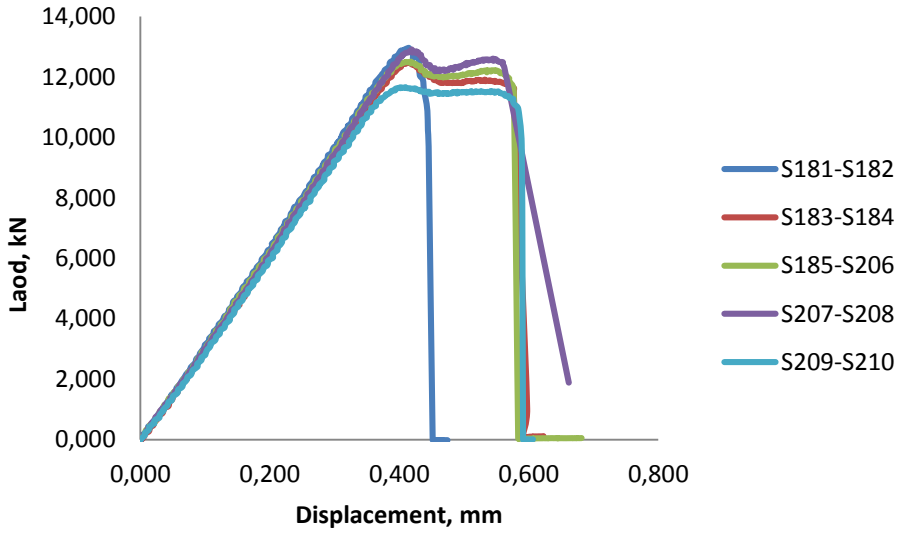

Figure B1 Load values versus displacement: peel ply side plus grit blasting pre-treatment.

Table B2 LSS values and failure type: peel ply plus manual abrasion pre-treatment

OUTPUT: Mechanical Testing				
#	**Sample designation**	**Max. Load (kN)**	**LSS (MPa)**	**Failure Type**
1	S186-S187	12.4	39.6	Cohesive Adhesive
2	S188-S189	11.6	37.0	
3	S190-S191	12.3	39.1	
4	S192-S193	12.3	39.3	
5	S194-S195	11.6	37.0	
			Mean:38.4 MPa Standard deviation: 1.1 MPa COV (%): 3.0	

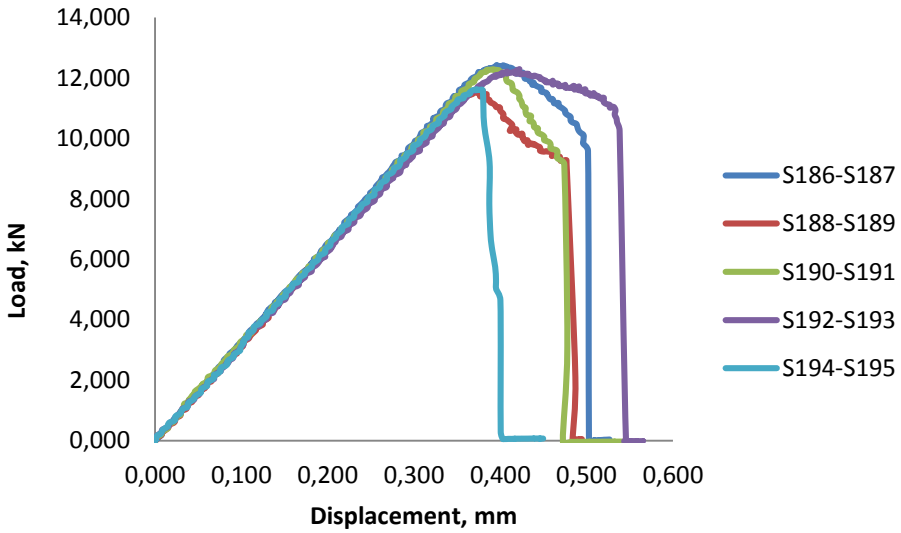

Figure B2 Load values versus displacement: peel ply plus manual abrasion pre-treatment.

Table B3 LSS values and failure type: peel ply pre-treatment

OUTPUT: Mechanical Testing				
#	**Sample designation**	**Max. Load (kN)**	**LSS (MPa)**	**Failure Type**
1	S196-S197	10.4	33.2	Cohesive
2	S198-S199	10.8	34.6	
3	S200-S202	10.5	33.7	
4	S201-S203	9.9	31.7	
5	S204-S205	10.5	33.6	
			Mean: 33.3MPa Standard deviation: 0.9MPa COV (%): 2.7	

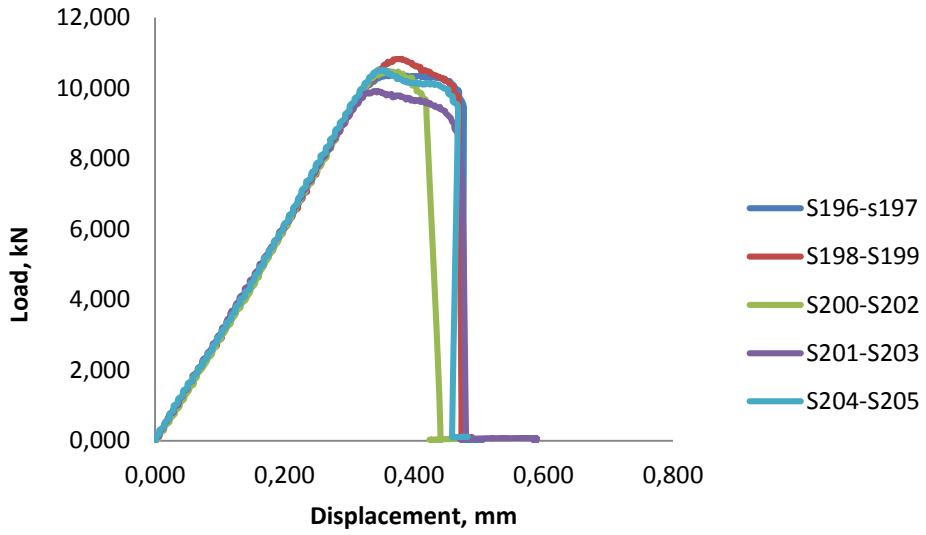

Figure B3 Load values versus displacement: peel ply pre-treatment.

Table B4 LSS value and failure type: peel ply side plus plasma pre-treatment (1pass, 500mm/min)

Plasma Parameters				
Gas Flow: 8l/min				
Gas type: Argon + Air				
Treatment distance, d=4mm				
Speed, v=500mm/min				
Number of passes =1				

	1	5	10
100			
500	✖		
1000			

OUTPUT: Mechanical Testing				
#	**Sample designation**	**Max. Load (kN)**	**LSS (MPa)**	**Failure Type**
1	S112-S113	11.1	35.6	Cohesive
2	S114-S115	11.3	36.1	
3	S116-S117	11.1	35.5	
4	S118-S119	10.6	33.9	
5	S120-S121	10.8	34.7	
			Mean: 35.1MPa Standard deviation: 0.7MPa COV (%):1.9	

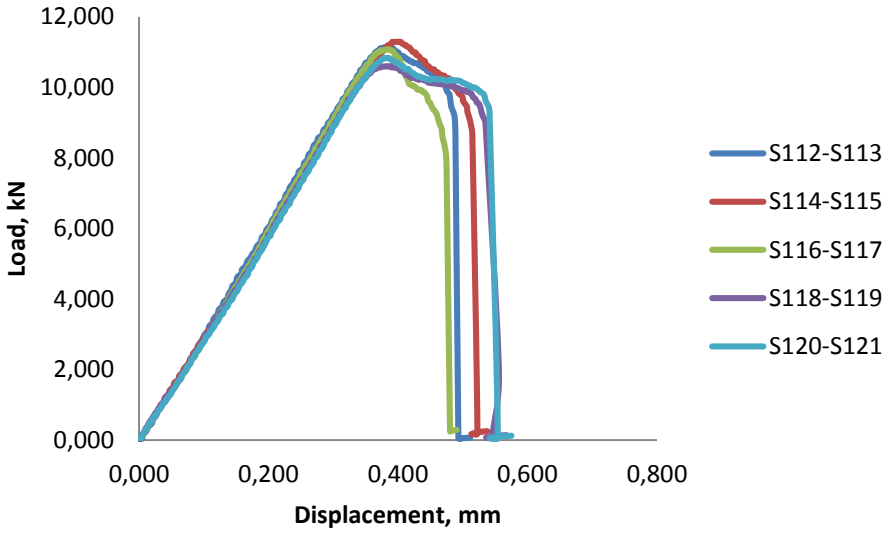

Figure B4 Load values versus displacement: peel ply side plus plasma pre-treatment (1pass, 500mm/min).

Table B5 LSS values and failure type: peel ply plus plasma pre-treatment (1 pass, 100mm/min)

Plasma Parameters				
Gas Flow: 8l/min				
Gas type: Argon + Air				
Treatment distance, d=4mm				
Speed, v=100mm/min				
Number of passes =1				
OUTPUT: Mechanical Testing				
#	**Sample designation**	**Max. Load (kN)**	**LSS (MPa)**	**Failure Type**
1	S130-S132	11.3	35.9	Cohesive
2	S133-S134	10.7	34.2	
3	S135-S137	10.6	34.1	
4	S136-S138	9.8	31.7	
5	S139-S140	10.8	34.7	
			Mean: 34.1MPa Standard deviation: 1.3MPa COV (%): 3.8	

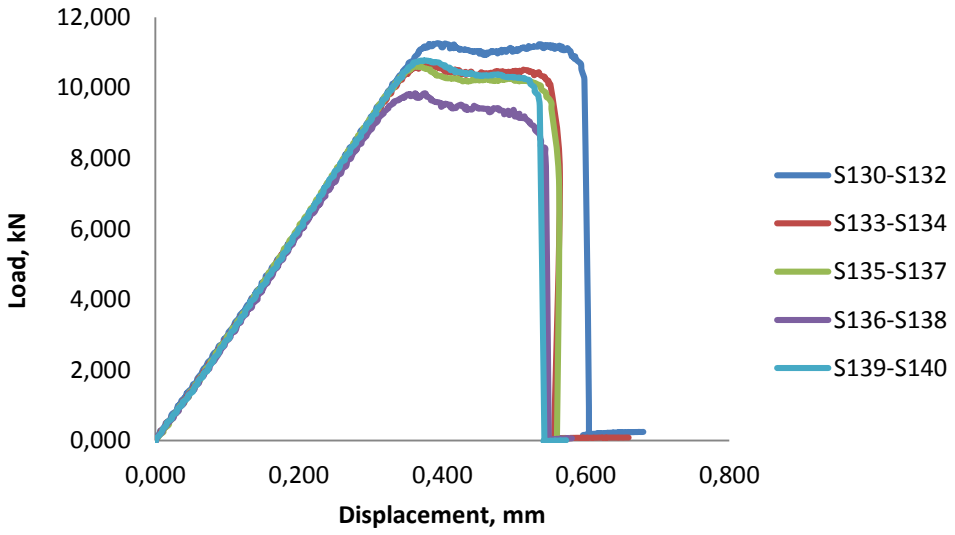

Figure B5 Load values versus displacement: peel ply plus plasma pre-treatment (1 pass, 100mm/min).

Table B6 LSS values and failure type: peel ply plus plasma pre-treatment (5 passes, 500mm/min)

Plasma Parameters				
Gas Flow: 8l/min				
Gas type: Argon + Air				
Treatment distance, d=4mm				
Speed, v=500mm/min				
Number of passes =5				

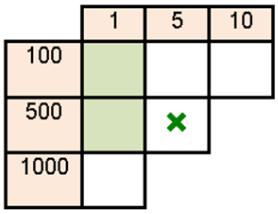

OUTPUT: Mechanical Testing				
#	**Sample designation**	**Max. Load (kN)**	**LSS (MPa)**	**Failure Type**
1	S141-S142	10.3	33.3	Cohesive
2	S143-S144	10.5	33.7	
3	S145-S146	10.1	32.3	
4	S147-S148	10.6	34.1	
5	S149-S150	10.8	34.7	
			Mean: 33.6 MPa Standard deviation: 0.8MPa COV (%): 2.3	

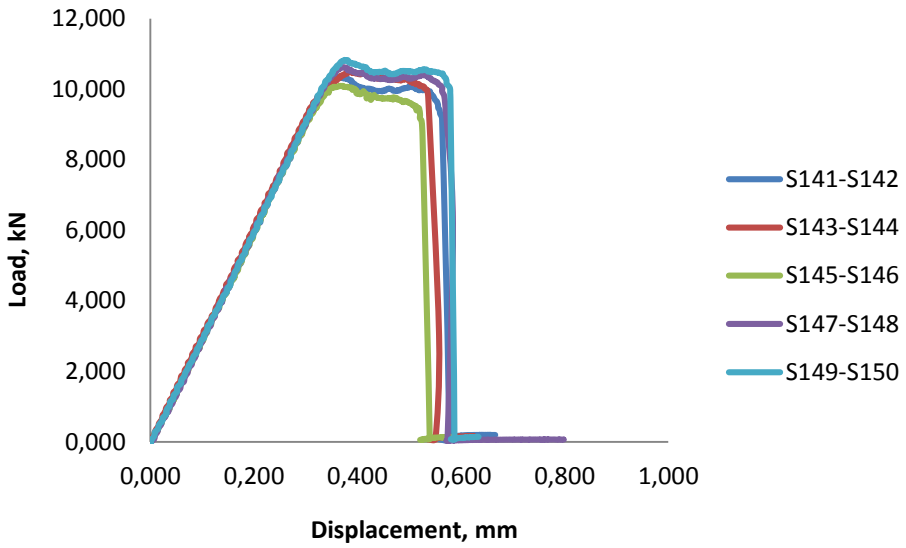

Figure B6 Load values versus displacement: peel ply plus plasma pre-treatment (5 passes, 500mm/min).

Table B7 LSS values and failure type: peel ply plus plasma pre-treatment (10 passes, 100mm/min)

Plasma Parameters				
Gas Flow: 8l/min				
Gas type: Argon + Air				
Treatment distance, d=4mm				
Speed, v=100mm/min				
Number of passes =10				

	1	5	10
100			✖
500			
1000			

OUTPUT: Mechanical Testing				
#	**Sample designation**	**Max. Load (kN)**	**LSS (MPa)**	**Failure Type**
1	S151-S152	10.9	34.9	Cohesive
2	S153-S154	10.8	34.8	
3	S155-S156	11.3	36.2	
4	S157-S158	10.9	35.01	
5	S159-S160	11.1	35.6	
			Mean: 35.3MPa Standard deviation: 0.5MPa COV (%): 1.4	

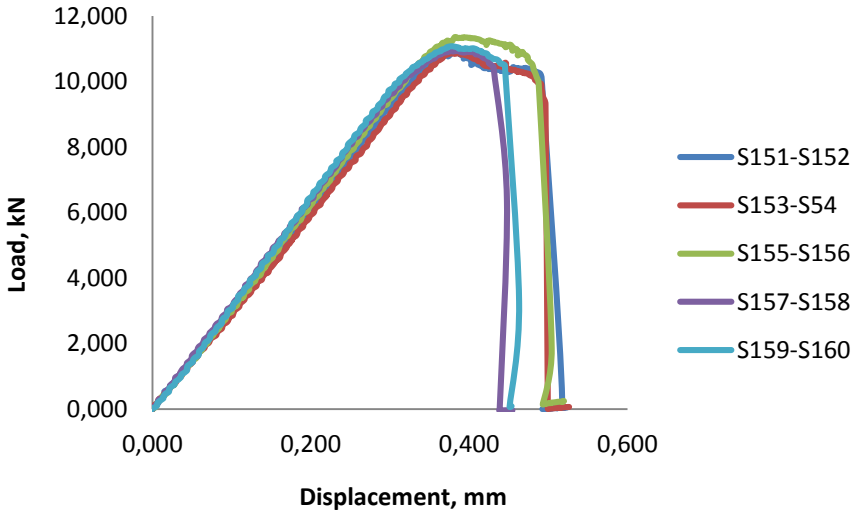

Figure B7 Load values versus displacement: peel ply plus plasma pre-treatment (10 passes, 100mm/min).

Table B8 LSS value and failure type: peel ply plus plasma pre-treatment (1pass, 1000mm/min)

Plasma Parameters				
Gas Flow: 8l/min Gas type: Argon + Air Treatment distance, d=4mm Speed, v=1000mm/min Number of passes =1	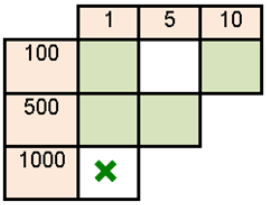			
OUTPUT: Mechanical Testing				
#	**Sample designation**	**Max. Load (kN)**	**LSS (MPa)**	**Failure Type**
1	S161-S162	10.3	33.1	Cohesive
2	S163-S164	9.9	31.8	
3	S165-S166	10.6	33.9	
4	S167-S168	10.2	32.8	
5	S169-S170	10.05	32.1	
			Mean: 32.7MPa Standard deviation: 0.7MPa COV (%): 2.1	

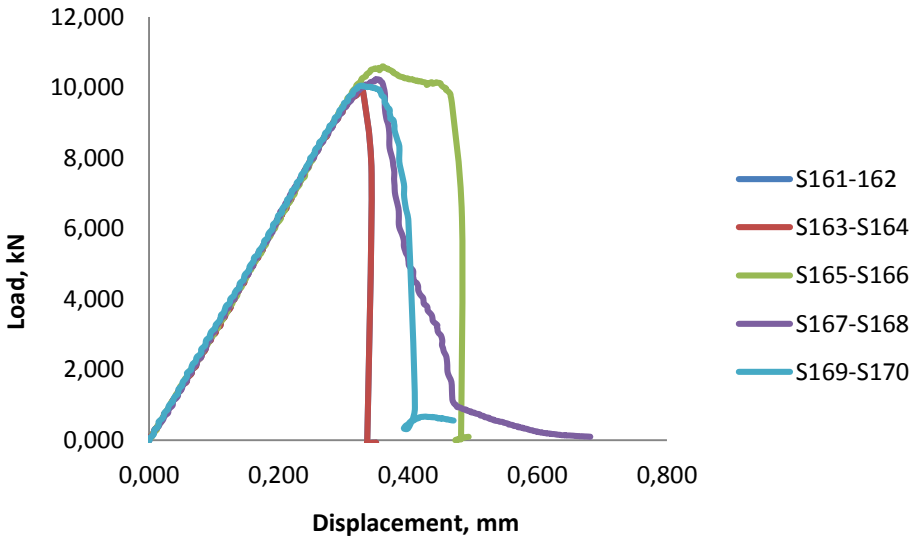

Figure B8 Load values versus displacement: peel ply plus plasma pre-treatment (1pass, 1000mm/min).

Table B9 LSS values and failure type: peel ply plus plasma pre-treatment (5 passes, 100mm/min)

Plasma Parameters				
Gas Flow: 8l/min Gas type: Argon + Air Treatment distance, d=4mm Speed, v=100mm/min Number of passes =5	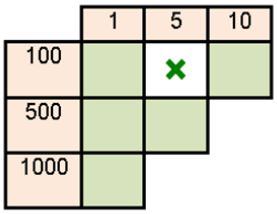			
OUTPUT: Mechanical Testing				
#	**Sample designation**	**Max. Load (kN)**	**LSS (MPa)**	**Failure Type**
1	S171-S172	11.6	37.3	Cohesive
2	S173-S174	11.1	35.3	
3	S175-S176	11.5	37.5	
4	S177-S178	11.6	37.2	
5	S179-S180	11.4	36.4	
			Mean: 36.7MPa Standard deviation: 0.8MPa COV (%): 2.1	

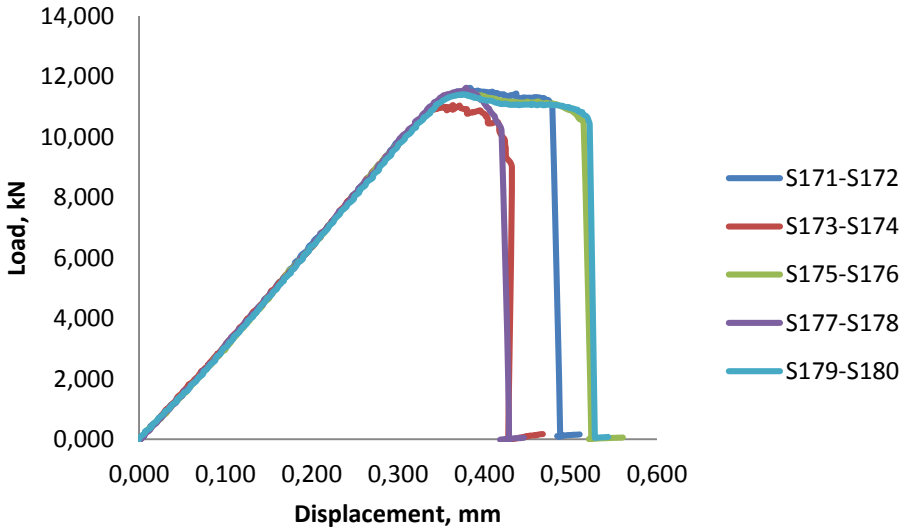

Table B9 Load values versus displacement: peel ply plus plasma pre-treatment (5 passes, 100mm/min).

Table B10 LSS values and failure type: bag side as received, no pre-treatment

OUTPUT: Mechanical Testing

#	Sample designation	Max. Load (kN)	LSS (MPa)	Failure Type
1	S221-S222	5.2	16.6	Adhesive
2	S223-S224	6.1	19.5	
3	S225-S226	5.7	18.2	
4	S227-S228	5.5	17.6	
5	S229-S230	4.8	15.3	
			Mean: 17.4MPa Standard deviation: 1.4MPa COV (%): 8.1	

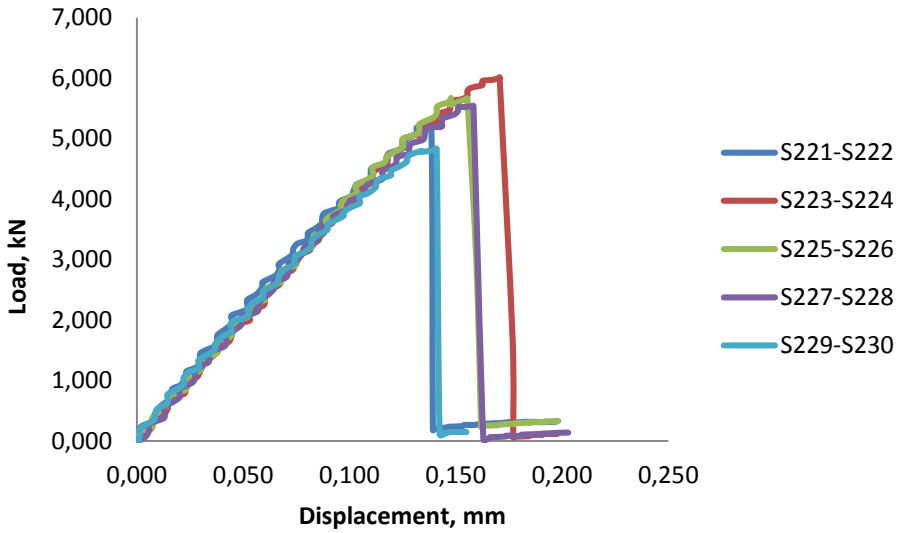

Figure B10 Load values versus displacement: bag side as received, no pre-treatment.

Table B11 LSS values and failure type: bag side plus plasma pre-treatment (5passes, 100mm/min)

Plasma Parameters				
Gas Flow: 8l/min Gas type: Argon + Air Treatment distance, d=4mm Speed, v=100mm/min Number of passes =5	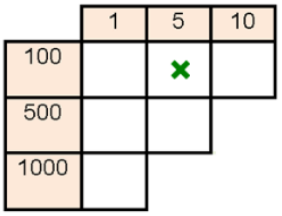			
OUTPUT: Mechanical Testing				
#	**Sample designation**	**Max. Load (kN)**	**LSS (MPa)**	**Failure Type**
1	S231-S235	13.9	44.3	Cohesive Adhesive
2	S233-S234	12.5	39.9	
3	S232-S236	14.1	45.0	
4	S237-S238	13.7	43.7	
5	S239-S240	12.8	41.1	
			Mean: 42.8MPa Standard deviation: 1.9MPa COV (%):4.4	

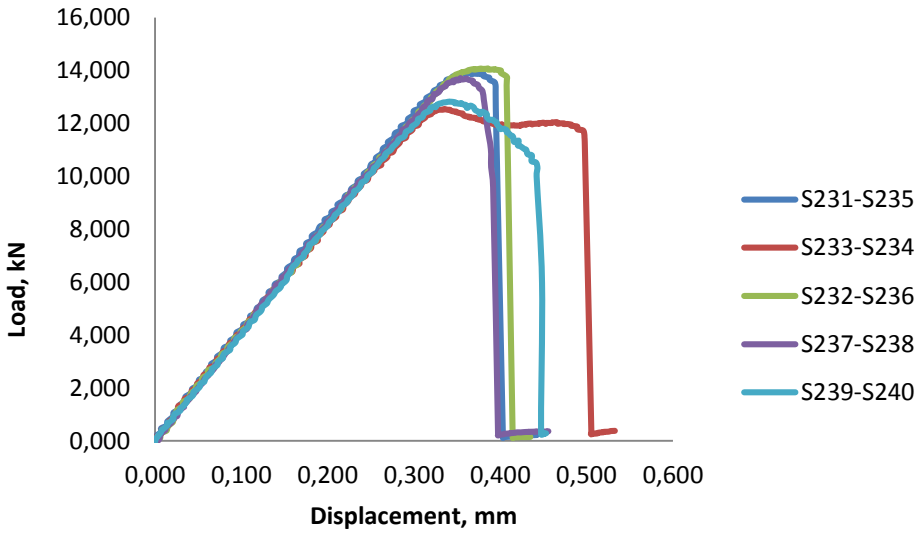

Figure B11 Load values versus displacement: bag side plus plasma pre-treatment (5passes, 100mm/min).

Table B12 LSS values and failure type: bag side plus plasma pre-treatment (1pass, 1000 mm/min)

Plasma Parameters				
Gas Flow: 8l/min Gas type: Argon + Air Treatment distance, d=4mm Speed, v=1000mm/min Number of passes =1	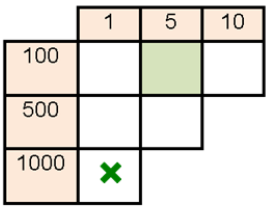			
OUTPUT: Mechanical Testing				
#	**Sample designation**	**Max. Load (kN)**	**LSS (MPa)**	**Failure Type**
1	S243-S244	12.1	38.8	Cohesive Adhesive
2	S245-S246	11.1	35.7	
3	S247-S248	12.1	38.7	
4	S249-S250	12.2	38.9	
			Mean: 38.03 MPa Standard deviation: 1.3MPa COV (%): 3.5	

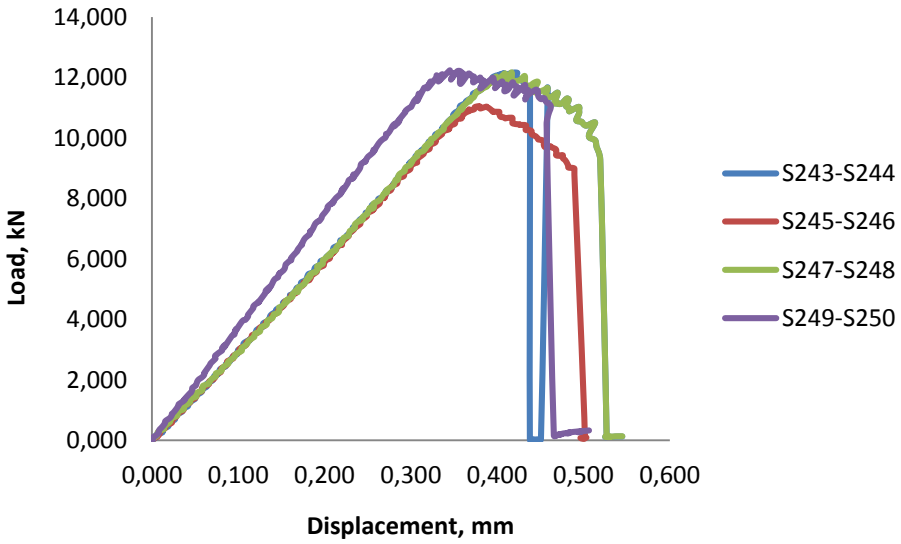

Figure B12 Load values versus displacement: bag side plus plasma pre-treatment (1pass, 1000mm/min).

Table B13 LSS values and failure type: bag side plus plasma pre-treatment (1pass, 100mm/min)

Plasma Parameters				
Gas Flow: 8l/min		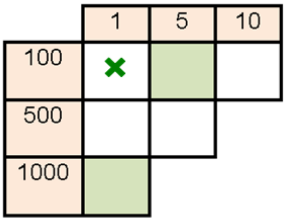		
Gas type: Argon + Air				
Treatment distance, d=4mm				
Speed, v=100mm/min				
Number of passes =1				
OUTPUT: Mechanical Testing				
#	**Sample designation**	**Max. Load (kN)**	**LSS (MPa)**	**Failure Type**
1	S251-S252	12.7	40.5	Cohesive Adhesive
2	S253-S254	12.1	38.6	
3	S255-S256	12.2	38.9	
4	S257-S258	12.6	40.6	
5	S259-S260	11.9	38.1	
			Mean: 39.4MPa Standard deviation: 1MPa COV (%): 2.5	

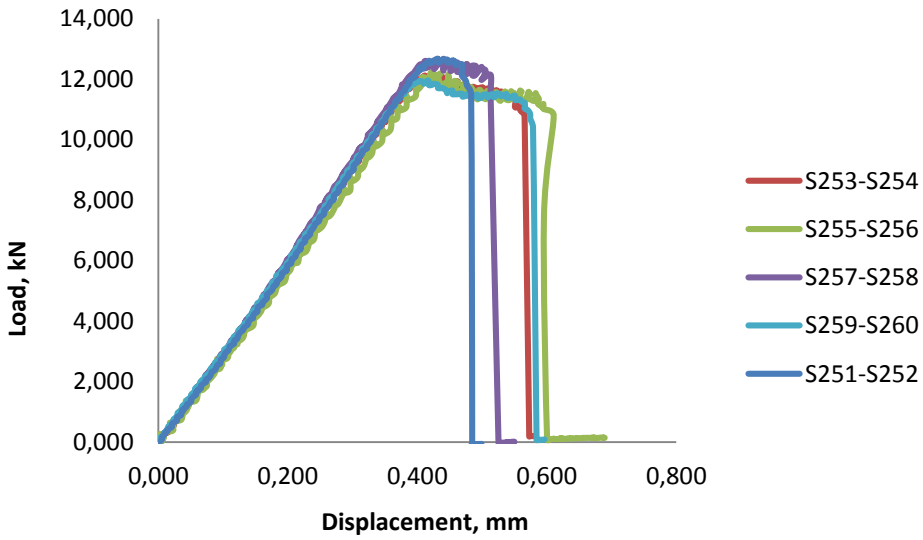

Figure B13 Load values versus displacement: bag side plus plasma pre-treatment (1pass, 100mm/min).

Table B14 LSS values and failure type: bag side plus plasma pre-treatment (10passes, 100mm/min)

Plasma Parameters				
Gas Flow: 8l/min				
Gas type: Argon + Air				
Treatment distance, d=4mm				
Speed, v=100mm/min				
Number of passes =10				

	1	5	10
100			✖
500			
1000			

OUTPUT: Mechanical Testing				
#	Sample designation	Max. Load (kN)	LSS (MPa)	Failure Type
1	S261-S262	12.4	39.6	Cohesive Adhesive
2	S263-S264	13.1	42.1	
3	S265-S266	11.9	38.2	
4	S267-S268	13.3	42.3	
5	S269-S270	13.6	43.3	
			Mean: 41.1MPa Standard deviation: 4.6MPa COV (%): 1.9	

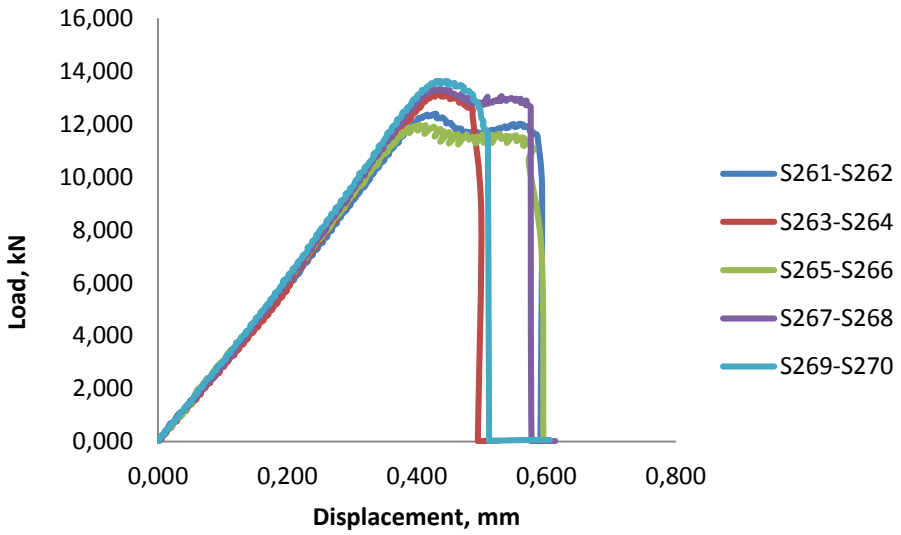

Figure B14 Load values versus displacement: bag side plus plasma pre-treatment (10passes, 100mm/min).

Table B15 LSS values and failure type: bag side plus grit blasting pre-treatment

OUTPUT: Mechanical Testing				
#	**Sample designation**	**Max. Load (kN)**	**LSS (MPa)**	**Failure Type**
1	S216-S217	12.9	41.1	Cohesive Adhesive (Delamination)
2	S218-S219	12.6	40.2	
3	S220-S271	12.7	40.5	
4	S272-S273	13.1	40.7	
5	S274-S275	12.7	40.5	
			Mean: 40.8MPa Standard deviation: 0.5MPa COV (%): 1.3	

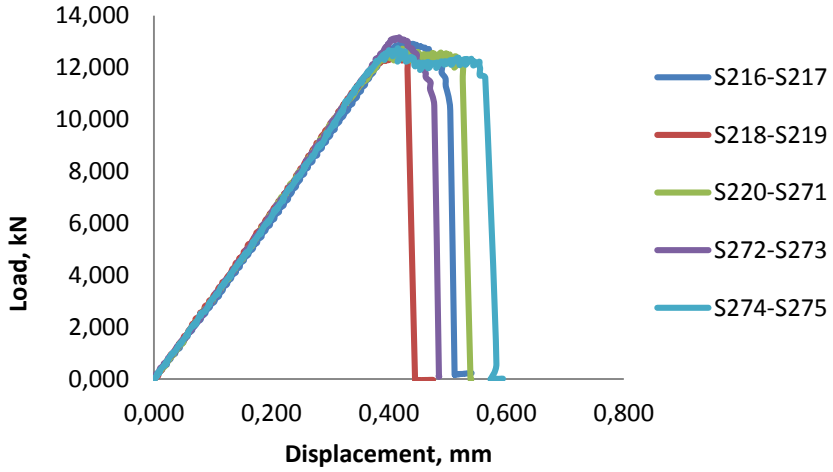

Figure B15 Load values versus displacement: bag side plus grit blasting pre-treatment.

Table B16 LSS values and failure type: bag side plus manual abrasion pre-treatment

OUTPUT: Mechanical Testing				
#	**Sample designation**	**Max. Load (kN)**	**LSS (MPa)**	**Failure Type**
1	S276-S277	11.7	37.4	Cohesive Adhesive
2	S278-S279	10.9	34.9	
3	S280-S281	11.1	35.1	
4	S282-S283	10.2	32.7	
5	S287-S288	10.4	33.1	
			Mean: 34.7MPa Standard deviation: 1.7MPa COV (%): 4.8	

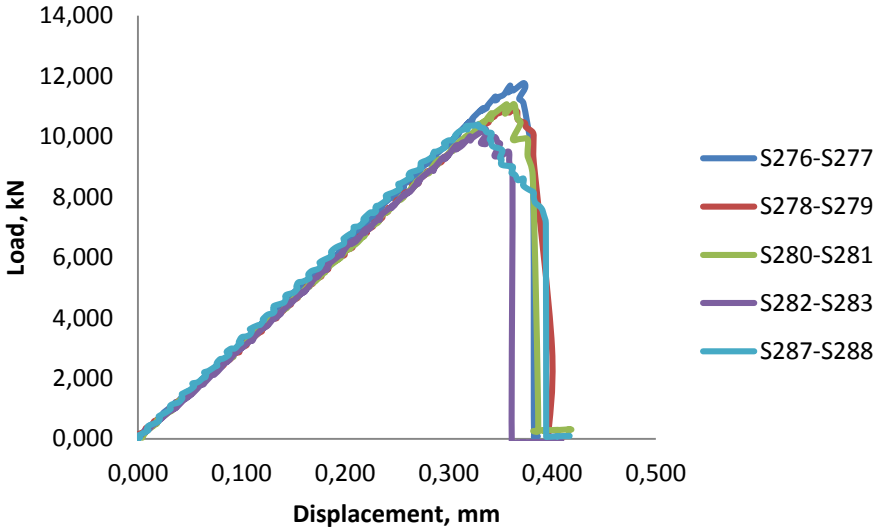

Figure B16 Load values versus displacement: bag side plus manual abrasion pre-treatment.

Table B17 LSS values and failure type: bag side plus plasma pre-treatment (1pass, 500mm/min)

Plasma Parameters				
Gas Flow: 8l/min				
Gas type: Argon + Air				
Treatment distance, d=4mm				
Speed, v=500mm/min				
Number of passes =1				

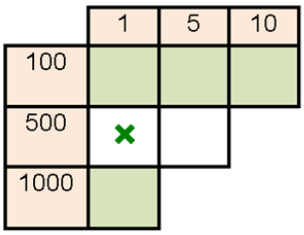

OUTPUT: Mechanical Testing				
#	Sample designation	Max. Load (kN)	LSS (MPa)	Failure Type
1	S289-S290	10.2	32.4	Cohesive Adhesive
2	S291-S292	10.2	34.4	
3	S294-S295	11.7	37.2	
4	S296-S297	11.2	35.8	
5	S298-S301	10.7	34.2	
			Mean: 34.4MPa Standard deviation: 1.9MPa COV (%): 5.5	

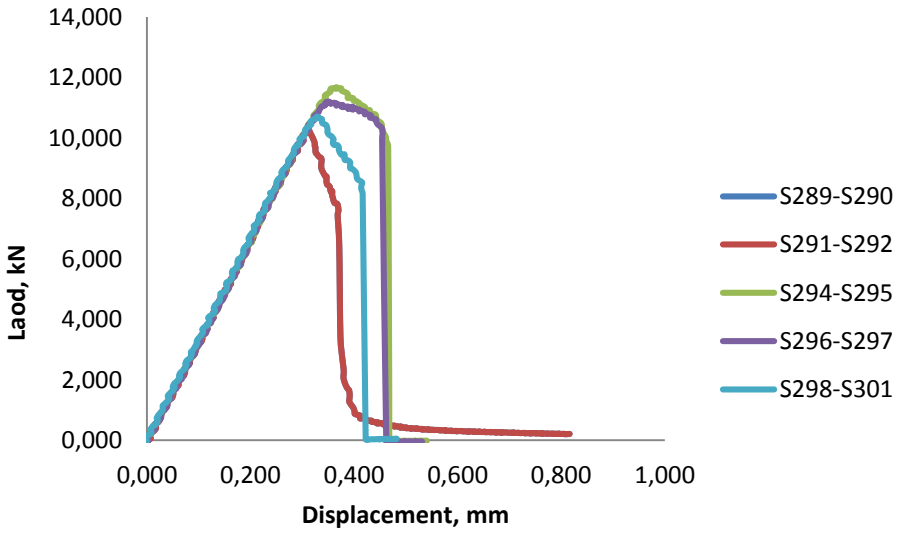

Figure B17 Load values versus displacement: bag side plus plasma pre-treatment (1pass, 500mm/min).

Table B18 LSS values and failure type: bag side plus plasma pre-treatment (5passes, 500mm/min)

Plasma Parameters				
Gas Flow: 8l/min Gas type: Argon + Air Treatment distance, d=4mm Speed, v=500mm/min Number of passes =5	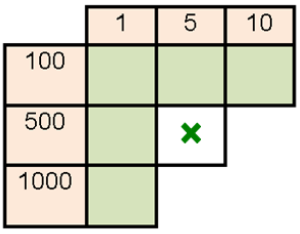			
OUTPUT: Mechanical Testing				
#	**Sample designation**	**Max. Load (kN)**	**LSS (MPa)**	**Failure Type**
1	S302-S303	11.5	39.7	Cohesive Adhesive
2	S304-S305	12.5	39.8	
3	S325-S326	11.1	35.4	
4	S311-S314	11.8	37.5	
5	S307-S301	10.9	34.6	
			Mean: 36.8MPa Standard deviation: 1.8MPa COV (%): 4.8	

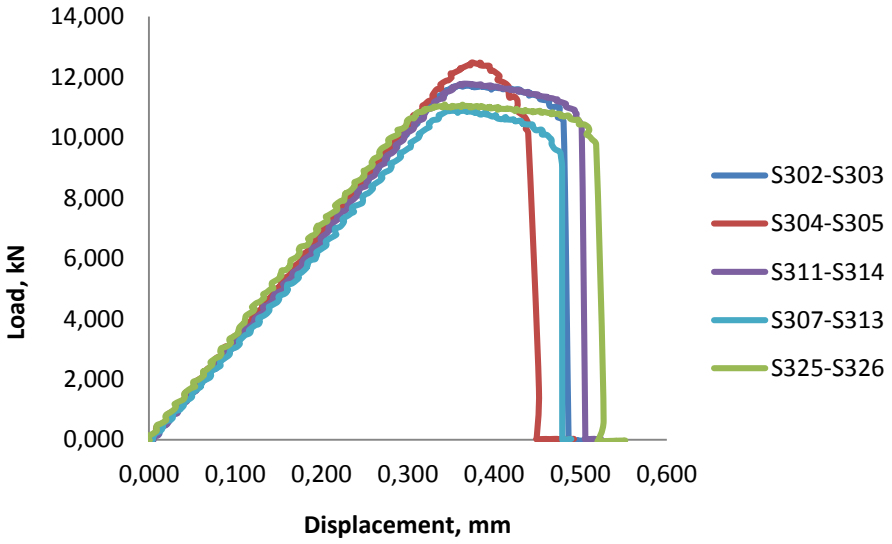

Figure B18 Load values versus displacement: bag side plus plasma pre-treatment (5passes, 500mm/min).

Appendix C:

X-ray Photoelectron Spectroscopy Results

Table C1 Elemental ID and quantification peel ply side as received

Name	Peak BE	Atomic %
C1s	285.06	75.66
C1s Scan A	286.80	5.43
C1s Scan B	289.30	0.89
O1s	532.58	13.14
S2p	162.40	2.34
Si2p	102.19	1.39
Zn2p3/2	1021.80	1.15

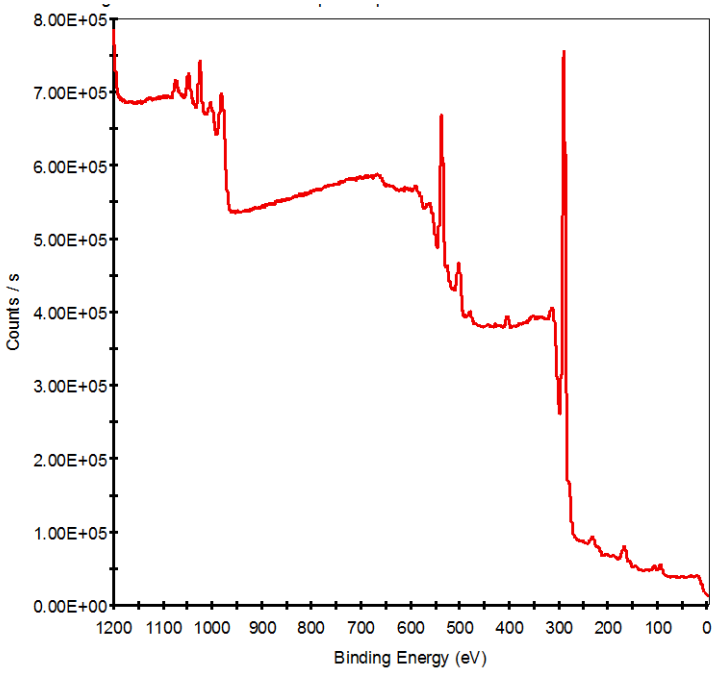

Figure C1 XPS spectra of surface pre-treatment peel ply side as received.

Table C2 Elemental ID and quantification peel ply side plus grit blasting

Name	Peak BE	Atomic %
C1s	285.12	61.81
C1s Scan A	287.00	2.85
C1s Scan B	284.50	0.37
N1s	399.30	8.91
O1s	532.52	22.41
S2p	167.93	2.76
Si2p	102.45	0.72
Zn2p3/2	1021.93	0.17

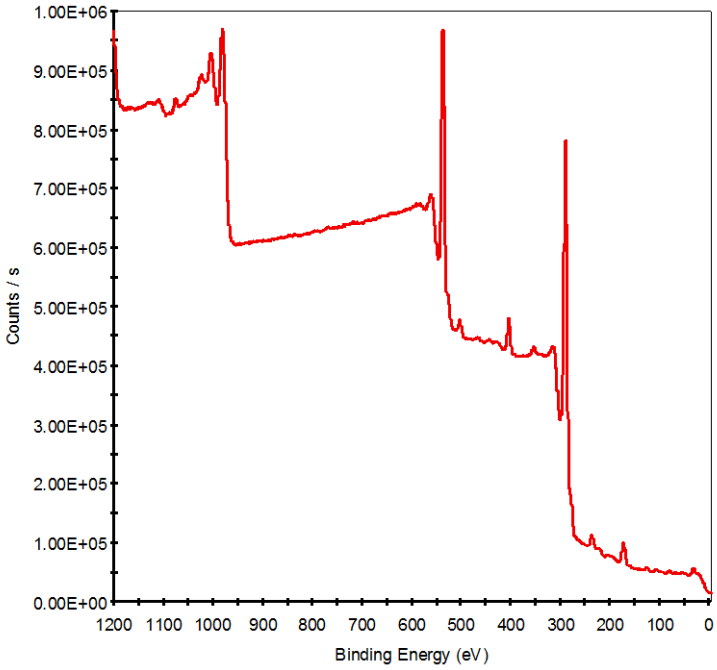

Figure C2 XPS spectra of surface pre-treatment peel ply side plus grit blasting.

Table C3 Elemental ID and quantification peel ply side plus plasma (5passes, 100mm/min)

Name	Peak BE	Atomic %
C1s	285.07	37.90
C1s Scan A	286.80	2.21
C1s Scan B	288.50	3.01
N1s	400.76	12.84
O1s	532.02	36.71
S2p	168.42	6.30
Si2p	103.07	1.03

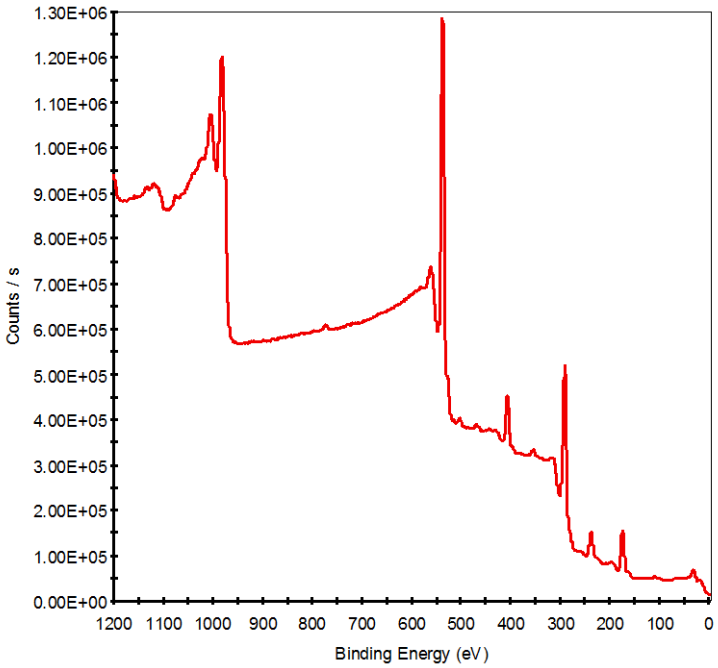

Figure C3 XPS spectra of surface pre-treatment peel ply side plus plasma (5passes, 100mm/min).

Table C4 Elemental ID and quantification peel ply side plus plasma (1pass, 1000mm/min)

Name	Peak BE	Atomic %
C1s	285.11	51.50
C1s Scan A	289.00	7.31
C1s Scan B	287.20	4.80
N1s	399.40	4.61
O1s	532.52	30.21
S2p	168.04	0.91
Si2p	102.91	0.44
Zn2p3/2	1021.89	0.22

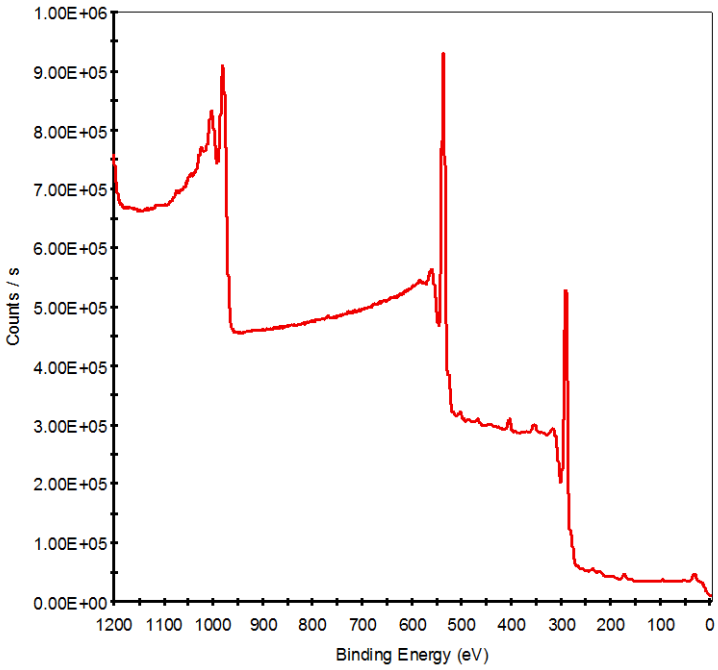

Figure C4 XPS spectra of surface pre-treatment peel ply side plus plasma (1pass, 1000mm/min).

Table C5 Elemental ID and quantification bag side (no pre-treatment)

Name	Peak BE	Atomic %
C1s	285.11	55.43
F1s	688.12	20.03
N1s	399.14	6.77
O1s	532.43	14.57
S2p	167.82	1.59
Si2p	102.62	1.61

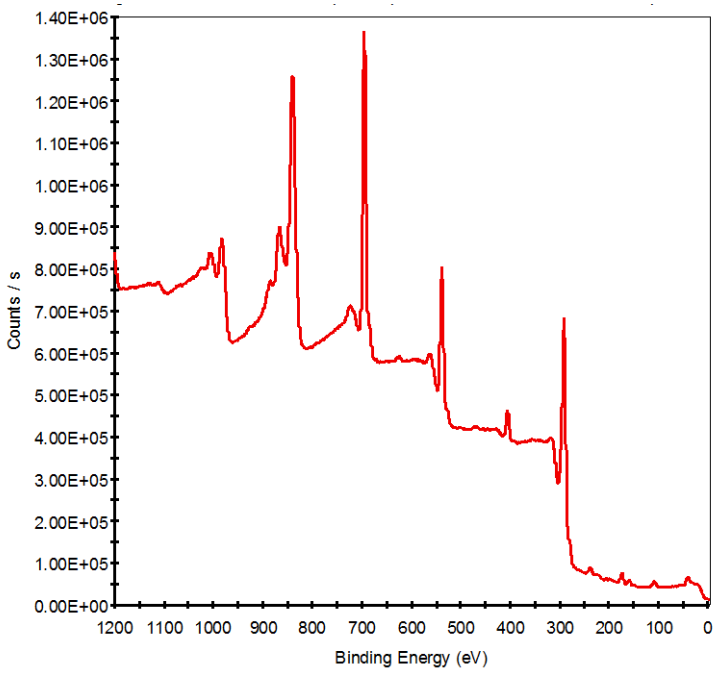

Figure C5 XPS spectra of surface bag side (no pre-treatment).

Table C6 Elemental ID and quantification bag side plus grit blasting

Name	Peak BE	Atomic %
C1s	285.03	66.77
N1s	399.36	7.49
O1s	532.56	21.96
S2p	167.99	2.74
Si2p	102.16	1.04

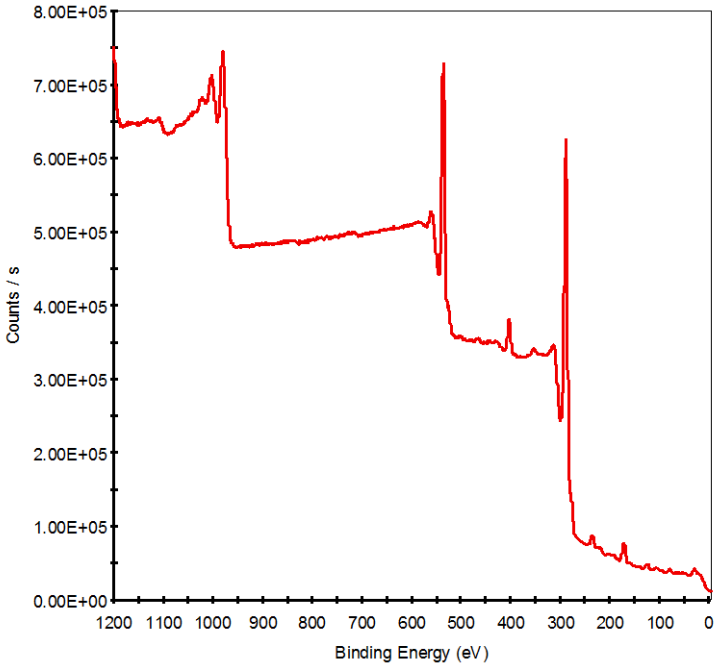

Figure C6 XPS spectra of surface pre-treatment bag side plus grit blasting.

Table C7 Elemental ID and quantification bag side plus plasma (5passes, 100mm/min)

Name	Peak BE	Atomic %
C1s	285.09	35.45
F1s	688.20	9.77
N1s	400.97	13.11
O1s	532.12	32.79
S2p	168.52	7.03
Si2p	103.13	1.85

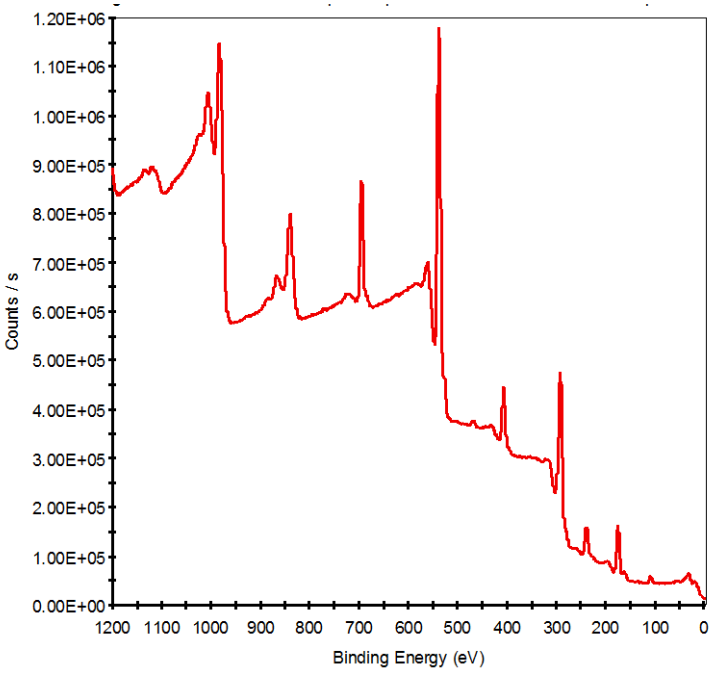

Figure C7 XPS spectra of surface pre-treatment bag side plus plasma (5passes, 100mm/min).

Table C8 Elemental ID and Quantification bag side plus plasma (1pass, 1000mm/min)

Name	Peak BE	Atomic %
C1s	285.18	39.77
F1s	688.54	29.32
N1s	399.22	8.98
O1s	532.39	18.43
S2p	168.09	1.75
Si2p	103.18	1.75

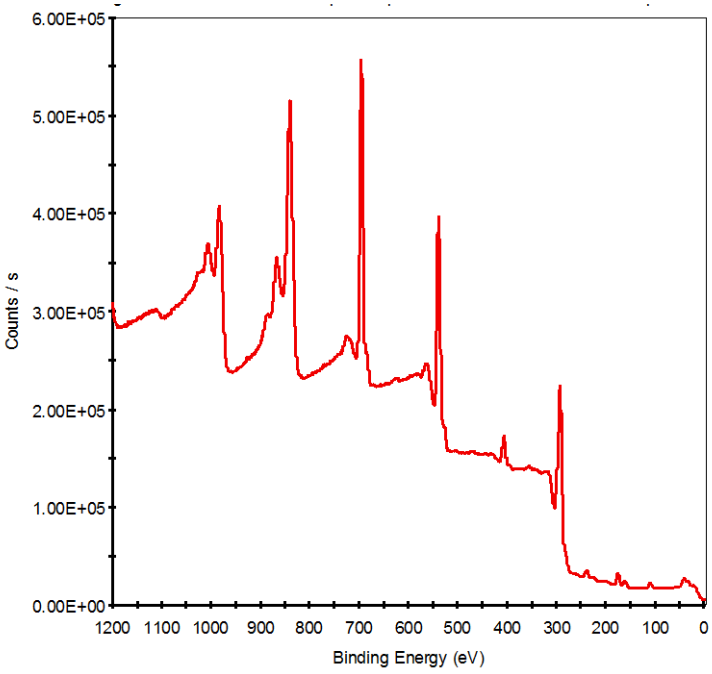

Figure C8 XPS spectra of surface pre-treatment bag side plus plasma (1pass, 1000mm/min).